



HAL
open science

An adaptive fault tolerant fusion framework for a precise, available and fail-safe localization

Khoder Makkawi

► **To cite this version:**

Khoder Makkawi. An adaptive fault tolerant fusion framework for a precise, available and fail-safe localization. Embedded Systems. Université de Lille; Université Libanaise, 2020. English. NNT : 2020LILUI069 . tel-03923919

HAL Id: tel-03923919

<https://theses.hal.science/tel-03923919>

Submitted on 5 Jan 2023

HAL is a multi-disciplinary open access archive for the deposit and dissemination of scientific research documents, whether they are published or not. The documents may come from teaching and research institutions in France or abroad, or from public or private research centers.

L'archive ouverte pluridisciplinaire **HAL**, est destinée au dépôt et à la diffusion de documents scientifiques de niveau recherche, publiés ou non, émanant des établissements d'enseignement et de recherche français ou étrangers, des laboratoires publics ou privés.

LILLE UNIVERSITY
&
LEBANESE UNIVERSITY
UMR 9189 - Laboratoire Centre de Recherche en Informatique,
Signal et Automatique de Lille

A thesis presented for the degree of
Doctor of Philosophy

Discipline : Automation, computer engineering and signal
processing

Khoder MAKKAWI

**An adaptive fault tolerant fusion framework for a
precise, available and fail-safe localization**

Defence at 18/12/2020 in front of the jury composed of :

Rapporteur

Roland CHAPUIS

Professor, Clermont Auvergne University

Chafic MOKBEL

Professor, Balamand University

Examiner

Isabelle FANTONI (President of the jury)

Research Director, LS2N Laboratory

Mohamad KHALIL

Professor, Lebanese University

Joelle AL HAGE

Ass. Professor, Sorbonne University - UTC

Thesis Director

Maan EL BADAOUI EL NAJJAR

Professor, Lille University

Nazih MOUBAYED

Professor, Lebanese University

Co-supervisor

Nourdine AIT-TMAZIRTE

Research engineer, IRT Ralenium

UNIVERSITÉ DE LILLE
&
UNIVERSITÉ LIBANAISE
UMR 9189 - Laboratoire Centre de Recherche en Informatique,
Signal et Automatique de Lille

Une thèse présentée pour le diplôme de
Doctor of Philosophy

Discipline : Automatique, Génie informatique, Traitement du
Signal et des Images

Khoder MAKKAWI

**Formalisme adaptative pour la fusion tolérante aux
fautes avec application à la localisation précise,
disponible et sûre**

Défense au 18/12/2020 devant le jury composé de :

Rapporteur

Roland CHAPUIS

Professeur, Université de Clermont Auvergne

Chafic MOKBEL

Professeur, Université de Balamand

Examineur

Isabelle FANTONI (Présidente du jury)

Directeur de Recherche, Laboratoire LS2N

Mohamad KHALIL

Professeur, Université libanaise

Joelle AL HAGE

MCF, Université de Sorbonne - UTC

Directeur de Thèse

Maan EL BADAOUI EL NAJJAR

Professeur, Université de Lille

Nazih MOUBAYED

Professeur, Université libanaise

Co-superviseur

Nourdine AIT-TMAZIRTE

Ingénieur de recherche, IRT Ralenium

Résumé

L'adoption d'une solution technologique comme moyen de localisation d'un Système de Transport Intelligent nécessite une validation des performances usuelles. Celles-ci sont principalement la précision, la disponibilité, la continuité et la sûreté de fonctionnement. Elles présentent pourtant un comportement antagoniste, dans la mesure où assurer la sûreté de fonctionnement est généralement au détriment de la disponibilité. Cette brique de localisation peut être utilisée dans des fonctions n'engageant pas la sécurité du système et de l'environnement l'entourant comme le suivi de flotte ou l'information voyageurs. Mais quand il s'agit de fournir une information de localisation au module de contrôle de trajectoire du véhicule, il paraît évident que l'erreur de positionnement inconnue doit être correctement bornée, c'est ce que l'on nomme l'intégrité de positionnement. Pour augmenter l'intégrité, la littérature préconise l'intégration d'une couche de diagnostic et de supervision. De même, le couplage de solutions de localisation complémentaires comme le GNSS utilisé pour ses facultés de positionnement absolu, et l'odométrie pour la justesse à court terme de ses données relatives est préconisé pour augmenter la précision, la disponibilité et la continuité du système. Dans ces travaux nous proposons un formalisme permettant la mise en place d'une fusion de données brutes GNSS et de données odométriques par le biais d'un filtre stochastique de fusion de données, le Maximum Correntropy Criterion Nonlinear Information Filter, robuste aux différents bruit de mesures (shot noises, mutli-gaussiens, etc...). Ce formalisme intègre également une couche de diagnostic conçue pour être adaptative au contexte de navigation ou au changement d'exigences opérationnelles par le biais d'une métrique informationnelle, l' α -Rényi Divergence, généralisant les métriques habituellement utilisées à ces fins, comme la divergence de Bhattacharyya ou la divergence de Kullback-Leibler. Cette divergence permet la conception de résidus paramétriques qui tiennent en compte du changement d'environnement et donc du changement de la probabilité a priori de faire face ou non à un défaut de mesures GNSS. Nous étudions la possibilité d'implémenter une politique de sélection de ce paramètre et étudions l'impact de cette politique sur l'ensemble des performances précédemment citées. Les résultats encourageants permettent d'envisager comme perspective la complexification de la politique et des algorithmes de fixation de la valeur du paramètre α par l'apport des technologies d'intelligence artificielle afin d'augmenter la discernabilité des défauts, minimiser la probabilité de fausse alarme (et donc augmenter la disponibilité) et minimiser la probabilité de détection manqué dans l'objectif d'augmenter la sûreté de fonctionnement du véhicule. Des données réelles fournies par la plateforme PRETIL du laboratoire CRISAL ont été utilisées pour le test et la validation des approches proposées.

Abstract

The adoption of a technological solution as a means of localization of an Intelligent Transport System requires validation of the usual performance metrics. These are mainly accuracy, availability, continuity, and safety. However, they present an antagonistic behavior, insofar as ensuring operational safety is generally to the detriment of availability. This localization brick can be used in functions that do not involve the security of the system and the surrounding environment, such as fleet tracking or passenger information. But, when it comes to providing localization information to the vehicle's trajectory control module, it seems obvious, that the unknown positioning error must be properly bounded, this is called positioning integrity. To increase integrity, the literature recommends the integration of a diagnostic and monitoring layer. Similarly, the coupling of complementary localization solutions such as GNSS for its absolute positioning capabilities, and odometry for the precision of its relative data is recommended to increase the accuracy, availability, and continuity of the system. In this work, we propose a framework allowing the implementation of merging GNSS raw data and odometric data, through the use of a data fusion stochastic filter, the Maximum Correntropy Criterion Nonlinear Information Filter, robust to different measurement noises (shot noises, multi-gaussian, etc...). This framework also integrates a diagnostic layer designed to be adaptive to the navigation context or to changing operational requirements through an informational metric, the α -Rényi Divergence, generalizing the metrics usually used for these purposes, such as the Bhattacharyya Divergence or the Kullback-Leibler Divergence. This divergence allows the design of parametric residuals that take into account the change in environment and thus the change in the a priori probability of facing or not facing GNSS measurement failures. We study the possibility of implementing a selection policy for this parameter and study the impact of this policy on all the above-mentioned performance. The encouraging results allow us to consider, as a perspective for this work, the complexification of the policy and the algorithms for setting the value of the α parameter by the contribution of artificial intelligence technologies in order to increase the discernibility of faults, minimize the probability of false alarms (and thus increase availability) and minimize the probability of missed detections (and thus increase operational safety). In this work, real data provided by the PRETIL plate-forme of CRISAL Lab are used in order to test and validate the proposed approach.

Remerciements

First of all, I would like to thank Lille University and Lebanese University for gave me the opportunity for a commune thesis between the EDST in Lebanon, and the CRISAL laboratory in France.

I would like to express, here, my respectful gratitude to Pr. Roland Chapuis (Clermont Auvergne University), and to Pr. Chafic Mokbel (Balamand University) who accepted to judge and review my work.

As well, I will thank Mme. Isabelle Fantoni (Research Director at LS2N Laboratory), Pr. Mohamad Khalil (Lebanese University), and Mme. Joelle El Hage (Associated Professor at Sorbonne University - UTC) who gave me the honor by accepting to be examiners of this work.

My sincere thanks also go to my thesis director in France, Prof. Maan El Badaoui El Najjar, and to my co-supervisor R.E. Nourdine Ait-Tmazirte for having supported and supervised me throughout this thesis, in good times and in times of discouragement. I was extremely touched by their human values in understanding and acting despite all the constraints. They taught me the meaning of research, and how to be a good researcher in my domain.

I also express my gratitude to my thesis director in Lebanon, Professor Nazih Moubayed for his responsibility, support and valuable advices.

I sincerely thank Dr. Imad Kassa'a (Director of AUF) and Youmna Sayour for supporting, and providing me the best technology services.

I would like also to thank all my friends for their encouragement, support and sympathy during these years, especially Dr. Marwan Osman, Dr. Abdallah Allouch, Dr. Ismat El Haffar, Dr. Souhayb El Kass, Rami Khoder, Zakaria Chmeit, Ahmad Kamal El Din, and Nesrine Harbaoui.

My last thanks go to my family, who sacrifice for providing me a successful carrier, my father and my mother whom I admire, for their support and trust, without whom I could not have accomplished all this work. I thank you from the deep of my heart for having always been there to help me. Thank you to my brothers and sisters and hope you a successful carrier in your life.

Finally, I would like to express my sincere gratitude to all those who have, directly or indirectly, participated in the elaboration of this work and who have accompanied me in this process, for a part of the way or for the totality of the journey.

Table Of Contents

1	General Introduction	1
1.1	General Introduction	1
1.2	Thesis Positioning	2
1.2.1	Context Of Work And Motivations	2
1.2.2	Localisation Systems For Intelligent Transportation Systems	4
1.3	Key Performance Indicators of a Localisation Function	5
1.3.1	Accuracy and Precision	6
1.3.2	Dependability and Availability	7
1.3.3	Robustness	7
1.4	Answers to the Three Main Operational Challenges	8
1.4.1	A Robust Multi-Sensor Integration to Ensure Continuity	8
1.4.2	Diagnostic as a Guarantee of Safety	8
1.4.3	Fault Tolerance as an Availability Booster	9
1.5	Contributions	9
1.6	Publications List	10
2	Multi-Sensors Localisation Architecture for High Accuracy and Availability	12
2.1	Chapter Introduction	12
2.2	Commonly Used Sensors and their Limitations	12
2.2.1	Global Navigation Satellites System	12
2.2.2	Odometers/Wheel Speed Sensors	17
2.2.3	Inertial Measurements Units	18
2.2.4	Other Possible Sensors	20
2.3	Sensor Fusion To Combine Them	23
2.3.1	Coupling Architectures	24
2.3.2	Stochastic Filtering	27
2.4	Chapter Conclusion	34
3	Adaptive Fault-Tolerant Fusion Framework to Ensure Fail-Safe and Available Localisation System	35
3.1	Chapter Introduction	35
3.2	A Brief State Of Art Of Diagnostic In State Estimation	35
3.3	Towards the New Concept of Adaptive Diagnostic for Safety	36
3.3.1	The Philosophy Behind Adaptive Diagnostic	36

3.3.2	How to Design an Adaptive Diagnostic Layer	38
3.3.3	Threshold Optimization	42
3.4	Fault Tolerance For Availability	45
3.4.1	Definition of Fault Tolerance	45
3.4.2	Fault Tolerance Applied To Fusion	46
3.4.3	Impact Of An Adaptive Diagnostic Layer In A Fault Tolerant Fusion Approach	48
3.5	Chapter Conclusion	49
4	Adaptive Fault Tolerant Fusion Framework for Performing a Robust, Precise, Available and Fail-Safe State Estimation	51
4.1	Chapter Introduction	51
4.2	General Approach Block Diagram	53
4.3	Toward a More Robust Criterion in Filtering	55
4.3.1	MMSE : The Ordinary KF Optimality Criterion	55
4.3.2	MCC : A More Robust Criterion	56
4.3.3	Development of MCC NIF	58
4.4	A Diagnostic based on α -Rényi Divergence	59
4.4.1	α -Rényi Divergence as a Parametric Residual	59
4.4.2	Physical Interpretation of α -Parameter	62
4.4.3	Establish A Residuals Parameterization Policy Based On Operational Requirements And Changes In Navigation Context	63
4.4.4	An Infinity Of Residuals Implies An Infinity Of Statistical Characterization ... How To Solve?	64
4.4.5	α -Rényi Criterion Generalizing Threshold Optimization	65
4.4.6	Threshold Optimization Algorithm	68
4.5	A Fault Tolerant Architecture based on UIO	68
4.6	Chapter Conclusion	71
5	Application : Robust and Fail-Safe Outdoor Localisation of an Autonomous Vehicle	72
5.1	Chapter Introduction	72
5.2	Technical Aspects	72
5.2.1	Data Acquisition Equipment Details	73
5.2.2	Trajectories details	74
5.2.3	Development And Processing Tools	75
5.3	MCCNIF Versus Classical MMSE-Based NIF Robustness Against Non-Gaussian Noises	77
5.3.1	Tight GNSS/Odometer Intergration Through MCCNIF	77
5.3.2	Impact Of GNSS/Odo Fusion	81
5.3.3	Impact Of MCC Compared To MMSE Criterion on non-Gaussian noises	81
5.4	Results of the Adaptive FTF proposed Framework	82
5.4.1	α -RD Residual Based On Unsupervised Clustering	83
5.4.2	Impact of α -Rényi On The Detection	84
5.4.3	Results using different α Strategy Scenarios	85

5.5	Chapter Conclusion	95
6	Conclusion	96
6.1	General Conclusion & Perspectives	96
6.1.1	Conclusion	96
6.1.2	Perspectives	97

List of Figures

1.1	Progress of automated driving levels	1
1.2	accuracy vs precision	6
2.1	Global Navigation Satellites System	13
2.2	Trilateration and Triangulation	14
2.3	GNSS problems faced	14
2.4	Protection Levels	16
2.5	Stanford Diagram	17
2.6	Stable platform IMU - gimbaled implementation (source (SAVAGE, 2013))	19
2.7	Strapdown platform IMU (source(KIKUTIS et al., 2012))	19
2.8	LiDAR applications	20
2.9	Stereo vision system	21
2.10	Benefits expected when merging different sensors observations	23
2.11	Combination of sensors for a robust localization system - (source :www.outsight.tech)	23
2.12	Loosely coupling architecture	25
2.13	Tightly coupling architecture	25
2.14	Ultra-Tightly/Deeply coupling architecture	26
2.15	Main Idea of the unscented transform	32
2.16	Particle Filter algorithm	34
3.1	Information transmission model	42
3.2	Different scenario probabilities	43
3.3	FDI categories and approaches	48
4.1	The proposed architecture for fault tolerant multi-sensor fusion	52
4.2	Detailed general diagram for the proposed approach	54
4.3	Kernel principal	57
4.4	illustration of the adjusting effect played by alpha in the residual rebalancing the probability distributions	62
4.5	Physical interpretation for α balanced	64
4.6	Diagram to create two probability distributions	64
4.7	Extracting estimated means and variances from real values	65
4.8	UIO architecture design	70
5.1	Septentrio receivers	73

5.2	PwrPak7 - NovAtel receiver	74
5.3	Trajectories references	75
5.4	goGPS interface	76
5.5	GNSS vs GNSS/odo without FDI	81
5.6	MCCNIF vs UIF without FDI	82
5.7	Experimental data PDFs of fixed α for the cases without/with faults	83
5.8	Effect of α -Rényi variation on the residuals	84
5.9	Effect of α variation on the detection	85
5.10	Positioning estimation without FDI algorithm vs reference in 3D/2D views	86
5.11	Elevation of each satellites during the whole trajectory	86
5.12	α -Rényi Residuals without FDI	87
5.13	Partials KLD observation for identification	87
5.14	KLD divergence without/with FDI with adaptive threshold	88
5.15	P0 during the whole trajectory	88
5.16	Partials Rényi observation for identification	89
5.17	Weighted Alpha balance	89
5.18	Estimated and real means & variances for faulty and non-faulty distributions	90
5.19	Rényi divergence without/with FDI with adaptive threshold	91
5.20	P0 during the whole trajectory	91
5.21	index of isolated satellites using fixed α	92
5.22	index of isolated satellites using α balance	92
5.23	The difference in decisions between fixed α and α balance	93
5.24	Final estimation positioning with FDI approach comparison	93
5.25	The effect of the decisions between fixed α and α balance on the position	94

List of Tables

2.1	Chronological table for estimation solution	27
4.1	Problems faced in localization and proposed solutions	53
5.1	Data acquisition information for trajectories	75
5.2	Mean error for GNSS and GNSS/odo without FDI	81
5.3	Median and mean error for MCCNIF and UIF without FDI	82
5.4	Type of errors removed	94

Acronyms

ADAS	Advanced Driver Assistance Systems
AFTF	Adaptive Fault Tolerant Fusion
AL	Alert Limit
ARAIM	Advance Receiver Autonomous Integrity Monitoring
AUC	Area Under Curve
BC	Bhattacharyya Coefficient
Bc	Bhattacharyya criterion
BD	Bhattacharyya Distance or Bhattacharyya Divergence
ChC	Chernoff coefficient
ChD	Chernoff Divergence
CIM	Control and Integrity Monitoring
CPRAIM	Carrier Phase Receiver Autonomous Integrity Monitoring
CUSUM	CUmulative SUM
DI	Deeply Integration
DoF	Degree of Freedom
EKF	Extended Kalman Filter
EM	Expectation Maximization
FD	Fault Detection
FDD	Fault Detection and Diagnosis
FDI	Fault Detection and Isolation
FT	Fault Tolerance
GLONASS	Globalnaya Navigazionnaya Sputnikovaya Sistema, or Global Navigation Satellite System
GNSS	Global Navigation Satellite System
GPS	Global Positioning System
HD	High Definition
HPL	Horizontal Protection Level
ICAO	International Civil Aviation Organization
IF	Information Filter
IMU	Inertial measurement unit
INS	Inertial Navigation System
IR	Integrity Risk
ITS	Intelligent Transportation Systems
KF	Kalman Filter
KLc	Kullback-Leibler criterion
KLD	Kullback-Leibler Divergence
KPI	Key Performance Indicator

LIST OF TABLES

LiDAR or LIDAR	Light Detection And Ranging
LGPR	Localizing Ground Penetrating Radar
MCC	Maximum Correntropy Criterion
MCCNIF	Maximum Correntropy Criterion Nonlinear Information Filter
MGn	Mixture Gaussian noise
MI	Mutual Information
MLE	Maximum Likelihood Estimation
MISE	Mean Integrated Squared Error
MMSE	Minimum Mean Square Error
MSE	Minimum Squared Error
NIF	Nonlinear Information Filter
NIS	Normalized Innovation Squared
NLOS	Non-Line-Of-Sight
odo	Odometer
OLS	Ordinary least square
P_D	Probability of Detection
<i>pdf</i>	probability density function
PE	Position Error
PF	Particle Filter
P_F	Probability of False alarm
PL	Protection Level
P_{md}	Probability of missed detection
PVT	Position, Velocity, and Time
QJSD	Quantum Jensen-Shannon divergence
RAIM	Receiver Autonomous Integrity Monitoring
Rc	Rényi criterion
RD	Rényi Divergence
ROC	Receiver Operating Characteristic
SLAM	Simultaneous Localization And Mapping
SS	Separation Solutions
THR	Tolerable Hazardous Rate
UIF	Unscented Information Filter
UIO	Unknown Input Observers
UKF	Unscented Kalman Filter
UT	Unscented Transformation
VPL	Vertical Protection Level
WLS	Weighted Least Square

Chapter 1

General Introduction

1.1 General Introduction

According to a study by the U.S. Department of Transportation’s National Highway Safety Administration, more than 90 per cent of road crashes are the result of driver error (SINGH, 2015), causing millions of people die from traffic accidents on roads worldwide each year. While other factors often come into play, such as distractions due to weather and/or other vehicles, and physical limitations such as vision and response time. These reasons are creating a great interest in providing safe driving technologies. Starting by helping the human driver through an Advanced Driver Assistance Systems (ADAS). This technology alerts drivers in case of traffic, speed limits, keeping drivers on track with lane-level data, and providing the visibility of road curves and slopes. The evolution is about progressing from detecting the problem to helping to avoid it passing with different level of automation (figure 1.1).

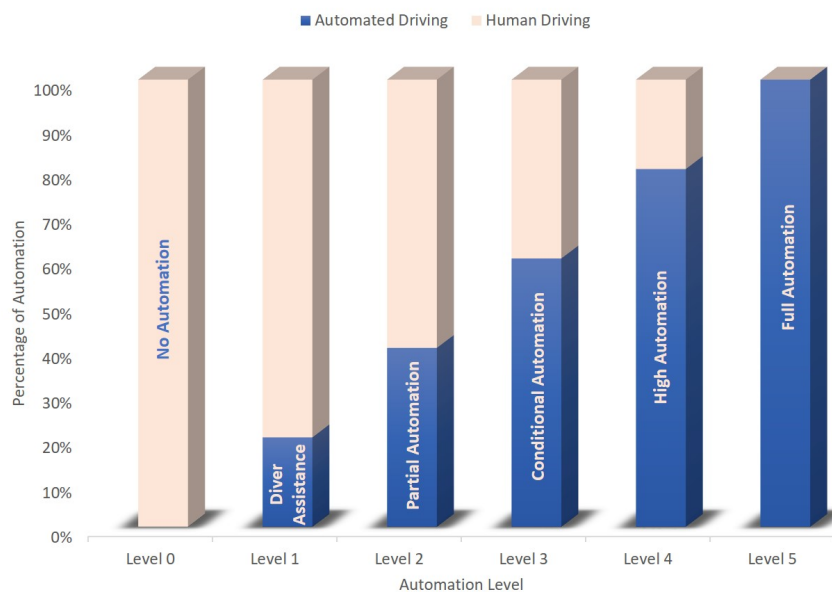


FIGURE 1.1 – Progress of automated driving levels

However, the race toward autonomous driving or self-drive vehicles have been in the development stage for decades, as automakers, like Google, Uber and Tesla at the forefront, have slowly begun to automate cars using sensory technology with a goal to deliver the world's first fully autonomous vehicle. Therefore, one of the goals of autonomous vehicles is to reduce accidents caused by human error, with the ambitious aim of eventually eliminating most accidents on the road. Nevertheless, introducing automated driving poses great potential for reducing crash rates (WOOD et al., 2019).

Although public opinion is still reluctant to adopt this type of vehicles, because of safety concerns, and so far no one is able to give a clear answer to the question "who is at fault when unmanned cars have an accident?", autonomous navigation is, relatively, a recent line of research that investigates methods that allow mobile systems to move around and reach specific and safe targets without any assistance or human intervention. Another important question concerning safety drive was proposed and take attention : "How many miles of driving would it take to demonstrate autonomous vehicle reliability?", and it is answered with details in (KALRA et al., 2016). From a theoretical point of view, autonomous navigation consists in solving three fundamental problems, which are location, trajectory tracking and trajectory planning.

On the other hand, research interest in the field of multi-sensor data fusion is growing due to the diversity of its application areas. More specifically, in the field of localization, the exploitation of the different information provided by the sensors is a crucial step in order to ensure a reliable estimation of the position. Precise and reliable localization has become a necessity in the development of Autonomous vehicles navigating in urban areas or in intervention zones presenting a danger to human life. The localisation techniques used differ according to the application and the sensors used.

1.2 Thesis Positioning

1.2.1 Context Of Work And Motivations

Safe autonomous navigation of vehicles especially for outdoor environments requires on board technologies, including fault-tolerant localization. Indeed, safe and accurate localization and its supervision have become essential criteria for the safe and secure operation of an autonomous vehicle.

Multi-sensor fusion localization is designed to estimate the states (position, heading, and speed) of a land vehicle (or even a set of vehicles). The main idea of the localization procedure is the fusion of relative measurements (proprioceptive sensors : odometry, inertial unit...), absolute measurements (GNSS (Global Navigation Satellite System), vision, telemetry), and information related to the vehicle's evolution environment (2D and/or 3D cartography, aerial images...). This integration can be done in a loosely, tightly or deeply coupled way. Nevertheless, the integrity of the localization is one of the main requirements of the multi-sensor fusion method in the framework of the work planned in this thesis. However, sensors embedded in vehicles can be affected by various

types of faults. In the absence of a diagnostic layer, the accuracy and integrity of the merging procedure are affected by errors and disturbances. To ensure the high integrity of localization with a multi-source fusion method, the addition of a Control and Integrity Monitoring (CIM) layer is one of the solutions considered. In the case of land vehicles, sensor redundancy makes Fault Detection and Isolation (FDI) algorithms more efficient. In the literature, the approaches to sensor FDI are mainly divided into three types of methods : methods based on the use of analytical models (recursive Bayesian filtering, parity relations ...), data-based methods (artificial neural networks, Bayesian networks ...) and methods based on the use of an expert system based on a priori knowledge.

The objective of this thesis is to develop an Adaptive Fault-Tolerant Fusion (AFTF) localization approaches for autonomous vehicles by multi-sensor data fusion : GNSS, proprioceptive sensors, exteroceptive sensors, in tightly coupling with an integrated CIM layer. The AFTF approach is developed through the integration of a diagnostic layer that allows the detection and isolation of faulty sensors. More specifically, we are interested in the development of systems to provide a measure of confidence in the calculated information and to improve the accuracy of the global positioning system. That is why, for the diagnostic part, our developments are oriented towards the use of informational approaches based on the use of filtering techniques and informational metrics more adapted to the design of residuals more reliable and more efficient than an Euclidean or Mahalanobis distance especially when manipulating random and noisy sensor signals. These methodological tools allow us to manipulate and quantify the amount of information brought by a sensor measurement or an observation, using informational metrics such as Mutual Information (MI), Kullback-Leibler divergence (KLD), Rényi divergence ... These informational measures allow to judge the relevance and the quality of the observations and their informational contributions. Besides, the use of informational filters allows the implementation of distributed or decentralized configurations to integrate a diagnostic and sensor management layer.

From a methodological point of view, the objective of the thesis work is to develop a multi-sensor fusion approach based on state estimators/observers with a fault detection layer based on an analytical model coupled with a phase of exploitation and processing of measurements/signals from sensors. The use of an analytical model based detection method allows the implementation of various architectures for the detection, isolation, and identification of sensor faults. The exploitation of data with an approach of type "information-driven techniques" allows, using informational metrics, a selection of relevant data.

From the application point of view, the objective of the thesis work is to test and validate the approach developed to improve and make reliable the autonomous navigation of an autonomous vehicle system at the level of accuracy and safety of operation. Where, the scientific and economic repercussions are expected in the field of the road transport and even railway transport for the implementation of geo-localization solutions.

1.2.2 Localisation Systems For Intelligent Transportation Systems

In this section, and before going deeply with our proposition, a brief state of art of localisation system must be provided in order to show the importance of this proposition in the scale of rapid innovation in the Intelligent Transportation Systems (ITS) domain. The framework by which autonomous driving is implemented should provide the robustness, the availability, the accuracy, the reliability, and of course the safety for the surrounding and the system itself. The most commonly used localization system for autonomous vehicles is the GNSS, as it is cheap and easily accessible. It also provides a first position without prior knowledge. But, GNSS standalone suffers from poor reliability due to limitation in precision which affects the safety-critical ITS (AMINI et al., 2014). Different techniques to enhance the performance of GNSS exist in the literature. In (JAGADEESH et al., 2004) and (BRAKATSOULAS et al., 2005) the map-matching algorithm is applied. One of the limits of this technique is that the performance of a map-matching algorithm depends strongly on the resolution of the digital map. As well, the processing time for the estimation is typically high (AMINI et al., 2014). The performance of map matching algorithms was continuously enhanced, where (EL NAJJAR et al., 2007) proposes a multi-criteria fusion technique based on the merging of GPS and ABS data through extended kalman filter. Sensors fusion is a well known technique (EL FAOUZI et al., 2011), based on combining multiple technologies information (e.g. LiDAR (Light Detection And Ranging), Camera, Radar, IMU (Inertial measurement unit), etc.), to develop robust, accurate, and reliable localization system. A GNSS/IMU sensor fusion approach for vehicle localization is presented in (ZHANG et al., 2012), in order to correct the accumulated errors of dead reckoning in intervals with absolute position readings. Another GNSS/IMU study provides a centimeter level of accuracy under no GNSS signal loss condition (Y. LIU et al., 2018). When the GNSS signal is lost for 3 seconds, the performance decreases obviously to meter level. By replacing the GNSS by the camera, a proposed method using only cameras is proposed in (LI et al., 2013). For better performance, (KAMIJO et al., 2015) uses the camera for lateral positioning based on lane markers recognition with the GNSS/IMU for global positioning. The same concept is applied in (SUHR et al., 2016), but the cameras are used for lateral positioning based on lane markers recognition, and for longitudinal positioning based on road markers recognition. With no landmark assumptions and avoiding data association problem, (VIVET et al., 2013) presents the first approach. Where, the paper presents and compares two SLAM (Simultaneous Localization And Mapping) approaches with a ground K2pi microwave radar sensors based on Frequency Modulation Continuous Wave (FMCW) with 360° of view for outdoor robotic applications. However, the second approach analyses the distortion caused by a rotating range sensor in high speed robotics to obtain the trajectory and map the environment. To decrease the cost of used sensors, (WARD et al., 2016) rely on a low cost pulse-based Short Range Radar (SRR) and was able to achieve a good accuracy in his application. CORNICK

et al., 2016 didn't rely only on GNSS/INS (Inertial Navigation System), but uses a novel Localizing Ground Penetrating Radar (LGPR) for localization of ground vehicle. The approach was able to perform in highway speeds and the LGPR was not affected by the changing weather and lightning surround like other existing radars. Nevertheless, authors clarified that deep study for potential and limitations in different other conditions should be done. In urban environment application, a LiDAR, IMU, and odometry are fused through a Particle Filter (PF) (KIM et al., 2017). Also in LEVINSON et al., 2007, GNSS, IMU, and odometer are integrated and the infrared LiDAR is used to generate high-resolution maps. Then, a SLAM relaxation algorithm based on PF localizes the vehicle in the created map. The two previous approaches offer good performance with an acceptable mean errors, but the drawback of the LiDAR, concerning the power needed, the computational requirements and its implementation costs, is considered high. For a low cost, light-weight sensors, (JUNG et al., 2009) proposes the integration of ultrasonic sensors with a gyroscope, two encoders, and a digital magnetic compass which have been used in a SLAM techniques. Despite the low cost and the low electric power consumption, it has a high computational time process (KUUTTI et al., 2018) and its mechanical waves can be affected by the bad weather.

As we have seen in this brief state of the art, sensors are indispensable elements in ITS, even if they have limitations that reduce system performance. These cited limitations are related to different elements that depend on the type of application and the surrounding environment of the system. That is why, a successful approach must study the key performance indicators (KPIs) that characterize the system, and accordingly, apply the most suitable algorithm in each case. Hence, an adaptive diagnosis approach may be one of the solutions to solve such problem.

Before, introducing the adaptive diagnosis, we must introduce the KPIs of the localization function and answer to three main operational challenges in this field.

1.3 Key Performance Indicators of a Localisation Function

As mentioned in the previous section, sensors measurements are affected by the environment, resulting in a lack of system security. Therefore, a sensor that is highly sensitive to the context in which it operates must be monitored with the appropriate diagnostic that can be adapted to the surrounding environment.

Indeed, when one thinks not only of the vehicle but also of the environment in which it evolves, it becomes obvious that the expected operational needs of the positioning system are also variable over time. Actually, whether the vehicle is driving in the open sky or in an urban canyon, the requirements in terms of expected precision or continuity differ. These operational requirements, through a complex process, impact the measures related to the level of

protection provided with the position estimation, or the probabilities of false alarms and missed detection of observation inconsistencies.

In this section, we define key performance indicators that define a frame in which an adaptive diagnostic layer was developed.

1.3.1 Accuracy and Precision

The terms "accuracy" and "precision" are two critical factors when dealing with data measurements. Their definitions are consistently misused and they are often used interchangeably while there are key differences that distinguish them. In fact, both accuracy and precision describe how close a measurement is to a real value. But, the difference lies in the definition of the real value itself. Where, the accuracy is defined as the correctness of the measurement with respect to a true or accepted value. The precision expresses the quality of being exact. It reflects how a series of measurements are reproducible, meaning that how close they are to each other in case of repeating under same conditions, regardless if any of them is accurate or not. Therefore, it is possible for measurements to be precise but not accurate. As well as, measurements can suffer from both inaccuracy and imprecision. Figure 1.2 can help visualize the difference between the two concepts :

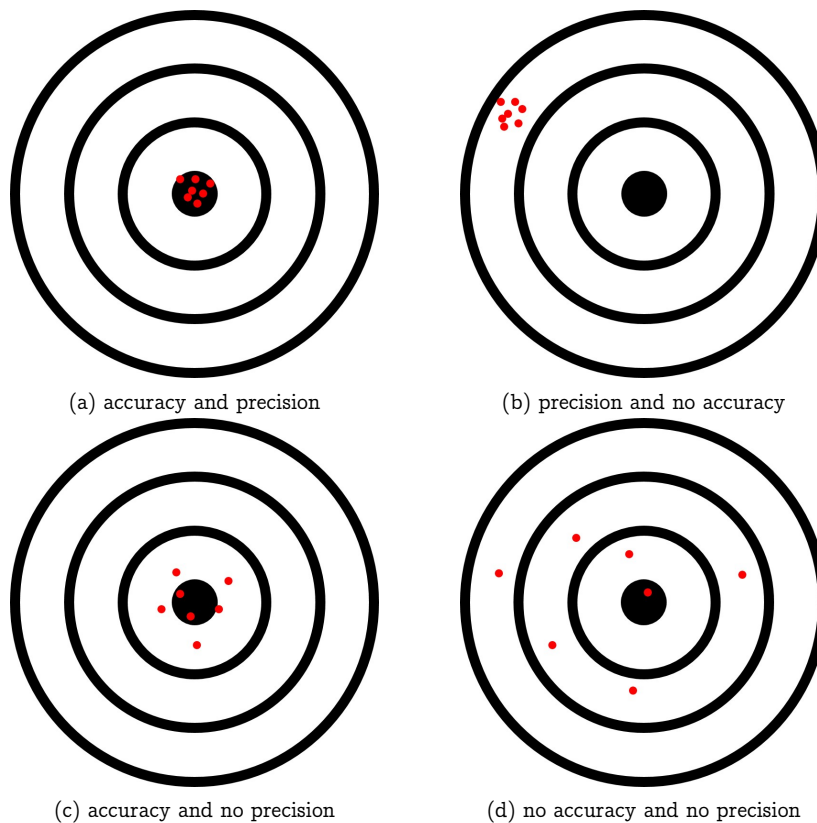


FIGURE 1.2 – accuracy vs precision

1.3.2 Dependability and Availability

In order to provide an accurate and precise position, a trustworthy dependable system must exist and be available at the needed time.

Usually, the two terms "dependability" and "reliability" make confusion when asking for definitions, and that is because of the interconnection between the two terms. The attribute of reliability is a feature of dependability, but the later is a much deeper character trait.

System dependability is the ability to provide trustworthy service and to avoid more frequent and more serious failures than is acceptable. It is a property of a system that justifies reliance on it. Going deeper in the definition of dependability, it is an integrative concept that embraces the following valuable features (KHAN et al., 2012) :

- **Reliability** : is the ability of systems to behave as expected, within a given scope, during a given period of time, regardless of internal or external faults,
- **Availability** : probability that a system will satisfactorily and effectively be capable to perform a function at the start of any random period of time,
- **Safety** : is the absence of any risk that may occur as a result of a decision or action and could harm humans and/or the environment,
- **Confidentiality** : data and other information must not be revealed without intention and authorisation.
- **Survivability** : is the quantified ability of a system to accomplish its mission independently of any disturbance encountered.
- **Integrity** : is the ability of a system to operate correctly according to the original system specification under a variety of conflicting conditions and to notify when faults are detected during its own operation.
- **Maintainability** : the ability to undergo easy modifications, and inexpensive repairs of a functional unit in accordance with the prescribed requirements.

1.3.3 Robustness

Along with dependability, accuracy and availability, robustness is one of the most important KPIs for evaluating the system. Many definitions in many different fields exist for robustness in the literature (CORRADINI et al., 2007, TANAKA et al., 1994, LOZANO et al., 2004). Furthermore, in some places, robustness and the definition of stability are correlated on some points, but as we are interested in the term "robustness", the details of this connection can be found in (JEN, 2005). Therefore, robustness is the ability of a system to respond appropriately to abnormal conditions, to handle errors during operation and to continue to function despite the existence of invalid inputs or challenging environmental conditions. In other words, it is the ability to tolerate disturbances that may affect system functionality.

On the other hand, it would be impractical and undesirable for systems to be robust to everything. Thus, for each system, one must ask "what does the

system need to be robust to?", in order to create a system that is robust to particular types of variation in its inputs, otherwise the drop in robustness may affect other features and lead to an unsafe system.

1.4 Answers to the Three Main Operational Challenges

After the main terms of KPIs are defined, one can see that achieving one KPI may affect the other(s). This link between the KPIs creates many important challenges that face the design of a robust, safe and available system. In this section, we highlight this relation by answering to the main operational challenges for any proposed estimation approach. Starting by a multi-sensor fusion algorithm which ensure the continuity through its robustness. As well for a guaranteed safety by a suitable diagnostic approach, and a high level of availability by monitoring and tolerating the fault along the whole operation.

1.4.1 A Robust Multi-Sensor Integration to Ensure Continuity

In order to be certified, and to be able to integrate an ITS, a localization function must be able to meet several requirements related to the expected final performance. These requirements, although not exhaustive, are mainly based on the usual performance metrics, i.e. the accuracy of the proposed estimate, availability, service continuity, and operational reliability. This last point, also called positioning integrity, can be defined as the capacity to limit the true (unknown!) positioning error at all times by a "protection level" (EL-MOWAFY et al., 2017), (N. ZHU et al., 2018) or, if necessary, to be able to alert the system within a defined time, called (ATT) in order not to use the proposed estimate.

1.4.2 Diagnostic as a Guarantee of Safety

Safety requirements are expressed in terms of Tolerable Hazardous Rate (THR) which represents a maximum limit for iteration of system failures. To achieve the objective, a very conservative diagnostic policy is required. At the slightest suspicion of error, this policy will prefer to render the localization function unavailable. We can see here the negative impact that this type of overly conservative policy can have on the availability and continuity of system. Having an adaptive diagnosis makes it possible to envisage to relax the constraints of operational safety according to the context all ensuring that the THR requested is not exceeded to improve availability.

In other words, a standard diagnostic allows to pursue a single objective (i.e. the probability of false alarm or the probability of missed detection). Where, an adaptive diagnostic adds a degree of freedom allowing, depending on the change of environment and/or KPIs, to reach a higher level of sensitivity to the various faults, and to compromise between these two objectives.

1.4.3 Fault Tolerance as an Availability Booster

As we have seen, a conservative diagnostic can affect the localization function availability. Hence, in order to mitigate this problem and achieve continuous and safe positioning solutions, a fault tolerant layer must monitor the health of the sensor measurements and analyzes the current situation to detect potentially dangerous and sudden situations, in order to provide an estimated appropriate system behavior to ensure a desired level of safety and maximum availability. In the literature, a well known FDI algorithms that supervise and tolerate the fault are based on Separation Solutions (SS) (JOERGER et al., 2014). These architectures are seemingly complex and very demanding in terms of computing resources, but have the advantage of detecting a fault, only if it has an impact on the estimated position.

1.5 Contributions

The main contributions of this thesis are the following :

Design of a coherent framework (Fusion + Diagnostic architecture with an advanced decision making part) :

We propose the design of a coherent framework that includes several consistent approaches from the fusion part to the diagnostic architecture. Where, the choice of a robust filter with an adaptive diagnostic layer, and decision making approach, are presented. The whole proposed method is developed within the framework of information theory, using an informational filter in the multi-sensor fusion step, and an informational metric for system monitoring. Indeed, a study of the feasibility of a real-time approach must be considered.

Design of a robust informational filter for a robust multi-sensor fusion architecture :

The Maximum Correntropy Criterion under the Non-linear Information Filter is relatively a new filter proposed. This filter allows to handle both non-Gaussianity and non-linearity of the system, which offers more robustness for the fusion part. Moreover, the advantage of the information theory in the updated step, based on the sum of the contributions, speeds up the operation process. This filter is therefore well adapted, in the case where the number of observations varies over time, and allows a simplified transition to distributed or decentralized architectures, making it suitable for the development of a fault tolerance approach.

Residuals generation based on the α -Rényi divergence :

The residual proposed in this work is based on the informational gain brought during the transition from the a priori distribution (based on prediction) to the a posteriori distribution (based on the informational contributions of the observations).

The proposed α -Rényi divergence is a generalisation of an infinity number of divergences, thanks to the alpha parameter. This parametric divergence opens the door for a new concept in the diagnostic domain, that we proposed in this thesis, called "the adaptive diagnostic". Through this concept, the residuals are generated from a new point of view, where the residuals change depending on each case, taking into consideration the surrounding environment.

Optimized thresholding based on adaptive criterion using the α -Rényi :

In order to take the optimal decision, risk should be minimized by choosing the best combination of missed detection and false alarm probabilities. To achieve this objective, there must be an appropriate criterion for each residual to obtain an optimal threshold.

In this thesis, we propose a new criterion based on α -Rényi. This criterion makes it possible to set the optimal threshold corresponding to each studied case by maximizing the amount of information provided.

Adaptive Fault Tolerant Fusion approach for a GNSS/odometer tight integration system :

In this thesis, an informational approach for sensor fault tolerant localization is developed. A method of tight coupling between GNSS and odometric measurements using a robust informational filter and an adaptive diagnostic layer based on informational metrics such as the α -Rényi divergence is presented.

1.6 Publications List

International conferences

K. Makkawi, N. Aittmazirte, M. E. El Najjar and N. Moubayed, « Combination of Maximum Correntropy Criterion & α -Rényi Divergence for a Robust and Fail-Safe Multi-Sensor Data Fusion », 2020 IEEE International Conference on Multisensor Fusion and Integration for Intelligent Systems (MFI), Karlsruhe, Germany, virtual conference, September 14–16, 2020.

K. Makkawi, N. Aittmazirte, M. E. El Najjar and N. Moubayed, « Fault Tolerant multi-sensor Data Fusion for vehicle localisation using Maximum Correntropy Unscented Information Filter and α -Rényi Divergence », 2020 IEEE 23rd International Conference on Information Fusion (FUSION), Pretoria, South Africa, virtual conference, July 6–9, 2020.

K. Makkawi, N. Aittmazirte, M. E. El Najjar and N. Moubayed, « Fault tolerant fusion using α -Rényi divergence for autonomous vehicle localization », The 15th European Workshop on Advanced Control and Diagnosis (ACD 2019), Bologna, Italy, November 21-22, 2019.

M. Kaddour, K. Makkawi, N. Aittmazirte, M. E. El Najjar and N. Moubayed, « Prediction optimization method for multi-fault detection enhancement : Application to GNSS positioning », 2018 IEEE International Conference on Vehicular Electronics and Safety (ICVES), Madrid, Spain, September 12–14, 2018.

International Journals

K. Makkawi, N. Aittmazirte, M. E. El Najjar and N. Moubayed, « Adaptive Diagnosis for Fault tolerant Data Fusion based on α -Rényi Divergence strategy for Vehicle Localization », Entropy, Special Issue "Fault Diagnosis Method Based on Information Theoretic : From Theory to Applications", MDPI : Submitted.

N. Harbaoui, K. Makkawi, N. Aittmazirte, and M. E. El Najjar, « Deep learning based adaptive decision making for a fail-safe, accurate and available autonomous context adaptive navigation », International Journal of Intelligent Robotics and Applications, Springer : Submitted.

Chapter 2

Multi-Sensors Localisation Architecture for High Accuracy and Availability

2.1 Chapter Introduction

The objective of this chapter is to present the most commonly used sensors in ITS localisation, explain how they deliver data to estimate the position, show the limitations of each sensor by highlighting the weakness points, and how these limitations affect the safety and/or the availability of the system. Then, we show the effect of combining these information by different coupling architectures through different kind of estimator and different type of criterion.

2.2 Commonly Used Sensors and their Limitations

2.2.1 Global Navigation Satellites System

Since the start of the current century, due to its ability to provide a position anywhere on the Earth without a priori knowledge, its relative accuracy, the good performances and different uses domain, the most extensively used system in outdoor navigation and positioning is the Global Navigation Satellite System (GNSS). GNSS is the generic term enclosing constellations such as the United States' Global Positioning System (GPS), Russian's Global Navigation Satellite System (GLONASS), Chinese's BeiDou Navigation Satellite System (BDS) called also Compass, the European Union's Galileo, and several regional satellite navigation systems (Figure 2.1) (RIZOS, 2013). Some of these systems start as military application to serve only military projects, as the GLONASS and the GPS devolpped by the US Department of Defense (LARSEN, 2001). Due to the fast development in technology, and the need of more and more accurate systems in outdoor navigation application, the GNSS is now an essential sensor used not only in military, but also in aerospace navigation, water

transportation, land applications and even available for personal civilian uses (DAWOUD, 2012). Under good conditions, these systems can deliver accurate positioning all time, where it can suffer out of these conditions.



FIGURE 2.1 – Global Navigation Satellites System

Fundamentals : How it works ?

Satellites broadcast signals holding valuable information for the receivers in order to estimate position, velocity, and time (PVT) of the vehicle, after measuring the transit time of the received signals and computing the distance to each satellite (HURSKAINEN et al., 2009). The transit time is measured as the signal is precisely marked by a very precise synchronous clock on the satellites (MISRA et al., p. d.). This position can be estimated if the constellation ensures that at least four satellites are visible at any point on the Earth (MAKKAWI et al., 2019). In fact, three satellites are enough to calculate longitude, latitude, and altitude (Figure 2.2), where the fourth satellite is used for solving synchronization problem caused by the type of clocks used in the receiver (DAWOUD, 2012).

So after receiving the three satellites signals, the possible location analysed by the first signal from the first satellite, can be any point on the surface of the sphere. The second sphere of the signal from the second satellite overlaps the first sphere and reduces the possible locations of the receiver to a surface between two points. When the third sphere signal is analysed from the third satellite, it overlaps between the surface of the sphere and the circle of the previous satellites. This overlapping reduces the receiver's location possibilities to only one point specifying the exact location of the receiver.

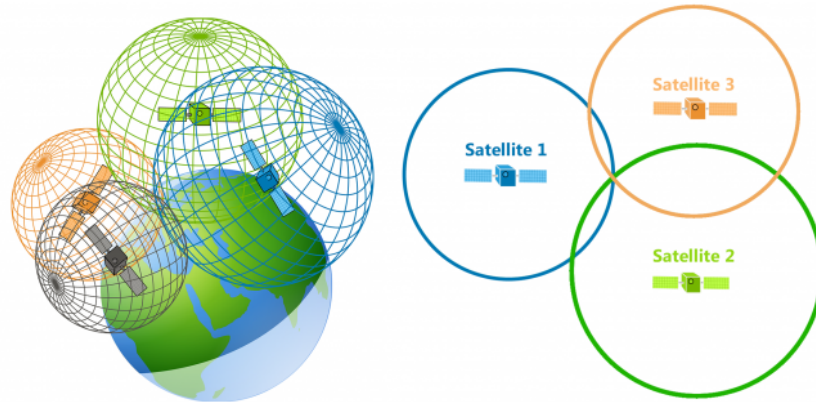
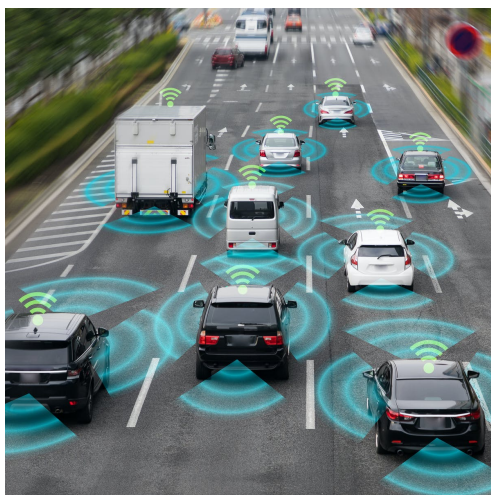


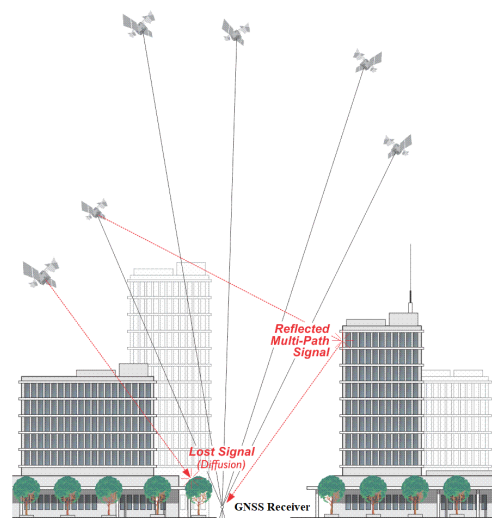
FIGURE 2.2 – Trilateration and Triangulation

Limitations : environment-dependent

Despite all the advantages that GNSS provides, it shows limitations in the performance under different environment and conditions. In case of an open-sky, where many strong satellite signals are present, the task of positioning is relatively easy. However, when navigating in harsher conditions such as urban areas with high building, trees, tunnels... which constitute real problematic environments for GNSS, a GNSS standalone solution shows the weakness of its performances, and is inoperative when dealing with substantial requirements to provide a safe and accurate position estimation. Indeed, in urban environment, many problems from different types, as GNSS gap or high multipath effects, caused by surrounding obstructions (MENG et al., 2018) will appear. These problems are due to GNSS signals reflection, interference, jamming/spoofing and blockage due to buildings, trees...(Figure 2.3) as well as other problems which can cause incorrect integer ambiguity values and an incorrect positioning solution will be provided (HUISMAN et al., 2010).



(a) Spoofing GNSS signals



(b) GNSS multipath

FIGURE 2.3 – GNSS problems faced

With the increase in the number of erroneous measurements caused by different feared local (multipath, NLOS, intentional/non-intentional interference ...) and/or global (atmospheric errors, clocks, ...) events, it will become hard on GNSS alone to deliver useful information to estimate the position (MENSING et al., 2010). In such cases, the receivers are unable to provide the estimated accuracy (RIZOS, 2013).

Receiver Internal Mitigation System : RAIMs algorithms

Incorrect integrity monitoring could lead to devastating consequences for safety-critical applications scenarios. Consequently, an algorithm bounding the mentioned feared events must exist to ensure their detection and avoid their relevant effects on the position.

Receiver Autonomous Integrity Monitoring (RAIM) is based on statistical detection theory (BROWN, 2003) and deals with the position error bounding. It is a technique, classified by the International Civil Aviation Organization (ICAO), used to monitor the integrity of the navigation signals in order to provide a measure of confidence that can be placed in the accuracy of the information provided by the whole system (HEWITSON et al., 2006). A RAIM method is based on the self-consistency check (BROWN, 2003), by comparing each GNSS measurement to the other available measurements. A minimum of five satellites is required to perform the detection of erroneous measurements and evaluate the reliability measure (HEWITSON et al., 2006). When there is a lack of observations and no redundancy, it is said that a RAIM cannot be performed. The best performance of RAIM algorithms is achieved by achieving high detection rates and low false alarm rates. To achieve such level, RAIM has three basic parameters : the statistical hypothesis, the decision threshold and the Protection Level (PL). The statistical hypothesis tests the existence of failure, then the threshold takes the decision based on specified confidence level. The Protection Level (PL) defined by the Convention On International Civil Aviation (ICAO) can provide the necessary bound for the position error. Actually, it is composed of two protection levels, one bounds the error in the horizontal plane, called Horizontal Protection Level (HPL), and the second in the vertical plane called Vertical Protection Level (VPL) (Figure 2.4) (ZABALEGUI et al., 2020). The two PLs bound the Position Error (PE) through a level of confidence based on the integrity risk (IR) requirement. Where, the IR is the probability of the PE to exceed a specified limit known as, the Alert Limit (AL), at any given moment. The detection will be occurred by RAIM after comparing the threshold with the protection level based on the missed detection probability (P_{md}) and false alarm probability (P_{fa}). This threshold is specified by minimizing the P_{md} (ZABALEGUI et al., 2020) taking into consideration that P_{fa} is constant.

RAIM algorithms are used since the nineties decades (YANG et al., 2016) for aircraft navigation applications and still getting improved by researchers till nowadays and known as Advanced RAIM (ARAIM) (NIKIFOROV et al., 2005, BLANCH et al., 2012). In the literature, many methods can

be considered as extension for the classical RAIM, as the Parity method, the Carrier Phase Receiver Autonomous Integrity Monitoring (CPRAIM) and others (KADDOUR, 2016). In plus, FDI methods are used as extensions for RAIM algorithms to enhance the accuracy of the estimated PVT solution (ZABALEGUI et al., 2020), hence to ensure the continuity of the system.

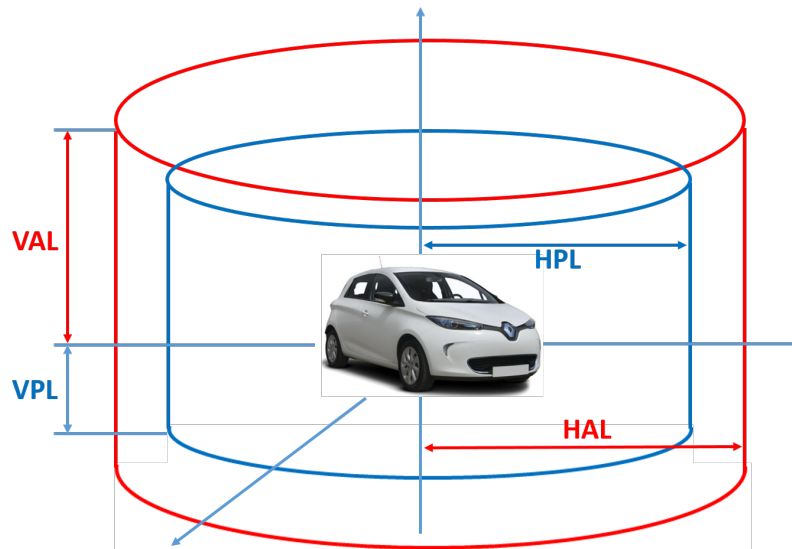


FIGURE 2.4 – Protection Levels

This process uses a minimum of six satellites to not only detect the faulty existence, but to exclude the erroneous satellite from the navigation solution, thus to ensure the availability of the system.

In order to evaluate the provided integrity solution, one can refer to the well known Integrity, Availability, Accuracy 2D diagram called Stanford diagram (or Stanford plot) provided by Stanford university (HANSEN, 2004). This diagram is a representation technique that illustrates the relation of the PE versus the PLs for a set of observations. This representation allows the distinction between the different cases of the system performance, and evaluate this performance through several events (figure 2.5) :

- The system operates normally when the PE is upper-bounded by the PL and the PL does not exceed the AL (white event),
- The moment that PL exceeds the AL, the system is considered unavailable (Yellow and orange events),
- If the PE exceeds the PL and still bounded by the AL, so the system is still available but the event is considered as a Misleading Information (pink event),
- The system becomes hazardous when the AL bounds the PL but the PE over bounds the AL.

For more deep details about RAIM, one can refer to (ZABALEGUI et al., 2020).

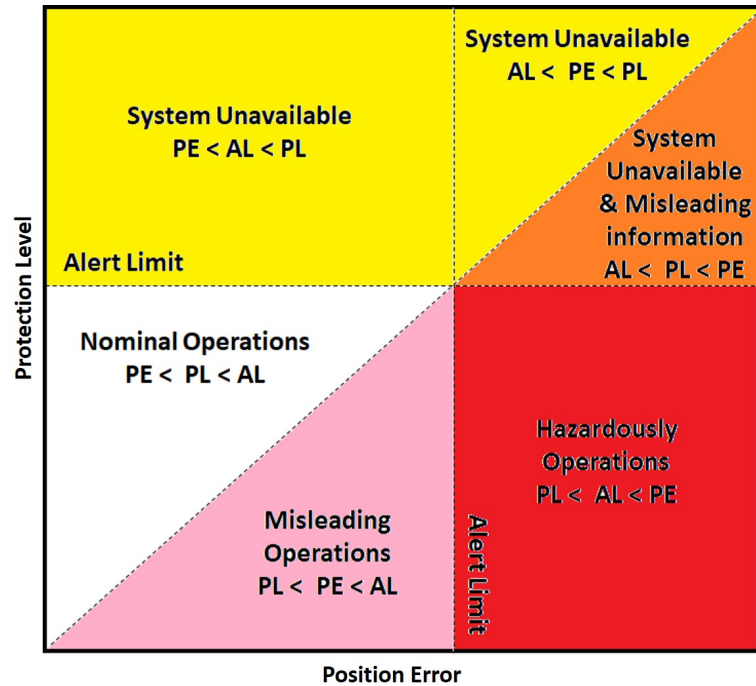


FIGURE 2.5 – Stanford Diagram

2.2.2 Odometry/Wheel Speed Sensors

The word "odometer" is derived from two Greek words "ὀδόμετρον, hodómetron", and "μέτρον, métron" meaning path and measure. It is a relative localization technique that is used for measuring the distance traveled by a vehicle. It is a simple device that can be implemented in real-time applications. An odometer (odo) may be digital or mechanical. In this paragraph we will explain how odometers or wheel speed sensors work and what are their limitations.

How it works ?

Most odometers work by counting wheel rotations and assume that the distance traveled is the number of wheel rotations times the tire circumference. Odometer relies on the measurements provided by the incremental encoders on the wheels to determine the vehicle's position. Based on the elementary displacement and the elementary rotation, the position (x, y) and orientation (θ) of the vehicle are calculated (T. ABBAS et al., 2006). Noting that, the starting position should be known.

Limitations : Susceptible to Sliding Phenomenon

Ensuring accurate odometer is still considered as challenging for researchers. As any existing sensor, odometers have disadvantages that limit their accuracy. These limitations are caused by different sources of errors which can be divided into two categories : systematic errors and non-systematic errors (T. ABBAS et

al., 2006). One of the main disadvantages of this technique is the accumulation of errors over the time. Another problem considered as non-systematic error is the wheel slippage caused by water, oil, and/or even because of the soil rugosity. This kind of error leads to wheel revolution reading despite no linear displacement occurs. For more details about odometer errors, one can refer to (T. ABBAS et al., 2006).

2.2.3 Inertial Measurements Units

Inertial Measurement Unit (IMU), is an electronic device that measures velocity, orientation, and other gravitational forces. It is used in many type of applications such as the navigation of aircraft, vehicles, spacecraft, submarines and ships. Different types of IMU sensors exist in the literature : IMU based on Fiber Optic Gyroscope (FOG) (ZHENG et al., 2009), IMU based on Ring Laser Gyroscope (A. CHEN et al., 2012), and IMU based on the Micro Electro-Mechanical Systems (MEMS) technology (CARDARELLI, 2002). It is a combination of accelerometers, gyroscopes, and sometimes magnetometers. An IMU sensor can have :

1. 6 Degrees of Freedom (6 DoF) - 3 accelerometers for linear acceleration measurement and 3 gyroscopes for angular velocity measurement, that is to say, one per axis for each of the three vehicle axes : roll, pitch, and yaw.
2. 9 DoF - 3 accelerometers, 3 gyroscopes, and depending on the heading requirement 3 magnetometers,
3. 10 DoF - 3 accelerometers, 3 gyroscopes, 3 magnetometers and a barometric pressure sensor that can be used to calculate altitude.

There are two ways to implement the IMU (CHIANG, 2004) : 1) stable platform systems called gimbaled implementation (Figure 2.6), and 2) strapdown implementation (Figure 2.7). The two implementation differ in the frame of reference where the gyroscopes and accelerometers operate.

In the first implementation, the inertial sensors are mounted on a gimbaled platform fixed regardless of any external rotations. These rotations are cancelled by the torque motors based on the gyroscopes information, hence keeping the platform aligned. The accelerometers calculate the position taking into consideration the gravity corrections by subtracting the acceleration from the vertical channel.

In the strapdown implementation, the inertial sensors are directly mounted onto the device creating one frame. Therefore, measurements are taken from the body frame rather than the global frame. As the stable frame, the gyroscopes and the accelerometers measure the rotations and the position respectively. Where, the difference between the two frames is the transformation matrix used in the strapdown platform between the body frame and the navigation frame.

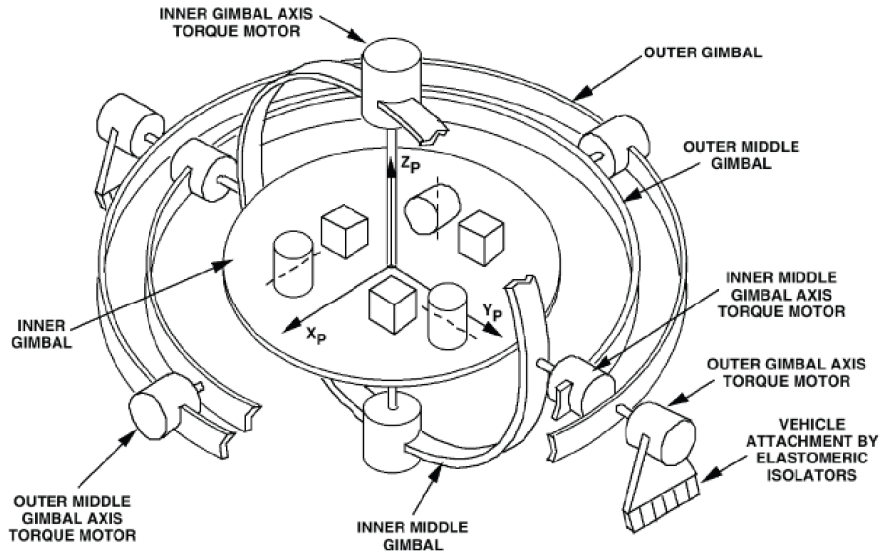


FIGURE 2.6 – Stable platform IMU - gimballed implementation (source (SAVAGE, 2013))

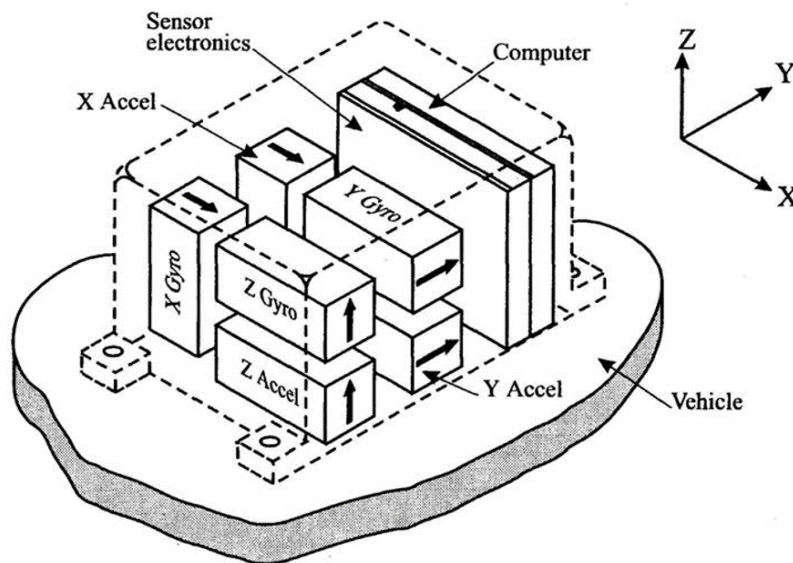


FIGURE 2.7 – Strapdown platform IMU (source(KIKUTIS et al., 2012))

The two implementations prove their performances with high accuracy and high reliability. Despite these advantages, the INS presents relatively low noise, but drift over time. In plus, gimballed implementation suffers from heavy weight and big size which makes it not practical in all applications. It is sensitive to external shocks and vibrations which makes it less immune to the environment. In general, the two platforms are based on the same underlying principles. But, the strapdown IMUs are more practical and become dominant as they have smaller size and less mechanical complexity which is reflected positively on the cost.

2.2.4 Other Possible Sensors

In this section, we introduce some of other possible sensors that can be useful as input data, depending on the application itself and the percentage of integrity needed. The chosen presented sensors are usually used in the localization applications for vehicles, robots, airplanes and other. The advantages and disadvantages of each sensor are discussed as well.

Radars/LiDAR

Light Detection And Ranging (LiDAR or LIDAR), is a remote sensing technology for measuring distances from a laser light source. It is an active sensor (R. WANG, 2013) with a special combination of laser and 3-D scanning. LiDAR is a widely used technique in different domain : terrestrial, airborne, mobile, autonomous vehicles applications (CLAWGES et al., 2008, GUAN et al., 2016, LIM et al., 2019), and many other (SHAN et al., 2018) (Figure 2.8). It can be adapted to detect objects in night mode conditions and can have high resolution with high position accuracy. It collects a georeferenced set of dense point clouds, then by computing the differences in laser return times and wavelengths, a three-dimensional map with detailed shapes is produced (SHAN et al., 2018).

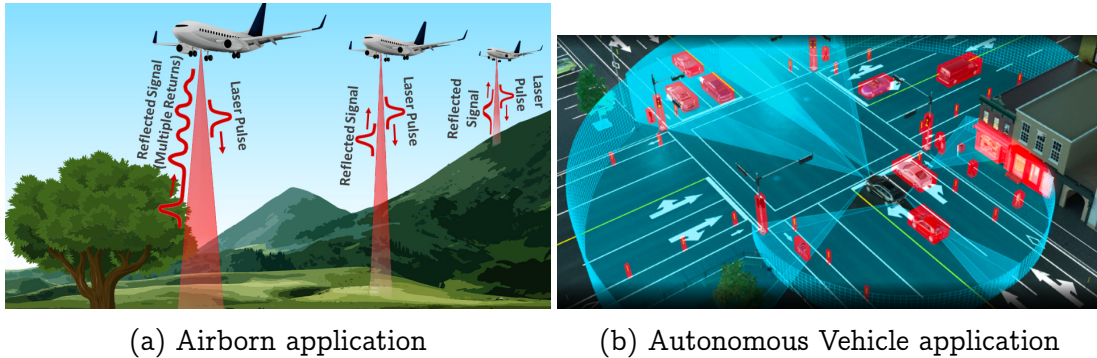


FIGURE 2.8 – LiDAR applications

The time for the round-trip, between the transmitted and received pulses, is calculated using accurate clocks. The basic equation to calculate the measured range between the sensor and the detected object can be written as (SHAN et al., 2018) :

$$R = \frac{c}{n_a} \frac{(t_r - t_s)}{2} \quad (2.1)$$

Where : R is the range in meters, c is the speed of light, n_a is the index of air refraction, t_r is the time when the signal is received, and t_s is the time when the pulse is sent. One of the problem faced by LiDAR, is the scenario of multiple reflected pulses. It can be caused by an edge of building or any other obstacle that reflects a part of the wave and the rest may continue to reach another object or maybe more. In present time, LiDAR technology is

improved to be able to record many returns at each time and some of these LiDARs can record the intensity of the returned pulses which is directly related to the characteristics of the targets. Another important problem related to the safety is still under improvements. Where, the LiDAR works well in good weather conditions but, it faces many perturbations in performance in case of bad weather or/and wet road surfaces which makes it unreliable in such cases (COMBS et al., 2019). In addition, LiDAR is considered as costly devices and suffer from limitations in recognising non-grounded objects at very close range which leads to lack in safety for human beings (LIM et al., 2019).

Mono/Stereo Vision

The current vision detection systems for vehicles are based on mono and stereo vision. This type of systems allows surrounding objects to be recognized by specifying their appearance or type of movement. Most researchers rely on a mono vision system to provide data input for an autonomous vehicle. Mono vision systems estimate distance using one camera, based on reference points in the camera's field of view (ESKANDARIAN, 2012). This is done by projecting the 3D view created onto a 2D image, which makes impossible to derive conclusions on the 3D geometry of the traffic case, and a loss for the depth information. This means that no distance values are directly available for categorized objects. Usually, to calculate the distances, a fusion with other sensor systems is performed, e.g. with a radar sensor or a laser scanner.

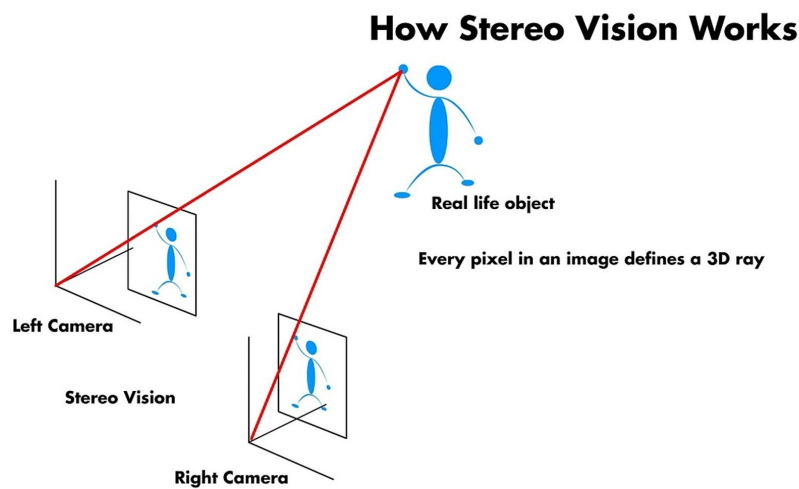


FIGURE 2.9 – Stereo vision system

In comparison, Stereo vision is considered as the only system that can provide an accurate information about the depth. It is a computer vision system based on stereo-tactic banding techniques to calculate the distance by extracting depth information from the same scene, at the same time, in the same manner as human eyes do, using two cameras acting together as one. The two

cameras are both horizontally oriented and vertically displaced in relation to each other. The use of this structure of the system allows to see the same scene from two different perspectives, then calculate the depth, created by the difference between pixels, with high accuracy as well as determine the relation and structure of the objects (Figure 2.9).

Although, mono vision has the advantage of shorter image processing, and the stereo vision provides the depth information, the performance of the both systems is largely influenced by surrounding light and suffer especially at dusk and at night. Moreover, they need a huge set of data to calculate the distances, that includes all type of objects and models, which is probably not possible. Another problem arises in the complexity of the chosen algorithm for objects' classification, specifically at overlapping cases (ZAARANE et al., 2020).

HD maps

As the world moves towards an autonomous future, vehicles need a new generation of highly accurate and realistic sensors. High-Definition (HD) maps are an important technology for autonomous driving, it is considered as critical feature of how vehicle sensors understand their surroundings.

In particular, these maps have high precision at the centimetre level to further improve the integrity of vehicle position estimation, specifically in urban environments. It also provide the vehicle with the necessary information to know exactly where it is on the road within a few centimetre of errors as well as the road conditions miles ahead. The HD card provides the necessary redundancy which permits the driver to take his eyes off the road for a few seconds or more. This redundancy may be crucial in case of sensors' failure, obscured in curves, mud road, fog and large vehicles blocking the vision of sensors, for example. In addition, it allows the vehicle to operate depending on the passengers' needs and other traffic participants.

HD maps are useful technique taking into consideration that the physical environment is not changing. However, this technology leads to significant problems if the HD maps are not up to date. Unfortunately, the current HD maps can not satisfy the needs for real-time applications, especially when facing urban environments with high traffic density. Where, in such cases the requirements to create HD maps are considerable not only in vehicle specifications, but also in infrastructure specifications. In addition, creating the HD maps is very costly and can creates problems concerning the transfer of data, where it is practically not possible to send huge amounts of data over networks in a very short periods of time. This will lead to computational load and transmission latency causing a significant drawbacks in performance. In order to overcome such difficulty, the necessary part of the HD maps can be loaded into the autonomous vehicles or by classifying information that needs to be shared in real time against information that does not need to be shared in real time.

2.3 Sensor Fusion To Combine Them

As shown in the previous sections, the robust localization of the vehicle and its surroundings remain a challenge. Every sensor suffers from one or more problems in different areas and conditions. The GNSS is not accurate enough, and has difficulty in situations such as urban canyons, IMUs are much more accurate than GNSS for short periods of time, until it reaches a high level of drifting. On the other hand, one can't rely on wheel encoders because of wheel slippage, diameter change and other factors (figure 2.10).

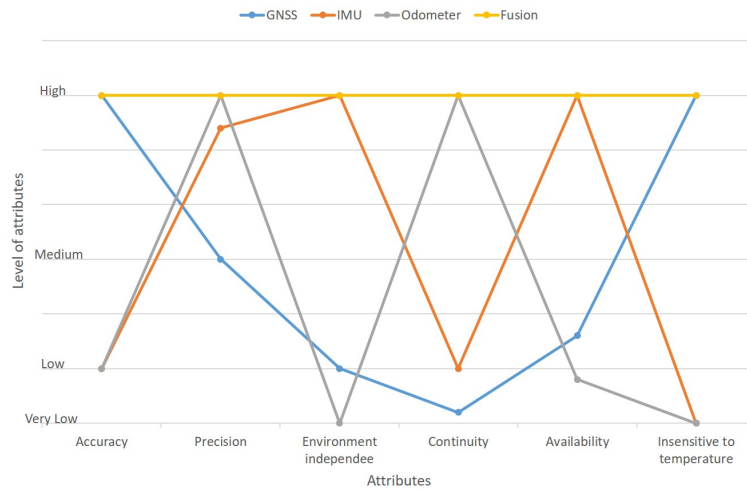


FIGURE 2.10 – Benefits expected when merging different sensors observations

For best results, the combination of these sensors leads to a more robust localization (figure 2.11).

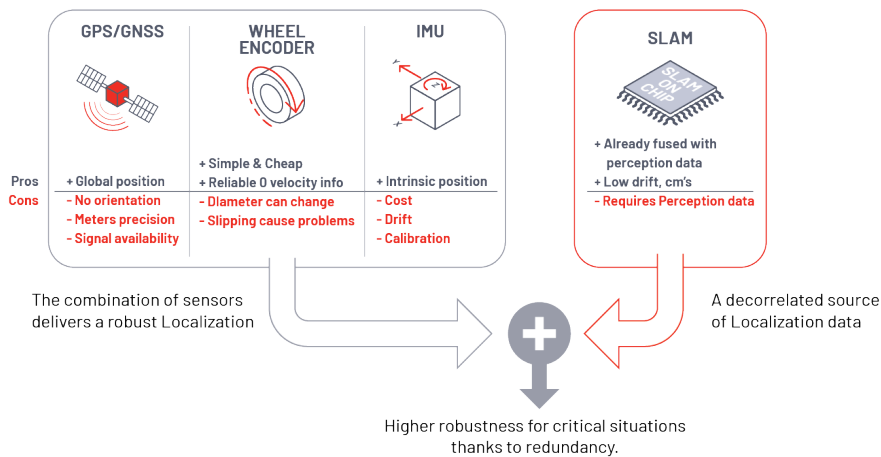


FIGURE 2.11 – Combination of sensors for a robust localization system - (source :www.outsight.tech)

Multi-sensors data fusion is a technology that provides unified, coherent,

and consistent picture, by combining different types of information from multiple sensors. It aims to deliver accurate, robust, and reliable estimation, and to overcome the limitations of standalone sensor (HU et al., 2005). The main advantages of multi-sensor data integration are resumed by (MITCHELL, 2007) :

- More accurate representation of information,
- Greater certainty in the data and results,
- Enhanced confidence and reliability of measurements,
- Enhanced continuity and availability of the localization function,

This leads to a better global view of the environment.

2.3.1 Coupling Architectures

In the literature different levels of integration are proposed (LASHLEY et al., 2010). They mainly differ on their ways of fusion which lead to different depth in integration with their corresponding advantages and disadvantages. There exist three levels with respect to fusion namely loosely coupled, tightly coupled and ultra-tightly coupled system called also deeply coupled.

The fusion algorithm takes into consideration the error characteristics of the sensor, the non-linearity of the position solution, and the user dynamics and it is usually realized through stochastic filters (Kalman filter or particle filter).

Loosely Coupling

This is the simpler coupling of the three levels of integration and is commonly used to equip older inertial systems with GNSS. The integration is normally done in the position domain. The main advantages of the loosely coupled integration are :

- The simplicity of the algorithm of fusion,
- The fused systems are totally separated,
- The components are less constrained to the platform.

These advantages prevent the influence of a fault in one system to affect the others, and reduce the inter-dependencies between components of a system and hence, it is easy to be replaced by other implementations providing the same services.

In the other hand, this type of integration suffers from several drawbacks. For example, the cascading architecture leads to a degradation in performance (LASHLEY et al., 2010). Furthermore, additional protocols for providing integrity are needed in case of systems are decoupled over time. Moreover, maintaining consistency when replicating data between different systems is a problem. Taking the GNSS/IMU loosely integration as example, it simply combines the output of the GNSS receiver with the measurements of the IMU (figure 2.12). Furthermore, the GNSS receiver does not benefit from the IMU with respect to signal tracking, and the GNSS/IMU filter does not collect GNSS data in case of less than four satellites are available.

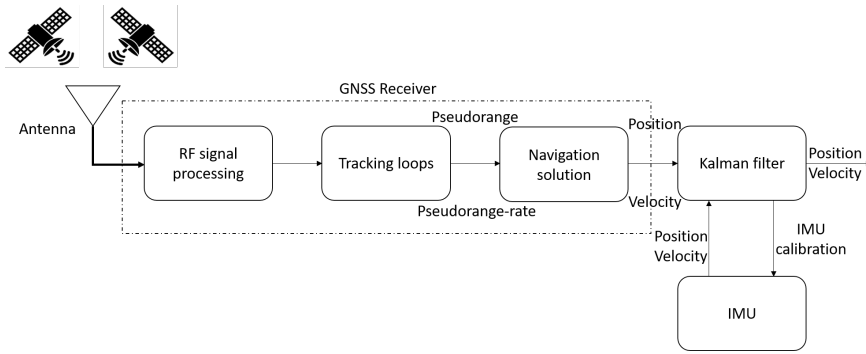


FIGURE 2.12 – Loosely coupling architecture

Tightly Coupling

Tight coupling means that components are dependent on one another. In another meaning, any change in one component requires changes to a number of other components, because of the high dependencies between components of the one system.

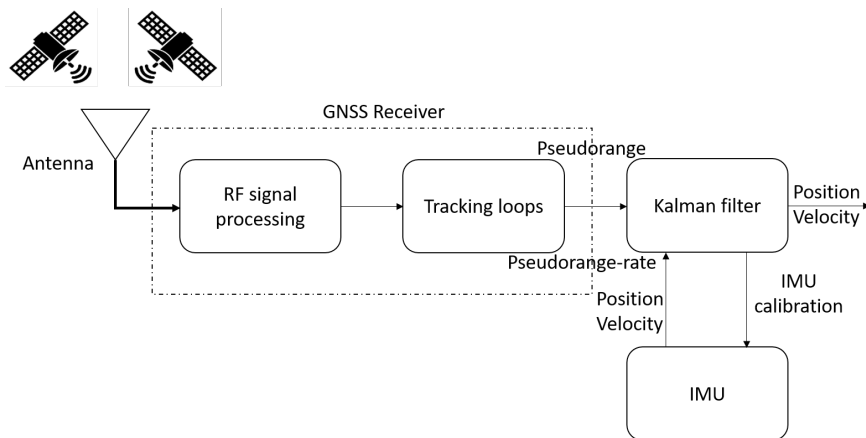


FIGURE 2.13 – Tightly coupling architecture

The main difference between the simplest integration and the tight integration is the measurement type. Where, in case of GNSS/IMU fusion for example, the position and velocity are the measurements in loosely coupled integration, while the tightly coupled integration deals with pseudoranges and doppler shifts. In plus, the fusion is made on pseudorange level and uses a centralized filter (for instance the Kalman filter) that integrates the estimated pseudoranges and Doppler shift from the GNSS receiver and the information of position, velocity and attitude coming from the mechanization equations of the inertial sensors (figure 2.13). In other words, the fusion filter is updated by pseudoranges and pseudorange-rates measurements rather than GNSS based position and velocity estimates, which make the tight integration more suitable in case of lack in number of available satellites (FALCO et al., 2018).

Deeply Coupling or Ultra-Tightly coupling

The first Deeply Integration (DI) proposing was by Abott in 2003 for GNSS/INS fusing approach. Up now, most researchers use this type of integration for GNSS fused with INS as the main sensors, and others add extra sensor to this combination depending on the application and the accuracy required.

The architecture that describes DI varies from one author to another. Whereas, most researchers categorize the DI by the way of filtering as either a centralized or federated filtering architecture. In the centralized architecture, the GNSS signals and inertial data are processed in the integrated filter (Kalman filter for example). Although relatively simple architecture, it has some disadvantages. With less computational burden, the performance of this structure degrades significantly when the filter makes accurate estimates only for the random errors of the IMU. Furthermore, reaching accurate estimation leads to much more sophisticated filter, hence, significant increasing in computation time. Otherwise, the federated architecture can accurately estimate as much as the centralized filter but with less computational time. The main difference between the two architectures is that the federated filter design distributes the tasks to multiple smaller residual filters, called also pre-filters, which improve the performance of the system and make it more suitable for real-time applications.

By comparing the three types of integration, in loosely and tightly integration, the GNSS receiver should obtain stable and strong signals in order to deliver good performance which can be hard to obtain in urban canyon and non-line of sight cases. Where, the DI overcomes in robustness and performance when dealing with high dynamics and high jamming cases under weak signals, but with relatively slow mobilisation. By implementing the replica code and carrier generation directly by the filter, the dynamic stress is reduced by involving the baseband signal processing of GNSS receivers. This is done through integrating the navigation data from the filter with the satellite ephemeris to re-configured the tracking loops (figure 2.14).

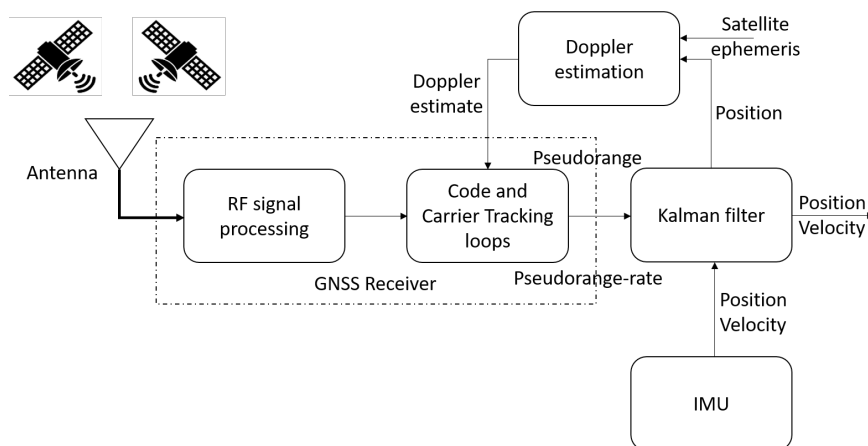


FIGURE 2.14 – Ultra-Tightly/Deeply coupling architecture

2.3.2 Stochastic Filtering

To design robust multi-sensor coupling architecture and to reach safe estimation, the chosen estimator should be selected carefully. The principal objective of the estimation process is to minimize the state error estimation while being robust to uncertainties and perturbations. In this section, we are presenting the principle of well-known filter techniques that help to achieve such needs. In the literature, the Bayesian estimation were first introduced (MR et al., 1763), then, the least square estimation was invented (LEGENDRE, 1805), followed by the Markov chain theory (SENETA, 1996). Few years later, Fisher Information theory was presented (EFRON, 1998). After a gap of time, the research took a quick slope, and the Monte Carlo method was introduced (ROBERT et al., 2011), followed by Wiener Kolmogorov filter (WIENER, 1949), Kalman filter (KALMAN, 1960), Particle filter (DEL MORAL, 1997), and finally the Unscented Kalman filter (JULIER et UHLMANN, 1997). Noting that different extensions of the KF are formulated in case of nonlinear systems, such as, the Extended KF (EKF) that use the first order linearization presented in (KLUGE et al., 2010), and the Second-order EKF using the second order of the Taylor series derived in (MEI et al., 2011). The following table 2.1 presents the main contribution theories invented chronologically.

TABLE 2.1 – Chronological table for estimation solution

Year	Estimation Theory Name
1763	Bayesian Estimation
1805	Least Square Estimation
1906	Markov Chain
1925	Fisher Information Theory
1930	Monte Carlo Mehtod
1949	Wiener Kolmogorov Filter
1960	Kalman Filter
1996	Particle Filter
1997	Unscented Kalman Filter

Ordinary and Weighted Least Square

Ordinary least squares (OLS) is a statistical method of analysis that estimates the relationship between one or more independent variables and a dependent variable in a regression model ; the method aims to solve an equation with no exact solution through estimating the relation by minimizing the sum of the squared residuals difference between the observed and predicted values of the dependent variable.

Consider the following no solution system :

$$AX = Z \quad (2.2)$$

Where A is considered as design matrix with $m \times n$ dimensions and $m > n$, X is a random variable with $n \times 1$ dimension, Z is the observation vector with

$n \times 1$ dimension and, X is the estimator that minimizes the estimation error \hat{e} , which is calculated as vector using :

$$\hat{e} = Z - AX \quad (2.3)$$

and its length is measured through the summation of squared residuals (SSR) :

$$\|e\|^2 = \sum_{i=1}^n (z_i - Ax_i^T)^2 = (Z - AX)^T (Z - AX) \quad (2.4)$$

This quadratic $\|e\|^2$ has a unique global minimum calculated using the gain k as :

$$X = kZ \quad (2.5)$$

Where k is the pseudo-inverse matrix given by :

$$k = (A^T A)^{-1} A^T \quad (2.6)$$

As OLS produces biased and unreliable estimators in stochastic equations in a complete linear system, a generalization of the OLS called the Weighted Least Squares (WLS) is presented. In WLS both the design matrix A and the observation vector Z should be multiplied by the weighting factor w_i (a greater value of W indicates a more trusted data point). Hence, the WLS estimates the position with the inverse of the variance-covariance matrix $R = \frac{1}{W}$ of the observations, called confidence criterion on the observations.

Thus, the solution can be represented using the new weighted gain k_w :

$$X = k_w Z \quad (2.7)$$

Where k_w is solved through the weight matrix W as :

$$k_w = (A^T W A)^{-1} A^T W \quad (2.8)$$

Kalman Filter and Variants

In this section, we introduce the Bayesian filters mostly used in multisensor data fusion. The Kalman filter (KF), named after the Hungarian electrical engineer Rudolf E.Kálmán, and its information form (canonical form) the informational filter are represented with their extensions and generalizations for the nonlinear systems, such as the Extended Kalman Filter and the Non-linear Information Filter (NIF).

Kalman Filter The KF is a recursive estimator that estimates the current state based on the previous step and the current measurement(s). One of the principles of KF is that it assumes errors as Gaussian and can deal perfectly with linear model. Its performance may degrade significantly for nonlinear systems. Consider the following linear system :

$$X_k = F_k X_{k-1} + B_k u_k + w_k \quad (2.9)$$

$$Z_k = H_k X_k + \epsilon_k \quad (2.10)$$

where, X_k is the state vector, F_k is the state transition model, u_k is the input vector, Z_k is the observations vector, $w_k \sim \mathcal{N}(0, Q_k)$ is the model noise considered as white Gaussian noise of zero mean value and covariance matrix Q_k^u , and ϵ_k is the observation noise vector considered as white Gaussian noise of zero mean value and covariance matrix $R_k = E[\epsilon_k \epsilon_k^T]$.

The KF alternates between two main steps called the prediction step (*a priori*) and the correction or update step (*a posteriori*). In the two steps, the information matrix and information vector are calculated. Where, in the prediction step the estimation is calculated using the previous state estimation and the observations are not included at this stage. This estimation is corrected using the observations received at the current step through the correction step. The prediction step equations are written as :

$$X_{k/k-1} = F_k X_{k-1/k-1} + B_k u_k \quad (2.11)$$

$$P_{k/k-1} = F_k P_{k-1/k-1} F_k^T + Q_k^u \quad (2.12)$$

The correction step equations are written as :

$$X_{k/k} = X_{k/k-1} + K_k \tilde{y}_k \quad (2.13)$$

$$P_{k/k} = P_{k/k-1} - K_k S_k K_k^T \quad (2.14)$$

Where \tilde{y}_k is the innovation calculated as :

$$\tilde{y}_k = Z_k - H_k X_{k/k-1} \quad (2.15)$$

K_k is seen as the gain of the KF written as :

$$K_k = P_{k/k-1} H_k^T S_k^{-1} \quad (2.16)$$

And S_k is the innovation matrix calculated as :

$$S_k = H_k P_{k/k-1} H_k^T + R_k \quad (2.17)$$

One of the disadvantages of the KF is the computing time required in the correction step caused by the inversion of a matrix S_k . In addition, the structure of the conventional KF (same for EKF) does not permit to easily isolate an observation when implementing a diagnostic strategy. Indeed it is necessary to recompute the whole matrices.

In order to avoid such problems, the information form of the KF is introduced.

Information Filter As the KF the Information Filter (IF) consists of prediction and correction steps. It uses the Fisher matrix, the inverse form of the information matrix.

The equations that represent the prediction in the information state space are given :

$$Y_{k/k-1} = [P_{k/k-1}]^{-1} = [F_k P_{k-1/k-1} F_k^T + Q_k^u]^{-1} \quad (2.18)$$

$$y_{k/k-1} = Y_{k/k-1} X_{k/k-1} \quad (2.19)$$

Following, the update step equations :

$$Y_{k/k} = Y_{k/k-1} + \sum_{i=1}^N gI_i(k) \quad (2.20)$$

$$y_{k/k} = y_{k/k-1} + \sum_{i=1}^N pI_i(k) \quad (2.21)$$

Where $gI_i(k)$ and $pI_i(k)$ are seen as information contribution (TMAZIRTE et al., 2014) calculated as :

$$gI_i(k) = H_{i,k}^T R_i^{-1}(k) H_{i,k} \quad (2.22)$$

$$pI_i(k) = H_{i,k}^T R_i^{-1}(k) Z_{i,k} \quad (2.23)$$

And N is the number of observations at instant k .

Despite the advantages that bring this type of filter in the correction step and dealing with the faulty measurements by offering the possibility of removing only the information related to the error from the calculation process, it still cannot provide good performance when dealing with non-linearity systems. In the following section, NIF is presented as a solution for non-linearity systems.

Nonlinear Information Filter The information form of the EKF called NIF (TMAZIRTE et al., 2014) is presented. As the EKF, the NIF consists of two main steps called the prediction and correction steps using the covariance matrix as information matrix and the state vector as information vector.

Consider the following non-linear system :

$$X_k = f(X_{k-1}, u_k) + w_k \quad (2.24)$$

where, X_k is the state vector, $f(\cdot)$ is the non-linear function, u_k is the input vector, and $w_k \sim \mathcal{N}(0, Q_k)$ is the model noise considered as white Gaussian noise of zero mean value and covariance matrix Q_k .

The non-linear observation model has the following form :

$$Z_k = h(X_k, \epsilon_k) \quad (2.25)$$

where, Z_k is the observations vector and ϵ_k is the observation noise vector considered as white Gaussian noise of zero mean value and covariance matrix

$$R_k = E[\epsilon_k \epsilon_k^T].$$

The first step of the NIF is called the prediction step and uses the following information matrix and information vector to predict the position :

$$Y_{k/k-1} = [F_k P_{k-1/k-1} F_k^T + B_k Q_k^u B_k^T + Q_k]^{-1} \quad (2.26)$$

$$y_{k/k-1} = Y_{k/k-1} X_{k/k-1} \quad (2.27)$$

taking as :

Q_k^u is the input vector variance-covariance matrix,

F_k is the Jacobian matrix of f : $F_k = \frac{\partial f}{\partial X} |_{X=X_{k-1/k-1}}$,

B_k is the Jacobian matrix calculated as : $B_k = \frac{\partial f}{\partial u} |_{u=u_k}$.

These equations are written in the second step called the correction step as follow :

$$Y_{k/k} = Y_{k/k-1} + \sum_{i=1}^N gI_i(k) \quad (2.28)$$

$$y_{k/k} = y_{k/k-1} + \sum_{i=1}^N pI_i(k) \quad (2.29)$$

Where $gI_i(k)$ and $pI_i(k)$ are seen as information contribution calculated as :

$$gI_i(k) = H_{i,k}^T R_i^{-1}(k) H_{i,k} \quad (2.30)$$

$$pI_i(k) = H_{i,k}^T R_i^{-1}(k) [(Z_{i,k} - \hat{Z}_{i,k}) + H_{i,k} X_{k/k-1}] \quad (2.31)$$

And N is the number of observations at instant k .

Unscented Transformation-based Filter Dealing with high nonlinearity systems can affect the performance of the KF and IF as well as the EKF and NIF (JULIER et UHLMANN, 1997). This degradation in performance is translated by the linearization of the underlying nonlinear model.

The Unscented KF (UKF) and the Unscented IF (UIF) offer a new concept in linearization through deterministic sampling technique called the Unscented Transformation (UT). The UT is a method calculating the statistics of a random variable that has been subject to a nonlinear transformation (BROWN, HWANG et al., 1992). The UT, approximates the probabilistic distributions by using a deterministic choice of sampling points, called sigma points. This method provides estimates of the mean and covariance of the random variable based on discrete samples projected exactly through the associated nonlinear transform (VAN DER MERWE et al., 2004). Each of these sample points are propagated through the nonlinear transformation of the nonlinear function to a corresponding set of sample points (Figure 2.15).

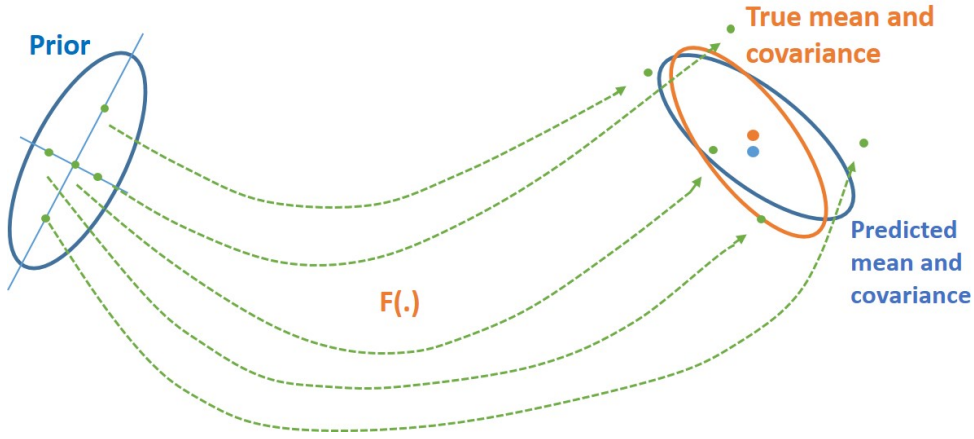


FIGURE 2.15 – Main Idea of the unscented transform

This set of weighted sigma points $\chi_{i,k-1}$ are calculated as :

$$\begin{aligned} \chi_{0,k-1} &= X_{k-1,k-1} \\ \chi_{i,k-1} &= X_{k-1/k-1} + \left(\sqrt{(n+\lambda)P_{k-1,k-1}} \right)_i \\ \chi_{i,k-1} &= X_{k-1/k-1} - \left(\sqrt{(n+\lambda)P_{k-1,k-1}} \right)_i \end{aligned} \quad (2.32)$$

Where $\lambda = \gamma^2(n+k) - n$, describes how far the points are from the mean, $0 \leq \gamma \leq 1$ determines the spread of sigma points, n represents the dimensionality of Gaussian distribution and k describes the influence how far the sigma points are away from the mean.

The corresponding weights for the mean and the covariance can be calculated using :

$$\begin{aligned} W_0^{(m)} &= \lambda / (n + \lambda) \\ W_0^{(c)} &= \lambda / (n + \lambda) + (1 - \gamma^2 + \vartheta) \\ W_i^{(m)} &= W_i^{(c)} = 1 / (2(n + \lambda)) \end{aligned} \quad (2.33)$$

Where $i = 1, \dots, 2n$, and ϑ is the third parameter for incorporating extra higher order effects.

As the UIF is one of the family of the KF, it consists of the two main prediction and correction steps to estimate the new state. In the prediction step the state vector is estimated through the UT using the information matrix :

$$Y_{k/k-1} = [P_{k/k-1}]^{-1} \quad (2.34)$$

Where the predicted state covariance matrix is :

$$P_{k/k-1} = \sum_{i=0}^{2n_a} W_i^{(c)} [\chi_{i,k}^x - X_{k/k-1}] [\chi_{i,k}^x - X_{k/k-1}]^T \quad (2.35)$$

The information vector is obtained through :

$$y_{k/k-1} = Y_{k/k-1} \sum_{i=0}^{2n_a} W_i^{(m)} \chi_{i,k}^x \quad (2.36)$$

The corrected information matrix $Y_{k/k}$ and vector $y_{k/k}$ are respectively represented as :

$$Y_{k/k} = Y_{k/k-1} + \sum_{i=1}^N gI_i(k) \quad (2.37)$$

$$y_{k/k} = y_{k/k-1} + \sum_{i=1}^N pI_i(k) \quad (2.38)$$

Where :

$$gI_i(k) = H_{i,k}^T R_i^{-1}(k) H_{i,k} \quad (2.39)$$

$$pI_i(k) = H_{i,k}^T R_i^{-1}(k) [(Z_{i,k} - \hat{Z}_{i,k}) + H_{i,k} X_{k/k-1}] \quad (2.40)$$

Particle Filters

Unlike the Kalman filters, where the state of the system is represented using only single Gaussian, this hypothesis is no longer necessary dealing with the Particle Filters (PF). This type of filters is based on sequential Monte Carlo approach (HOWARD, 2006), and a solution to solve non-Gaussian noises by using a set of weighted particles (samples), to reproduce the *a posteriori* distribution of a given stochastic process based on noisy and/or partial observations. PF techniques offer a methodology for generating particles from the required distribution without previous knowledge about the state model or state distributions. PF can keep track of as many hypotheses as there are particles, thus, if new information emerges that leads to a complete change towards the best hypothesis, it is easy to do so.

Firstly, the new state is predicted by the filter using the state transition, then it is corrected in a statistical manner, where the noise information is integrated into the correction stage (figure 2.16). At each stage a set of weighted particles are generated to represent the sampling probability of the sample from the probability density function (*pdf*). The weighted particles produce a discrete approximation to the *a posteriori* distribution of the state history. The bad particles are then eliminated through the re-sampling process, and the good particles are multiplied and propagated through time according to the dynamics of the states. Finally, the weights are corrected taking into account the information from each measurement.

In summary, the superiority of PF algorithm can be noticed in nonlinear and non-Gaussian systems. However, these type of algorithms do not perform well when applied to very high dimensional systems and some disadvantages can be noticed :

- The performance is directly related to the number of particles, where the higher number of particles is, the better estimation will be, but it is more costly.
- Its particles degeneracy and sample impoverishment are disadvantages that can restrain its performance (TONG et al., 2006).
- Disparity of weights leads to weight collapse, particle depletion (one particle with a way higher likelihood than any of the other particles),

and areas in *a posteriori* with high probability not represented well. However, it can be attenuated by including a re-sampling step before the weights become very uneven which lead to very computational time makes it unsuitable in real-time for some applications.

- In terms of parameter estimation, fixed parameters are generally considered to be part of the extended state vector, but since the parameters are static, particles will rapidly degrade into sample.

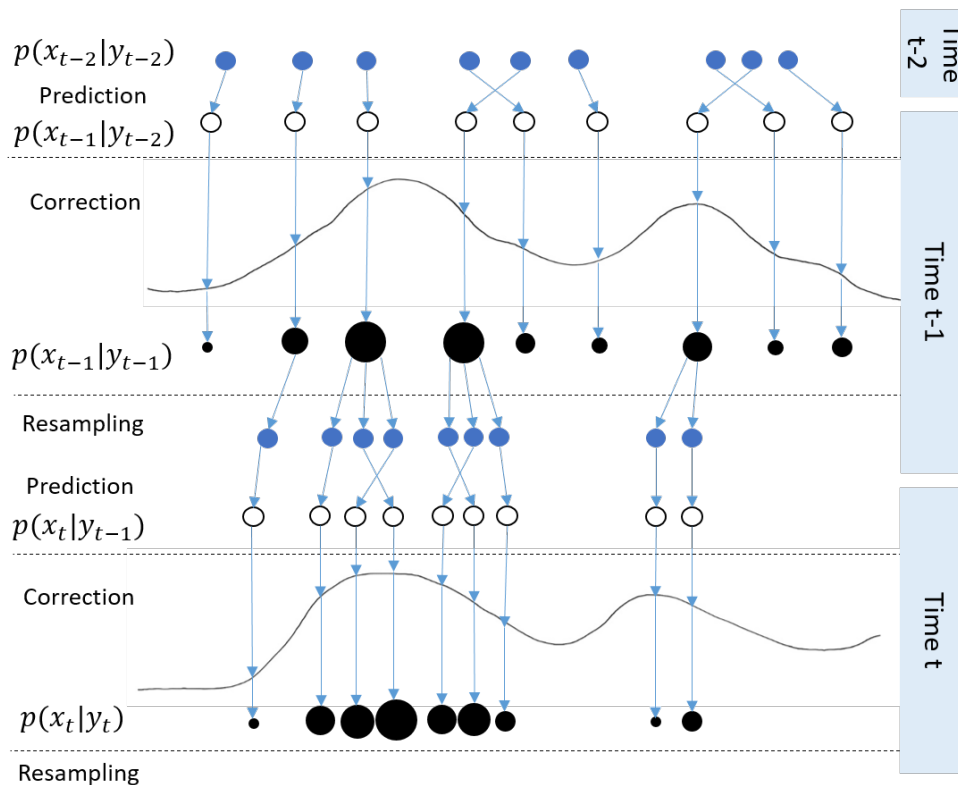


FIGURE 2.16 – Particle Filter algorithm

2.4 Chapter Conclusion

In this chapter, we introduced the used sensors with their advantages and disadvantages for localization purpose. Then, the idea and benefits of combining their observations is explained and the different possible architectures were presented. To achieve such combination or fusion sensors, some popular stochastic filters were discussed, among them the well-known Kalman Filter and its canonical version the NIF. In chapter 4, we introduce a more robust criterion for a much more robust filter.

Chapter 3

Adaptive Fault-Tolerant Fusion Framework to Ensure Fail-Safe and Available Localisation System

3.1 Chapter Introduction

Safety, integrity, dependability, availability, accuracy, and precision, valuable terms becoming essential demands in every safety-relevant navigation system. These requirements should be provided in high quality, hence, there must be a way to monitor the system and take appropriate decision in case of faults' existence.

The diagnostic layer is a procedure of testing, designed to provide information on the general condition of the system and/or reveal localization of potential problems. The main objective of diagnostic technologies is to ensure the correctness of the provided service during the operation of a system. In safety-relevant application, diagnostic is associated to a supervision system enabling the quality of decisions to be checked and its status to be evaluated, where any suspicious decision should trigger an alarm. Therefore, problems and faults due to feared events can be detected and corrected while the system is still available and safe. This avoids future failures in the system as well as costs resulting from repairs.

In navigation systems, detecting the fault is not enough to ensure the availability, hence, the fault must be monitored, and evaluated in order to isolate or identify the error.

3.2 A Brief State Of Art Of Diagnostic In State Estimation

Fault tolerance is a feature that allows the system to continuously operate safely in the case of failure of some of its components. Advanced methods of diagnostic, fault tolerance and fault management called Fault Detection and Isolation (FDI) (ISERMANN, 2006), are valuable tools for satisfying such needs.

FDI methods can be classified into model based methods and model free methods (called data based) (GERTLER, 1998). The process of FDI consists of the generation of residuals, their interpretation and a decision making policy. Through FDI techniques, the system aims at achieving a given objective not only in normal conditions, but also in given faulty situations.

In the literature, FDI methods are widely used, and proved their efficiency in many different domains (Z. CHEN et al., 2019, GENG et al., 2017, ESCOBAR et al., 2011).

In navigation localisation applications, needs are growing more and more and should be ensured. The particle Filter with a multi-sensor fusion approach, are proposed in (CANEDO-RODRIGUEZ et al., 2016), and show good results. However, the use of cameras with other sensors for increasing the accuracy will lead to high cost in localisation system. A Fault Detection (FD) algorithm, based on the EKF to track the outputs from the localization methods followed by the CUMulative SUM (CUSUM) to test the filter's residual, is proposed in (SUNDEVALL et al., 2006) to identify any unexpected large deviation. Authors in (MORALES et al., 2008) propose an FD method for a woodland vehicle localization. A data fusion is occurred using GPS, encoders, and IMU under EKF estimator after a Normalized Innovation Squared (NIS) tests to deal with GPS measurements.

In the rest of this chapter, we will introduce and explain the new concept we propose for the diagnosis, and show how it will affect the way of understanding things from a new perspective.

3.3 Towards the New Concept of Adaptive Diagnostic for Safety

3.3.1 The Philosophy Behind Adaptive Diagnostic

Outdoor navigation, and by consequence outdoor localization is a field of research that does not stop, insofar as the problems encountered have never been so topical. For many years, the addition of sensors and new technologies made it possible to meet industrial demands for concepts whose cost could be high. But nowadays, in order to be commercialized, technologies must reach a cost allowing a mass deployment. Localization is one of those technologies that aims to achieve this goal. The sensors considered, such as GNSS, IMU and odometers, must therefore be inexpensive sensors. All the added value being moved into the algorithms developed for integration, diagnostics and integrity monitoring. These algorithms are more and more advanced, but must be certifiable for applications requiring the agreement of regulatory authorities before being placed on the market. For localization, the evolution of algorithms tends to take into account what is called context-adaptive navigation. In this subsection we detail the impact of taking into account contextual navigation on the diagnostic layer and develop a framework based on α -Rényi divergence, parameterizing the synthesis of residuals.

Change In Environment Conditions

The main difficulty, when it comes to ensuring the safety of a localization block in a safety-relevant application integrating GNSS data, is the impossibility of considering this technology as a sensor with a single operating point. It is unthinkable to consider a single value for the system failure rate. This rate is highly variable, depending on the number of visible satellites, their geometric arrangement, the local reception conditions (obstacles, interference), and other parameters that would take too long to list. It is therefore a sensor that is very sensitive to the context in which it operates. Adopting a diagnostic layer that would consider constant statistics of the presence of faults would not be rigorous.

Normally, localisation systems assume that the surrounding environment is static, without taking into consideration the dynamics inherited from most real-world situations. Corresponding scenarios include buildings, trees and bridges, where the location of certain objects such as vehicles, obstacles or pedestrians change through time. Not only the change of objects, but also the change in atmosphere as temperature, humidity (SALMANPOUR et al., 2017), and wind or/and the change in the surrounding geographic area as valleys or mountain slopes, in the same mission lead to unexpected measurements. Thus, it decreases the accuracy (TIPALDI et al., 2013) of the location measure, due to reflections which generate multi-path signals arriving with a variable time delay to the receiver, or even prevent the localization of the vehicle caused by blocking completely the signals.

In order to avoid such problematic issues, the adaptive diagnostic is able to evaluate each case by case, then take the suitable decision based on the available information. In cases where the reception of the measurements is optimal, the diagnostic layer must be able to give a high level of confidence to the measurements in the residual, which will allow the detection of faults related to the models. In the opposite case where the reception of the measurements cannot be done in good conditions, the residual will be able to take advantage of the model.

Change in KPI Requirements

Other elements lead to think about the development of an adaptive diagnostic layer. Among them, an element which requires a macroscopic view of the system. Indeed, when one does not think only of the vehicle but of the environment in which it operates, it becomes obvious that the operational requirements expected from the positioning system are also variable over time. In fact, whether the vehicle is traveling in the countryside or whether it is traveling in an urban canyon, the requirements on the expected accuracy or on the continuity are not the same. These operational requirements, through a process explained later, impact metrics related to the Protection Level or even the probabilities of false alarms and miss-detections of observations inconsistencies.

Trade-Off Policy between Availability and Safety Requirements

A trade-off is a situational judgement resulting in the reduction or loss of a quality, quantity or property of a set or design in exchange for gains in other features. Simply defined, a trade-off is a situation in which one thing increases and another should decrease.

Requirements related to safety and those related to availability are typically the type of conflicting requirement that leads to this type of situation where a compromise must be found. Obviously, the term compromise may seem inadequate, and should not be added to the term safety. Generally, the requirements related to safety are expressed in terms of Tolerable Hazardous Rate which represent a limit of failure rate to be reached per maximum hour. In order to be achieved, they require a very conservative diagnostic policy, which at the slightest suspicion of error will prefer to make the observation unavailable. We can see here the negative impact that this type of overly conservative policy can have on the availability and continuity of service. Having an adaptive diagnostic makes it possible to consider relaxing the constraints on safety while ensuring that the requested THR is not exceeded in order to improve availability. In other words, a standard diagnosis allows only one objective to be reached (depending on whether the Probability of False Alarm or the Probability of missed detection is taken into account) where an adaptive diagnosis adds a degree of freedom allowing according to the change of environment and/or KPI to achieve a compromise between these two objectives.

3.3.2 How to Design an Adaptive Diagnostic Layer

The analysis in the past sections shows the need for an diagnostic method to cope with the changing in the environment and the KPI requirements. In this section, we will explain how the proposed diagnostic method can be adaptive and what are the tools and/or metrics needed.

The whole proposed approach is composed of three main elements : the informational filter, the diagnostic layer, and the exclusion step. After the informational filter is chosen (NIF, MCCNIF ...) to estimate the state of the system, the diagnostic layer based on FDI uses what called residuals to test and evaluate this estimation. The residuals are designed through a bank of the chosen Informational Filter using the α -RD as test between the predicted and the corrected distributions of the chosen estimator. These residuals can be created by different existing metrics. Starting by the euclidean metric called also euclidean distance (AY et al., 2015), which is considered the simplest way to compare the two distributions using the distance between their means. But taking only the mean as comparison factor leads to a big lose in information related to the characteristics of the distributions, such the volume, the form and the orientation. Claude Elwood Shannon proposes in 1948 (SHANNON, 1948) a new concept dealing with information, called Shannon's entropy. This information theory allows to generate residuals taking into consideration the means as well as the uncertainty as an important factor. Recently, in order to reach higher integrity and accuracy through FDI methods, researchers resorted to

involve information metrics as support for the design in the residuals in FDI methods. The MI in (H.-M. CHEN et al., 2003) and (TMAZIRTE et al., 2014), is used as similarity measure for the residual created and shows higher accuracy and better results comparing with other methods. In (MONDAL et al., 2008), a robust unknown input observer for a class of nonlinear systems is designed for an FDI methods through the Bhattacharyya Distance (BD). The Quantum Jensen-Shannon divergence (QJSD) is used in pattern recognition (BAI et al., 2015), chemical physics (ANTOLIN et al., 2009), and other applications (RADHAKRISHNAN et al., 2016),(DE DOMENICO et al., 2015). As well, the Kullback-Leibler Divergence proved its efficiency in different domains, in FTF approach with FDI method for multi-robots localization in (AL HAGE et al., 2017). A general survey for the various informational divergences and measures used in the literature can be found in (BASSEVILLE, 2013).

In the work cited above, in order to design residuals, the hypothesis, through the chosen information metric, is that the evolution model is always considered as a reference with respect to the observation model, despite the relevance of the cases where the observations are very reliable. Besides, in cases where the uncertainty may be high on both models, this assumption may lead to problems of missed detection in cases of possible faulty cases.

In this thesis, we propose a new way to generate these residuals by weighting with a suitable way the two covariance matrices of the models using α as a weight in the α -RD. Through the variation of $\alpha \in [0, \infty]$, the α -RD generalizes a large number of possible informational measures. Corresponding residuals are then created based on proposed models for the fault-free cases and the faulty cases. After residual creation, an adaptive thresholding method based on α -Rényi criterion (α -Rc) is proposed in order to make decisions. In case of error detection, an isolation algorithm based on UIO is used to remove the error from the correction step of the chosen estimator.

In summary, to design an adaptive diagnostic layer, residuals must be compatible with system information as long as the system is activated, regardless of environmental conditions. The proposed α -RD can provide this coherence through its parameter α .

Before introducing α -RD and present the advantages, well known divergences as the Kullback-Leibler, Bhattacharyya and others will be briefly presented.

Flash Back : Kullback-Leibler and Bhattacharyya Divergences as Residuals

1. Kullback-Leibler Divergence

Note that this section is inspired from (AL HAGE, 2016).After two years of presenting the Shanon's entropy, Solmon Kullback and Richard Leibler invent the KLD at 1951 as the directed divergence between two probability distributions P and Q (KULLBACK et LEIBLER, 1951). Then, the divergence is discussed in Kullback's book at 1959 (KULLBACK, 1959).

Consider two probability distributions P and Q . Normally, P represents data, observations, or a computed probability distribution and Q distribution nor-

mally represents a theory, model, description, or approximation of P . So the KLD can be seen as the informational surprise provided by the observations :

For continuous case :

$$KLD(P||Q) = \int_x p(x) \log \left(\frac{p(x)}{q(x)} \right) \quad (3.1)$$

For discrete case :

$$KLD(P||Q) = \sum_x p(x) \log \left(\frac{p(x)}{q(x)} \right) \quad (3.2)$$

It is also defined as the expectation of a log likelihood ratio which plays an essential role in detection theory, and in realizing the detectability of change (TARTAKOVSKY et al., 2014), where it can be written as :

$$KLD(P||Q) = E_p \left(\frac{p(x)}{q(x)} \right) \quad (3.3)$$

In case of P and Q are two Gaussian distributions with means μ_p and μ_q and covariance matrices Σ_p and Σ_q respectively, the KLD is written as :

$$KLD(P||Q) = \frac{1}{2} \left[\text{trace}(\Sigma_q^{-1}\Sigma_p) + \log \left| \frac{\Sigma_q}{\Sigma_p} \right| - M + (\mu_p - \mu_q)^T \Sigma_q^{-1} (\mu_p - \mu_q) \right] \quad (3.4)$$

Where M is the dimension of distributions.

Based on the equation 3.4, the KLD can be interpreted as the sum of two tests : 1) the test of averages represented by $(\mu_p - \mu_q)^T \Sigma_q^{-1} (\mu_p - \mu_q)$. And this test assimilated to the Mahalanobis distance. 2) the test on the covariance matrices illustrated by $\text{trace}(\Sigma_q^{-1}\Sigma_p) + \log \left| \frac{\Sigma_q}{\Sigma_p} \right| - M$, and this test has the form of the Bregman divergence and includes the mutual information between two Gaussian distributions represented by $\log \left| \frac{\Sigma_q}{\Sigma_p} \right|$.

2. Bhattacharyya Distance

Like the KLD, the Bhattacharyya Divergence also called the Bhattacharyya distance is a metric that measures the similarity between two discrete or continuous distributions. The BD between two probability distributions P and Q is written as (BHATTACHARYA, KAR et al., 2009) :

$$BD(P||Q) = -\log BC(P||Q) \quad (3.5)$$

Where \log represents the natural logarithm, and BC is the Bhattacharyya coefficient described as :

$$BC(P||Q) = \int \sqrt{p(x)} \cdot \sqrt{q(x)} dx \quad \text{continuous case} \quad (3.6)$$

$$BC(P||Q) = \sum \sqrt{p(x)} \cdot \sqrt{q(x)} dx \quad \text{discreet case} \quad (3.7)$$

The BC itself is related to the squarred Hellinger distance through the following relation :

$$\begin{aligned} Hell^2(P||Q) &= \frac{1}{2} \int \left(\sqrt{p(x)} - \sqrt{q(x)} \right)^2 dx \\ &= \frac{1}{2} \left[\int p(x) dx + \int q(x) dx - 2 \int \sqrt{p(x)} \cdot \sqrt{q(x)} dx \right] \\ &= 1 - BC(P||Q) \end{aligned} \quad (3.8)$$

The BD is also related to different other divergences as Chernoff and Rényi, where for more details about Bhattacharyya one can refers to (BOUSSAD, 2019).

One of the important advantages of BD is that there is no need to specify a reference distribution, which is not the case for the KLD.

3. Chernoff Divergence

The Chernoff divergence known as Chernoff Information and Chernoff α -divergence was first introduced by Chernoff in 1952. It is well known in information theory for upper bounding the error probability of the Bayesian decision rule. In the literature, it is used as a concept of symmetric distance in different domains and applications, such as sensor networks (JULIER, 2006), face recognition (ZHOU et al., 2005), and many others (NIELSEN, 2013, NIELSEN, 2011). The Chernoff information between two *pdfs* P and Q is calculated through :

$$ChD(P||Q) = -\log \min_{\alpha \in (0,1)} \int p^\alpha(x) q^{1-\alpha}(x) dv(x) \quad (3.9)$$

Where p and q are the Radon-Nikodym densities for P and Q with respect to v , which is known as dominating measure (NIELSEN, 2013).

When the P and Q distributions belong to the same exponential family, equation 3.9 can be written as follow :

$$ChD(P||Q) = -\log ChC(P||Q) \quad (3.10)$$

Where ChC is called the Chernoff coefficient and written as :

$$ChC(P||Q) = \int p^\alpha(x) q^{1-\alpha}(x) dx \quad (3.11)$$

Chernoff information is defined as the maximal ChD by minimizing the ChC in the Bayes error upper bound, with $0 < ChC(P||Q) \leq 1$.

For multivariate Gaussian distributions, the Chernoff divergence between P and Q with means μ_p and μ_q , and covariance matrices Σ_p and Σ_q respectively can be seen if $\alpha > 0$ as (ZHOU et al., 2005) :

$$ChD(P||Q) = \frac{1}{2} \log \frac{|\alpha \Sigma_p + (1 - \alpha) \Sigma_q|}{|\Sigma_p|^\alpha |\Sigma_q|^{1-\alpha}} + \frac{\alpha(1 - \alpha)}{2} (\mu_p - \mu_q)^T (\alpha \Sigma_p + (1 - \alpha) \Sigma_q)^{-1} (\mu_p - \mu_q) \quad (3.12)$$

One of the advantages that brings the Chernoff concept is that the Chernoff distance generalizes many other distances, such as the Bhattacharyya distance which is achieved through $\alpha = \frac{1}{2}$, and the Bregman distance with few conditions cited in (NIELSEN, 2013). However, the Chernoff bound is considered difficult to calculate or even approximate in practice (NIELSEN, 2011).

3.3.3 Threshold Optimization

After defining the residual, it must be evaluated in order to make the optimal decision for each case and assure the extraction of the faulty measurements in case of existence. To do so, two hypotheses should be defined to represent the faulty and non-faulty cases. By supposing that H_0 and H_1 represent the hypothesis of non-faulty and faulty cases respectively (AL HAGE et al., 2017), Figure 3.1 illustrates the probability of each possible decision that can be made. Where, u_0 is the decision of choosing H_0 and u_1 is the decision of choosing H_1 .

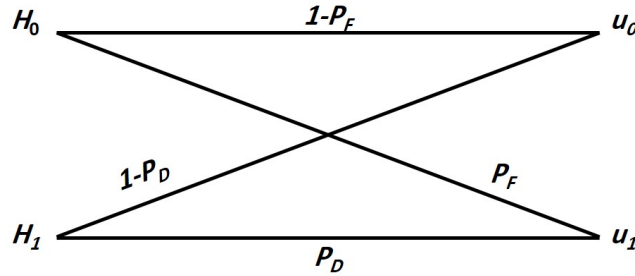


FIGURE 3.1 – Information transmission model

based on figure 3.1 and 3.2, we can define the following probabilities :

- P_D : the probability of detection is the decision of choosing H_1 where H_1 is true :

$$P_D = p(u_1/H_1) = \int_{th}^{\infty} p(x/H_1) dx \quad (3.13)$$

- P_F : the probability of false alarm is the decision of choosing H_1 where H_0 is true :

$$P_F = p(u_1/H_0) = \int_{th}^{\infty} p(x/H_0) dx \quad (3.14)$$

- P_{md} : the probability of missed detection is the decision of choosing H_0 where H_1 is true :

$$P_{md} = p(u_0/H_1) = \int_0^{th} p(x/H_1) dx \quad (3.15)$$

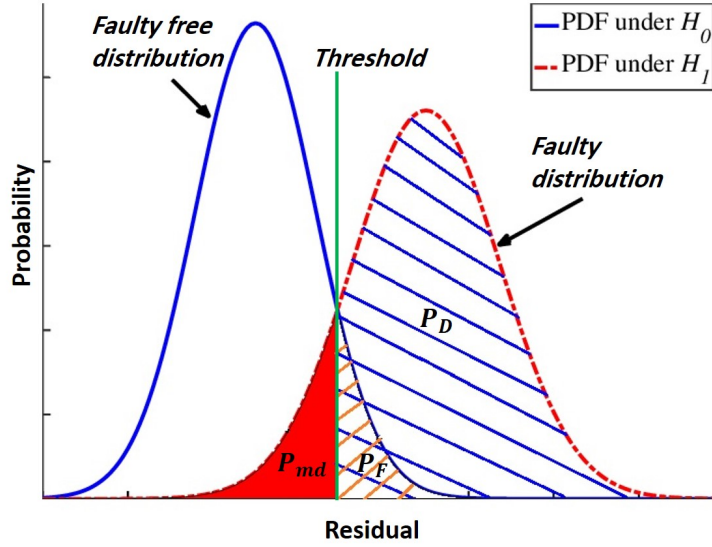


FIGURE 3.2 – Different scenario probabilities

As we can see in figure 3.2, the overlapping between the probabilities, especially the zone that concerns the P_{md} , is a very precise zone, which makes decision making very sensitive. In the next sections we will briefly present some of the existing criterion for decision making, then we will introduce the new adaptive criterion as a new contribution, in the next chapter, in order to choose the optimal threshold.

Kullback-Leibler criterion

In this paragraph, the Kullback-Liebler criterion (KLc) introduced by (AL HAGE et al., 2017), is presented briefly.

Using the information surprise, the optimization problem when a particular value is observed can be done. The informational gain associated with a decision u_j corresponds to KLD between *aposteriori* and *apriori* distributions is :

$$KLD(p(H/u_j)||p(H)) = \sum_{i=\{0,1\}} p(H_i/u_j) \log \frac{p(H_i/u_j)}{p(H_i)} \quad (3.16)$$

Note that : $p(H_0) = P_0$, $p(H_1) = P_1 = 1 - P_0$

By defining the KLc as the summation of the KLD between the prior and posterior distributions of chosen IF, one can write as following :

$$KLc = KLD(p(H/u_0)||p(H)) + KLD(p(H/u_1)||p(H)) \quad (3.17)$$

Which can be written as :

$$\begin{aligned}
 KLc &= \frac{\alpha_0}{\alpha_0 + \beta_0} \log \frac{\alpha_0}{P_0(\alpha_0 + \beta_0)} \\
 &+ \frac{\beta_0}{\alpha_0 + \beta_0} \log \frac{\beta_0}{(1 - P_0)(\alpha_0 + \beta_0)} \\
 &+ \frac{\alpha_1}{\alpha_1 + \beta_1} \log \frac{\alpha_1}{P_0(\alpha_1 + \beta_1)} \\
 &+ \frac{\beta_1}{\alpha_1 + \beta_1} \log \frac{\beta_1}{(1 - P_0)(\alpha_1 + \beta_1)}
 \end{aligned} \tag{3.18}$$

Where,

$$\begin{aligned}
 \alpha_0 &= P_0(1 - P_F) \\
 \alpha_1 &= P_0 P_F \\
 \beta_0 &= (1 - P_0)(1 - P_D) \\
 \beta_1 &= (1 - P_0)P_D \\
 P_0 &= p(H_0)
 \end{aligned} \tag{3.19}$$

The optimization of the threshold can be occurred by minimizing the probability of missed detection P_{md} and maximizing the probability of detection P_D which are equivalent to maximizing KLc . This maximization is reached by getting the derivative of KLc equal to zero : $\frac{\delta KLc}{\delta th}|_{th=\lambda} = 0$, where th represents the threshold, and written as follow :

$$\begin{aligned}
 \frac{\partial KLc}{\partial v} &= \\
 \sum_{i \in \{0,1\}} &\left[\frac{\partial \alpha_i}{\partial v} \left[\frac{\beta_i}{(\alpha_i + \beta_i)^2} \log \left(\frac{1 - P_0}{P_0} \frac{\alpha_i}{\beta_i} \right) \right] + \frac{\partial \beta_i}{\partial v} \left[\frac{\alpha_i}{(\alpha_i + \beta_i)^2} \log \left(\frac{P_0}{1 - P_0} \frac{\beta_i}{\alpha_i} \right) \right] \right]
 \end{aligned} \tag{3.20}$$

The derivative of KLc is detailed in (AL HAGE et al., 2017). P_0 is calculated using the following equation :

$$\hat{P}_0 = 1 - \frac{\sum_{i=1}^n h^i}{n} \tag{3.21}$$

Where $h^i = 0$ if the decision is H_0 or $h^i = 1$ if the decision is H_1 . So $\sum_{i=1}^n h^i$ represents the windows taken for n past hypotheses.

Bhattacharyya Criterion

As the KL, the Bhattacharyya has its own criterion that will be presented in this section.

The informational gain associated with a decision u_j corresponds to Bhattacharyya divergence (BD) between *aposteriori* and *apriori* distributions is :

$$BD(p(H/u_j)||p(H)) = -\log \sum_{i \in \{0,1\}} p(H_i/u_j)^{\frac{1}{2}} q(H_i)^{\frac{1}{2}} \tag{3.22}$$

Thus, the summation of BD associated with decisions u_0 and u_1 , is given by the following equation :

$$Bc = BD(p(H/u_0)||p(H)) + BD(p(H/u_1)||p(H)) \quad (3.23)$$

By minimizing the summation of BD the threshold is optimized, the Bc can be written as :

$$Bc = - \left[\log(\alpha_0 + \beta_0) + \log(\alpha_1 + \beta_1) - \frac{1}{2} \log(\gamma_0) - \frac{1}{2} \log(\gamma_1) \right] \quad (3.24)$$

Where :

$$\begin{aligned} \gamma_0 &= \frac{\alpha_0^2}{P_0} + \frac{\beta_0^2}{1 - P_0} \\ \gamma_1 &= \frac{\alpha_1^2}{P_0} + \frac{\beta_1^2}{1 - P_0} \\ \alpha_0 &= P_0 \sqrt{1 - P_F} \\ \alpha_1 &= P_0 \sqrt{P_F} \\ \beta_0 &= (1 - P_0) \sqrt{1 - P_D} \\ \beta_1 &= (1 - P_0) \sqrt{P_D} \end{aligned} \quad (3.25)$$

3.4 Fault Tolerance For Availability

3.4.1 Definition of Fault Tolerance

Before defining the term Fault Tolerance (FT), we must differentiate between three overlapping terms : failure, fault, and error.

- Failure : a failure is a permanent interruption event that occurs when the system breaks its specifications and becomes unable to properly perform its mission under specific conditions. One or more faults may cause the system failure, resulting in the termination of system operation, as well the failure of a component leads to an error creation that appear as a fault in the system.
- Fault : a fault is an unauthorized behavior of at least one system characteristic that disrupts normal standard operation, that may not affect the overall system operation but degrades system performance, or that may eventually lead to a failure, but which may be tolerable. A failure is the assumed cause of an error, it is said to be active when it produces an error, and latent when it has not yet been enabled. A latent error is usually undetectable and can only be detected once it generates an error or after a detailed analysis.
- Error : an error is incorrect information that, when processed by the system's normal algorithms, results in a subsequent failure. It does not always lead to failure, but it can also cause other errors in the system,

until this propagation finally causes a failure by deviating the system from its proper function.

The existence or the generation of some faults and failure is something that can be avoided totally. Whereas, these faults must be tolerated and compensated to not cause a failure system. This can be achieved by the principle of fault-tolerance.

Fault tolerance is the property that allows a system to continue to operate with satisfactory performance despite the presence of one or more faults or, more seriously, the failure of certain system components. The quality of performance is directly proportional to the severity of the failure, where even a small failure can result in total breakdown. The concept of fault tolerance can be seen as an assurance of system reliability through testing and diagnostics, this concept is concluded from the paper (DENNING, 1976) when author said : "Reliability means not freedom from errors and faults, but tolerance against them". At a deeper level, fault tolerance not only tolerates faults caused by physical hardware degradation, software defects or environmental disturbances, but also includes the ability to tolerate design faults that have not been detected to date. Strictly speaking, a system is said to be fault-tolerant only if it does not require external assistance for its fault tolerance.

Finally, and in order to design a fault tolerant system, one must be rigorous dealing with three key features of fault tolerance :

1. the systematic identification and characterization of all the faults to be tolerated,
2. development and choice of the technique(s) that provide protection against detected faults,
3. analytical or experimental prediction of the effectiveness of the chosen technique(s).

3.4.2 Fault Tolerance Applied To Fusion

In order to apply fault tolerance to data fusion, the specificity of the fusion algorithms and how to choose the appropriate FT algorithm must be studied. Before going into details, the purpose of FT needs to be clarified.

The FT attempts to react to the failure, where it normally contains a specific strategy that monitors the state of the system and alerts a secondary algorithm at the failure or damage level. This algorithm is called Fault Detection and Diagnosis (FDD), which can be either Fault Detection and Isolation (FDI) or Fault Detection and Identification (FDI).

Fault Detection detects the occurrence of a fault in the system. Then, fault isolation locates the fault in the system upon detection. Where, fault identification estimates the amount of the fault in the system. Once the fault is detected, isolated or identified, suitable separation procedures can be implemented to minimize or remove its impact on the system. Thus, the main advantage of FDI algorithm is that it keeps the system available and safe wherever the source of disturbance was. On the other hand, the most important feature is to avoid choosing a slow detection procedure in order to avoid one or more failures.

Specificity Of Fusion Algorithms

Information fusion is the combination of information through different sensors. Hence, as much as the number of sensors increases, the probability to detect fault(s) increases. Thus, the need for a fault tolerant method becomes necessary in order to avoid any system failure. The exciting approaches in the literature are based on the duplication and comparison techniques which can be divided into two categories (3.3) (BADER et al., 2017) :

— **Hardware Redundancy approaches**

The basic concept of the hardware redundancy approaches is to measure a single crucial input parameter with two or more sensors (usually three or more), then the operation of detection is done through consistency checking provided by the redundant sensor measurements, and the isolation for the faulty sensor using majority voting process. As advantage, the hardware redundancy approaches are easy to implement, and can provide a high degree of certainty for FDI. Nevertheless, the use of redundant sensors is not always possible due to cost and space restrictions. In addition, there is a quite probability for failure as the redundant sensor are working in the same environment and exposed to the same conditions which lead to the same expectation for measurements.

— **Analytical Redundancy approaches**

Analytical redundancy also known as functional, inherent, or artificial redundancy. This idea of this approach is achieved based on the functional relationships between the measurements itself, providing a model for the system. The approach finds the relation between the measured inputs based on mathematical model, and generates residuals in order to detect and isolate the faulty sensor (JIANG, 2011). Where, the mathematical model is created using the underlying physics or deduced from the measurements. And the generated residuals are in the form of differences between the model outputs created and the actual received measurements, taking into account the chosen techniques for FDI that does not need any additional redundant sensors. After the residuals generation, a decision is made through thresholding technique to evaluate the residuals and make the final decision for detection and isolation. The analytical redundancy approaches can be applied using three different theory (figure 3.3) :

1. Model-based methods
2. Knowledge-based expert systems
3. Data-driven methods

As we are interested in model-based methods, one can refer to (JIANG, 2011) for more details about knowledge-based expert systems and data-driven methods.

A model-based method with its three different way : 1) parity relations,

2) Luenberger observers and Kalman filter, and 3) parameter estimation, requires a strict mathematical model of the target system. Then, the residuals (r) are generated based on the difference between the estimation of the model (\hat{y}), and the actual sensor measurements (y), as follow :

$$r_k = y_k - \hat{y}_k \tag{3.26}$$

Noting that, the FDI layer added between the *a priori* and *a posteriori* play a critical rule in the decision of detection and isolation depending on the coherence between the chosen divergence and the environmental around which affect directly the residual.

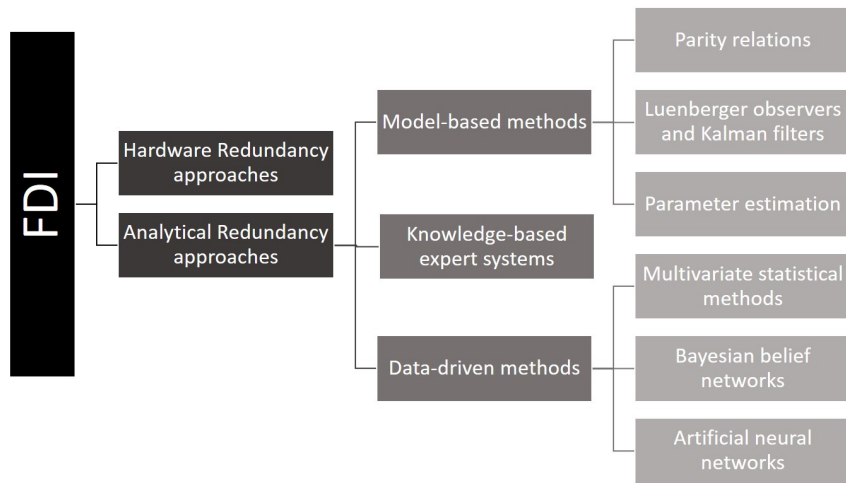


FIGURE 3.3 – FDI categories and approaches

3.4.3 Impact Of An Adaptive Diagnostic Layer In A Fault Tolerant Fusion Approach

In the previous sections, we mentioned the importance to design a suitable fusion architecture for a fault tolerance approach, and we also discussed the necessity to use adaptive diagnostic to deal with the different factors that can affect the system performance. In this section, we explain in detail the impact of adaptive diagnostics in a FTF architecture, and the points to focus on in order to progress towards the robust choice.

The problem of robustness can be solved by defining the independent sensitivities of the residual to uncertainties and faults. Hence, a robust FDI approach is one in which the residual is insensitive to uncertainties while being sensitive to faults (J. CHEN et al., 2012). In analytical redundancy approaches, residuals are the difference resulting from the consistency checking of the different variables. In case of normal operation for the system, the residual has a zero value, where it deviate from zero in case of fault existence. Through this residual propriety, the fault can be detected in the system. More general definition,

residual can be seen as fault indicator or emphasis signal reflecting the faulty status or behavior of the system being supervised. Through these definitions, we conclude that one of the key characteristics of the residual, in ideal case, is its independence from the inputs and outputs of the system. However, in practical systems, and due to the different problems to which it is exposed by the environment, and taking into consideration the type of applications and the number of sensors used, these are factors that can force the system to accept the failure at a certain level but keep it tolerated so as not to cause a failure. In addition, the diagnosis of hard and sudden faults is considered particularly easy due to their heavy impact on the FDI system and can be detected by applying an appropriate threshold to the residue. Nevertheless, incipient and/or light defects have a small effect on the residue and can be considered as an uncertainty in the modeling of the supervised system. Furthermore, it often develops continuously and can grow slowly with very serious consequences. This will not necessarily lead to a significant decrease in system performance, but these faults will indicate that the sensor needs to be replaced before more serious malfunctions appear. Although it may be tolerable in its initial phase. Based on these points, the generation of residual is now considered as a key solution for a robust FDI method, that carries fault information. Thus, a good residual design reduces the loss of some fault information which must be as small as possible. Finally, we can resume that an adaptive diagnostic based on robust FDI approach through a good residual design will have a good impact on the FTF architecture, by tolerating such types of faults whatever the conditions surrounding the system environment.

3.5 Chapter Conclusion

The goal of the chapter is to present a diagnostic concept for fault tolerant fusion approach. The main idea is to create a diagnostic layer that will be sensitive to the system environment and able to adapt to the surrounding problems. The main objectives of the fault tolerant fusion system is to provide the following points :

- Fast response to faults,
- The FTF system will be at the maximum feasible performance level considering the current state of the system's functionality,
- The FTF system must deals with the maximum simultaneous faults can reached,
- The FTF system should handles multi-faults as much as possible.

In order to achieve these points, the concept of adaptive diagnostic is introduced gradually. Starting by the explanation of the reasons to use "adaptive", where we present different factors that affect the diagnostic, such as the surrounding environment, the key performance indicators requirements, and the need of the trade-off between the attributes of dependability. After that, the way to design an adaptive diagnostic layer is detailed, where different divergences are presented.

Going to the heart, we explained the importance of the FT to be applied in

fusion and the two existing approaches in the literature were presented then detailed. The conclusion was that the impact of residuals is very important in both detection and isolation parts, and an FDI method is considered a robust method if the residuals are well generated and well related to surrounding environment around the system. Finally, the impact of the adaptive diagnostic, that brings in an FTF architecture, highlighted its importance and its effect on the residuals generation with the minimum loss of information.

Chapter 4

Adaptive Fault Tolerant Fusion Framework for Performing a Robust, Precise, Available and Fail-Safe State Estimation

4.1 Chapter Introduction

The main goal of this chapter is to deliver a concept of fault tolerant fusion for a robust and fail-safe outdoor localisation of an autonomous vehicle. The principle objectives that we aim, can be listed in :

- The proposed approach must have the ability to run in real time at any conditions,
- The proposed approach should ensure the availability and the needed safety,
- The FDI approach should provide good performance regardless of the problems encountered in adapting to the surrounding environment,
- As the residuals are adaptive to the environment, the decision should also be adaptive and take into consideration the multiple conditions that affect the level of the decision, for example, the number of available sensors, the type of application itself,...
- All type of faults as sudden faults, soft faults, external and/or internal faults should be detected, and isolated from the final estimation step.

In order to achieve such needs, different problems should be solved. The proposed approach deals with these problems by different strategies in different levels. In term of data fusion, we propose a multi-sensor fusion (section 2.3) approach based on the informational framework to overcome the problem of availability of the system and its accuracy. Non-linearity problems are faced through the non-linear Kalman filter in its informational form. As well, the Maximum Correntropy Criterion (section 4.3.2) performs well dealing with non-Gaussian noises. In term of fault tolerance, the unpredictable environment

and conditions, as well the problem of coherence between the evolution model and the observations are treated with the use of adaptive diagnosis level, based on weighted α -RD residuals (section 4.4) created in the FDI layer. The weighted α -RD residuals calculated between the predicted and the corrected distributions of the MCCNIF are developed to discriminate between normal and abnormal sensors behavior. In the thresholding level, basically the decision is then taken by a threshold by considering a fixed false alarm probability (HARMOUCHE et al., 2015), or by using a fixed threshold like in (MAKKAWI et al., 2019), through the Receiver Operating Characteristic (ROC) curve. (QIAN et al., 2015) proposes the MI criterion, in order to evaluate candidate features in an incomplete information system. The maximization of MI criterion is proposed in (HOBALLAH et al., 1989), in order to minimize the ambiguity between the hypothesis and the decision. As well, the Bayes criterion, and the maximization of P_D in Neyman-Pearson criterion, are presented in (VARSHNEY, 2012). In AL HAGE et al., 2017, the KLC is proposed in order to select an optimal threshold from an interval of thresholds. In this work, an adaptive threshold based on α -Rc is proposed. The α -Rc (section 4.4.5) selects the optimal threshold, which lies in an interval, related to the historical behavior of the system, using the Maximum Likelihood Estimation (MLE). The proposed framework for the multi-sensor AFTF approach consists of four main parts (Figure 4.1) :

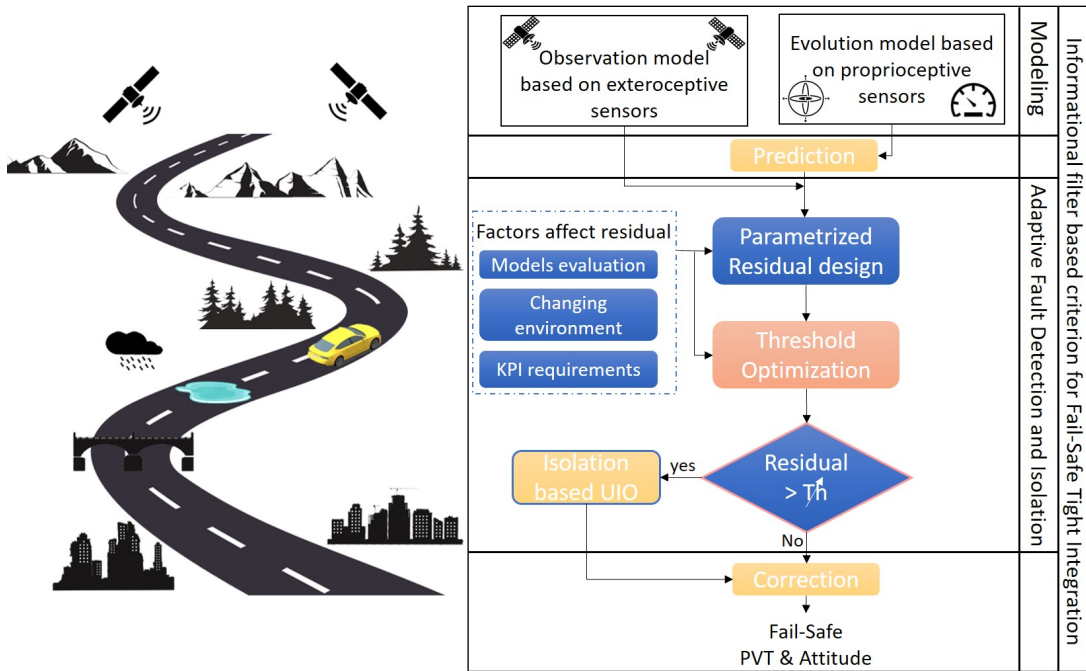


FIGURE 4.1 – The proposed architecture for fault tolerant multi-sensor fusion

- In the first part, the n^{th} number of sensors data are combined using the chosen estimator through the corresponding model.
- The detection stage of the FDI method represents the second main part.

Where, a global residual is designed based on the α -RD after calculated the weighted value of α .

- The third part consists of an adaptive threshold, optimized by the α -Rc in order to find the optimal missed detection (P_{md}) and detection (P_D) probabilities.
- The fourth part is only activated if the threshold in the third part indicates the fault(s) existence. This part is based on the UIO, where a bank of the chosen IF is created for different observations combinations at each instant k . Then, a set of α -RD residual is calculated for each sub-filter and a decision-making step realized to indicate the existence or not of fault(s).

In summary to the faced problems in localization and how it is proposed to be solved, one can refer to table 4.1.

TABLE 4.1 – Problems faced in localization and proposed solutions

Problems faced	Proposed solutions
System availability and accuracy	Multi-sensor data fusion
Non-linearity state estimation problems	Nonlinear Kalman Filter in informational form
Non-Gaussian noises	Maximum Correntropy Criterion as criterion
Changing in environment and KPI requirements	Adaptive diagnostic layer
Multipath/NLOS, and other local feared events causing safety issues	Fault Detection (FD) layer using information metrics
Multipath/NLOS, and other local feared events causing poor accuracy and availability problems	Fault isolation layer using solution separation method
Misestimation of evolution and/or observation covariance matrices	Residuals design using α -Rényi Divergence
Difficulty to choose between False alarm and missed detection rate	Adaptive thresholding using α -Rényi criterion

4.2 General Approach Block Diagram

In this section, we detail the proposed approach in its different levels. In this diagram, we used general terms like "chosen IF", " α -RD", and " α -Rc" without specifying the chosen information filter or the value of α , in order to explain after the importance of the proposed filter and α value.

The proposed fault tolerant multi-sensor fusion approach is illustrated in figure 4.2. The algorithm is applied by fusing GNSS observations (pseudo-ranges) and odometer data using the chosen IF as the main estimator.

4.2. GENERAL APPROACH BLOCK DIAGRAM

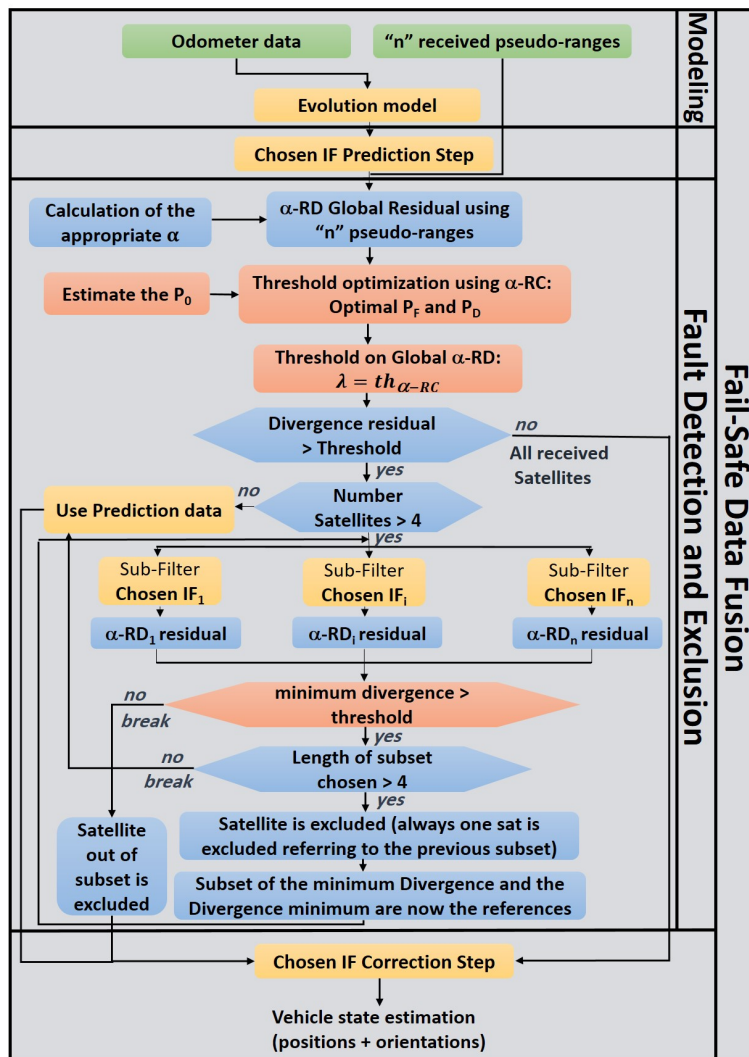


FIGURE 4.2 – Detailed general diagram for the proposed approach

After specifying the value of α (detailed in the next sections), all the received observations are involved in the calculation of the global α -RD. The global residual is then tested with the threshold provided by the α -Rc. The α -Rc is used in order to provide the optimal missed detection and detection probabilities for each case. If the global residual is below the specified threshold, so the use of all observations in the correction step of the chosen IF is safe to estimate the position. Where in the opposite case, the isolation step is activated to remove the erroneous measurements. The isolation method is a hierarchical algorithm based on the UIO, where at each level, sets of the chosen IF sub-filters are created using the number of observations available at the previous level minus one ($n - 1$). At each level, local α -RD residuals are calculated for each sub-filter and one erroneous satellite measurement is removed from the next level. This process continues until all erroneous measurements are removed and the final subset of observations has an α -RD below the threshold. Finally, the final safe subset is used in the correction step of the chosen IF and the estimated position is calculated.

Noting that, during the whole process, the number of satellites is taken into consideration. As it should not be less four satellites at instant k in order to deliver a position (LEWANDOWSKI et al., 2010).

4.3 Toward a More Robust Criterion in Filtering

The estimation task comes from the need to find the expected monitoring parameters of a "black" system from its outputs (measurements), which is essential for many type of applications such as : wireless communication, signal processing, image reconstruction, and etc.

Linear and Gaussian MMSE capabilities are a popular choice because they are easy to use, easy to calculate and flexible. It has given rise to many famous estimators such as the Wiener-Kolmogorov filter and the Kalman filter.

4.3.1 MMSE : The Ordinary KF Optimality Criterion

The Minimum Squared Error (MSE) criterion is an estimator with minimum squared errors (which means that it is perfect in terms of statistics). In the Bayesian perspective, the MMSE concept refers more specifically to the estimation based on the square loss function. Popularly, the Linear and Gaussian MMSE is a frequently used choice because it is easy to use, easy to calculate and flexible. It has given birth to many well-known estimators such as the Wiener-Kolmogorov filter and the Kalman filter. Where, KF technique uses the MMSE as a linear processing algorithm to recursively solve estimation problems.

Let x and z be two jointly distributed random vector variables with different dimensions. Taking z as the observation known vector, and the estimator $\hat{x}(z)$ of x as any function of the measurement z . Hence, the estimation error vector is given by $e = \hat{x} - x$ and its mean squared error (MSE) is given by the trace of error covariance matrix as :

$$MSE = tr [E(\hat{x} - x)(\hat{x} - x)^T] = E [(\hat{x} - x)^T(\hat{x} - x)] \quad (4.1)$$

Taking into account statistical information such as the a priori $p(x)$, the MSE can be written as :

$$MSE = \int_x p(x/z)(\hat{x} - x)^T(\hat{x} - x)dx \quad (4.2)$$

Where, the a posteriori $p(x/z)$ is calculated through Bayesian chain rule as :

$$p(x/z) = \frac{p(z/x)p(x)}{p(z)} \quad (4.3)$$

Thus, the optimal MMSE estimator is then defined as the estimator by finding minimal MSE :

$$\hat{x}_{MMSE}(z) = argmin_{\hat{x}} MSE \quad (4.4)$$

Regardless of all the advantages of MMSE criterion, as it is easy to understand, and deal well with many types of applications, it still very sensitive to heavy disturbances. Where in highly non-linear and heavy non-Gaussian conditions, the well-known KF and its extensions show drop of the robustness when dealing with large outliers caused by the MMSE criterion (Wu et al., 2015).

4.3.2 MCC : A More Robust Criterion

Despite all the advantages that KF (or its informational form) has, its performance can decline significantly under non-Gaussian noises in a non-linear system. In this section, we introduce the Maximum Correntropy Criterion (MCC) as a proposed solution to overcome this strong limitation.

Correntropy Definition

The correntropy defines a metric in the data space and is directly related to information entropy. It is defined as a generalized correlation function, which is directly related to the similarity probability of two scalar random variables X and Y (IZANLOO et al., 2016) defined by :

$$C(X, Y) = E [ker(X, Y)] = \int \int ker(x, y) f_{XY}(x, y) dx dy \quad (4.5)$$

Where, E is the expectation and $f_{XY}(x, y)$ is the joint probability density function of X and Y , which is unknown, and a finite number of sample data are available. Therefore, the correntropy can be estimated by the sample mean estimator as the summation of all statistical instants generated by the kernel :

$$C(X, Y) = \frac{1}{N} \sum_{i=1}^N ker(x_i, y_i) \quad (4.6)$$

Where N samples drawn from $f_{xy}(x, y)$ and ker is the positive definite translation-invariant Gaussian kernel function calculated as the most popular kernel called Mercer kernel under the form of :

$$ker(x, y) = \frac{1}{\sqrt{2\pi}\beta} exp\left(-\frac{e^2}{2\beta^2}\right) \quad (4.7)$$

with $e = \|x - y\|$ and β is the kernel bandwidth.

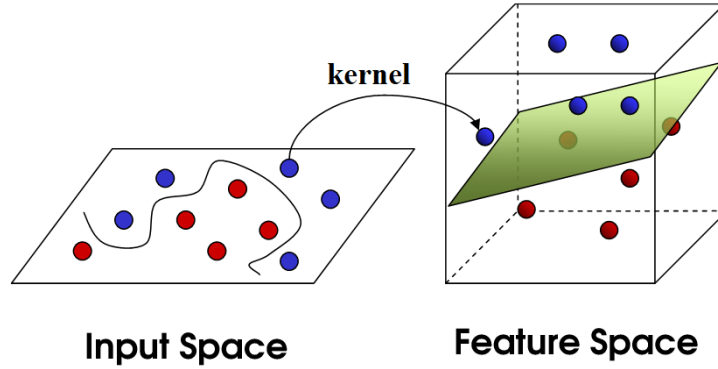


FIGURE 4.3 – Kernel principal

The basic idea of kernel algorithms is to transform the data from the input space to a high dimensional feature space (SANTAMARIA et al., 2006). It is a way of placing two dimensional plane into a higher dimensional space, so that it is curved in the higher dimensional space. In general, what the kernel does is that any plane in the three-dimensional space intersects the two-dimensional plane that contains the data in a curved line rather than a straight line giving more flexibility to choose the curve that separates the data (figure 4.3).

Maximum Correntropy as a Criterion

Given X a random vector variables with $n \times 1$ dimensions, Z as the observation known vector with $m \times 1$, the estimator $\hat{X}(Z) = f(Z)$ of X as any function of the measurement Z , and the estimation error vector is given by $e = \hat{X} - X$ with a pdf $p_e(\epsilon)$. Hence, by maximizing the correntropy between X and \hat{X} under the MCC, the estimator f can be written as :

$$f_{MCC} = \underset{f \in \mathcal{F}}{\operatorname{argmax}} C_r(X, \hat{X}) = \underset{f \in \mathcal{F}}{\operatorname{argmax}} E [ker(X - f(Z))] \quad (4.8)$$

Where, the term maximization is chosen as the MCC estimator has been shown to be a smoothed estimate of the maximum posterior probability, where the PDF reaches its maximum value (B. CHEN et PRINCIPE, 2012). \mathcal{F} represents the set of measurable functions of Z , and $p_e(\epsilon)$ is calculated through :

$$p_e(\epsilon) = \int_{\mathbb{R}^m} p_{X|Y}(\epsilon + f(y)|y) dG_Y(y) \quad (4.9)$$

With G_Y the distribution function of Y and $p_{X|Y}(x|y)$ is the conditional pdf of the variable X .

Finally, the estimator f under the MCC is written as follow :

$$f_{MCC} = \underset{f \in \mathcal{F}}{\operatorname{argmax}} \int_{\mathbb{R}} ker(\epsilon) \int_{\mathbb{R}^m} p_{X|Y}(\epsilon + f(y)|y) dG_Y(y) d\epsilon \quad (4.10)$$

The MCC shows a superiority in performance over other similarity measures, as the MMSE and the correntropy. These advantages can be summarized as follows (B. CHEN et PRINCIPE, 2012) :

- It is always bounded for any distribution,
- It includes all even-order moments, and the Kernel size plays a significant role in the behavior of correntropy filters by weighting high-order moments,
- Deals with high non-linearity and very useful for the case where the signals are contaminated by heavy non-Gaussian noises,
- It is a measure of local similarity, and is very robust to aberrant points.

4.3.3 Development of MCC NIF

The filters which adopts the MCC, utilize correntropy between two random variables as a cost function for designing the estimation (IZANLOO et al., 2016). This kind of filters based on MCC can achieve high performance in highly non-linear and heavy non-Gaussian conditions (B. CHEN, X. LIU et al., 2017).

To overcome such problems, we introduce an original filter called the Non-linear Information Filter (NIF) under the MCC (MCCNIF). The NIF deals well with Gaussian noises but, its performance decreases when abruptly facing heavy non-Gaussian noises causing a divergence. Conversely, the NIF deals fairly with nonlinearity problems. Hence, to deal with non-Gaussian noises, the MCC shows good performance especially with shot noises and Gaussian mixture noises.

To estimate the position, MCCNIF uses two main steps :

The prediction step calculates the information matrix, represented by :

$$Y_{k/k-1} = [F_k P_{k-1/k-1} F_k^T + B_k (Q_u)_k B_k^T + Q_k]^{-1} \quad (4.11)$$

Where :

Q_u is the input vector variance-covariance matrix,

Q_k is the model noise variance-covariance matrix,

F_k is the Jacobian matrix calculated as : $F_k = \frac{\partial f}{\partial X} \Big|_{X=X_{k-1/k-1}}$,

B_k is the Jacobian matrix calculated as : $B_k = \frac{\partial f}{\partial u} \Big|_{u=u_k}$.

And the information vector by using :

$$y_{k/k-1} = Y_{k/k-1} X_{k/k-1} \quad (4.12)$$

The corrected information matrix $Y_{k/k-1}$ vector $y_{k/k-1}$ are now calculated through the chosen kernel respectively as :

$$Y_{k/k} = Y_{k/k-1} + \sum_{i=1}^N g I_i(k) \quad (4.13)$$

$$y_{k/k} = y_{k/k-1} + \sum_{i=1}^N pI_i(k) \quad (4.14)$$

Where :

$$gI_i(k) = \text{ker}_{i,k} H_{i,k}^T R_i^{-1}(k) H_{i,k} \quad (4.15)$$

$$pI_i(k) = \text{ker}_{i,k} H_{i,k}^T R_i^{-1}(k) [(Z_{i,k} - \hat{Z}_{i,k}) + H_{i,k} X_{k/k-1}] \quad (4.16)$$

Where, $R(k)$ is the covariance matrix of the observation noise ε_k , related to the kind of noise in each case as follow :

— For white Gaussian noise :

$$R(k) = E [\varepsilon_k \varepsilon_k^T] \quad (4.17)$$

— For mixture Gaussian noise (MGn) (IZANLOO et al., 2016) :

$$R(k) = \phi N(\mu_{y1}, R_1) + (1 - \phi) N(\mu_{y2}, R_2) \quad (4.18)$$

4.4 A Diagnostic based on α -Rényi Divergence

After a robust sensors fusion, an effective diagnostic layer has to be presented. In this work, we propose the α -RD for residual design, and we present in details the features, and the advantages for this divergence.

The α -RD choice is based on the wide range of divergence measures offered, by changing the value of α (HISTACE et al., 2015), which makes the divergence more flexible with the type of application.

In chapter 5, we will see, that changing the parameter α has an important impact on the residual design, which affect the detection layer, the decision-making part, and the estimation.

4.4.1 α -Rényi Divergence as a Parametric Residual

For two probability distributions P and Q , the α -RD between P and Q is non-decreasing as a function of its order α , and it is continuous on the set of α for which it is finite. It can be written as :

$$RD_\alpha(P||Q) = \frac{1}{\alpha - 1} \ln \int P^\alpha(x) Q^{1-\alpha}(x) d(x) \quad (4.19)$$

Where $\alpha \in R^+ \setminus \{1\}$ (VAN ERVEN et al., 2014).

As α approaches to zero, the Rényi entropy weights all possibilities more equally, regardless of their dissimilarities. In the limit $\alpha \rightarrow 0$, the α -RD slides to the negative log probability under Q that P is non-zero (RÉNYI et al., 1961) :

$$RD_0(P||Q) = \lim_{\alpha \rightarrow 0} RD_\alpha(P||Q) = -\log Q(p > 0) \quad (4.20)$$

If the two distributions have the same support then the $\lim_{\alpha \rightarrow 0} RD_\alpha(P||Q) = 0$

This divergence is symmetric only in its arguments when $\alpha = 0.5$, which yields to the Bc and BD seen in equation 3.5 (BHATTACHARYA, KAR et al., 2009) :

$$RD_{\frac{1}{2}}(P||Q) = -2 \log \int \sqrt{P(x)} \cdot \sqrt{Q(x)} dx = 2BD(P||Q) \quad (4.21)$$

We recover the relativity entropy in the limit of $\alpha \rightarrow 1$, where the relation between α -RD and the *KLD* appears using the Hospital theorem (BHATTACHARYA, PATI et al., 2019). This relation can be shown by the following equation :

$$RD_1(P||Q) = \lim_{\alpha \rightarrow 1} (RD_\alpha(P||Q)) = KLD(P||Q) \quad (4.22)$$

Note that, the $RD_\alpha(P||Q)$ is non-decreasing in α on $[0, 1] \cup \{\alpha \in [1, \infty] | RD_\alpha < \infty\}$.

The $RD_\alpha(P||Q)$ is skew symmetry for $0 < \alpha < 1$ where it can be written as $RD_\alpha(P||Q) = \frac{\alpha}{\alpha-1} RD_{1-\alpha}(Q||P)$, and for $\alpha = 2$ the divergence becomes related to the χ^2 (BOBKOV et al., 2019).

Studying the convexity of Rényi entropy, it is neither convex nor concave but considered as pseudo-concave for $\alpha > 1$, where it is Schur concave for $\alpha > 0$ (HO et al., 2015). Its divergence $RD_\alpha(P||Q)$ is jointly convex in (P, Q) for $\alpha \in [0, 1]$, convex in Q for $\alpha \in [0, \infty]$ and jointly quasi-convex in (P, Q) for $\alpha \in [0, \infty]$ (ERVEN et al., 2010).

The generation of residuals through α -RD makes the residual more flexible and adaptable with the environment, the dynamic and the kind of errors. Hence, to calculate the divergence between the two probability distribution functions (*pdfs*) $g(k/k-1) \sim \mathcal{N}(X_{k/k-1}, \Sigma_{k/k-1})$ and $g(k/k) \sim \mathcal{N}(X_{k/k}, \Sigma_{k/k})$, representing the two covariance matrices of the prediction and the correction steps provided by the chosen IF estimator, the α -RD can be written as the following equation (HOBZA et al., 2009) :

$$RD_\alpha(g(k/k-1)||g(k/k)) = \frac{\alpha}{2} (X_{k/k-1} - X_{k/k})^T (\Sigma_\alpha)^{-1} (X_{k/k-1} - X_{k/k}) - \frac{1}{2(\alpha-1)} \log \frac{|\Sigma_\alpha|}{|\Sigma_{k/k-1}|^{1-\alpha} |\Sigma_{k/k}|^\alpha} \quad (4.23)$$

Taking into consideration that $\Sigma_\alpha = \alpha \Sigma_{k/k} + (1-\alpha) \Sigma_{k/k-1}$, $\Sigma_{k/k-1} = \frac{1}{Y_{k/k-1}}$, and $\Sigma_{k/k} = \frac{1}{Y_{k/k}}$. And, by considering that $\frac{\alpha}{2} (X_{k/k-1} - X_{k/k})^T (\Sigma_\alpha)^{-1} (X_{k/k-1} - X_{k/k})$ is the term *A*, and $-\frac{1}{2(\alpha-1)} \log \frac{|\Sigma_\alpha|}{|\Sigma_{k/k-1}|^{1-\alpha} |\Sigma_{k/k}|^\alpha}$ is the term *B* :

Term A can be written as :

$$\begin{aligned}
 & \frac{\alpha}{2} (X_{k/k-1} - X_{k/k})^T (\Sigma_\alpha)^{-1} (X_{k/k-1} - X_{k/k}) \\
 &= \frac{\alpha}{2} (X_{k/k-1} - X_{k/k})^T \left(\frac{1}{\frac{\alpha}{Y_{k/k}} + \frac{1-\alpha}{Y_{k/k-1}}} \right) (X_{k/k-1} - X_{k/k}) \\
 &= \frac{\alpha}{2} (X_{k/k-1} - X_{k/k})^T \left(\frac{Y_{k/k-1} Y_{k/k}}{\alpha Y_{k/k-1} + (1-\alpha) Y_{k/k}} \right) (X_{k/k-1} - X_{k/k})
 \end{aligned} \tag{4.24}$$

Term B can be written as :

$$\begin{aligned}
 & - \frac{1}{2(\alpha-1)} \log \frac{|\Sigma_\alpha|}{|\Sigma_{k/k-1}|^{1-\alpha} |\Sigma_{k/k}|^\alpha} \\
 &= - \frac{1}{2(\alpha-1)} \log \left[\left| \frac{\alpha Y_{k/k-1} + (1-\alpha) Y_{k/k}}{Y_{k/k-1} Y_{k/k}} \right| \frac{1}{\left| \frac{1}{Y_{k/k-1}} \right|^{1-\alpha} \left| \frac{1}{Y_{k/k}} \right|^\alpha} \right] \\
 &= - \frac{1}{2(\alpha-1)} \log \left| \frac{\alpha Y_{k/k-1} + (1-\alpha) Y_{k/k}}{Y_{k/k-1} Y_{k/k}} \right| - \frac{1}{2(\alpha-1)} \log \frac{|Y_{k/k}|^\alpha}{|Y_{k/k-1}|^{\alpha-1}} \\
 &= \frac{1}{2(\alpha-1)} \log \left| \frac{Y_{k/k-1} Y_{k/k}}{\alpha Y_{k/k-1} + (1-\alpha) Y_{k/k}} \right| + \frac{1}{2(\alpha-1)} \log \frac{|Y_{k/k-1}|^{\alpha-1}}{|Y_{k/k}|^\alpha}
 \end{aligned} \tag{4.25}$$

Hence, the equation 4.23 can be written in the following form :

$$\begin{aligned}
 RD_\alpha(g(k/k-1) || g(k/k)) &= \\
 & \frac{\alpha}{2} (X_{k/k-1} - X_{k/k})^T \left(\frac{Y_{k/k-1} Y_{k/k}}{\alpha Y_{k/k-1} + (1-\alpha) Y_{k/k}} \right) (X_{k/k-1} - X_{k/k}) + \\
 & \frac{1}{2(\alpha-1)} \log \left| \frac{Y_{k/k-1} Y_{k/k}}{\alpha Y_{k/k-1} + (1-\alpha) Y_{k/k}} \right| + \frac{1}{2(\alpha-1)} \log \frac{|Y_{k/k-1}|^{\alpha-1}}{|Y_{k/k}|^\alpha}
 \end{aligned} \tag{4.26}$$

This residual consists of three kind of tests that deal with the two *pdfs* in different ways :

1. The first test : $(X_{k/k-1} - X_{k/k})^T \left(\frac{Y_{k/k-1} Y_{k/k}}{\alpha Y_{k/k-1} + (1-\alpha) Y_{k/k}} \right) (X_{k/k-1} - X_{k/k})$ represented by the weighted Mahalanobis distance, is to measure the distance between the means, taking into the consideration the α value which weights distance through its impact on the covariance matrices,
2. The second test : $\log \left| \frac{Y_{k/k-1} Y_{k/k}}{\alpha Y_{k/k-1} + (1-\alpha) Y_{k/k}} \right|$ can be compared to the weighted Bregman, taking into account the weight of α for each covariance matrix,
3. The third test : $\log \frac{|Y_{k/k-1}|^{\alpha-1}}{|Y_{k/k}|^\alpha}$ represented by the weighted MI, where in this test, the two *pdfs* are compared based on their weighting value related to the value of α .

These tests creating the generalized α -RD residual, show a weighty flexibility related to the value of α .

4.4.2 Physical Interpretation of α -Parameter

To interpret the impact of using α in the α -RD residual and its effect on the residual by a physical interpretation, let's take the pdfs of the prediction and correction covariance matrices to judge them on the balance of α .

Fig.4.4 explains the effect of α on the residual by rebalancing the confidence between the pdfs of prediction and correction covariance matrices in different cases.

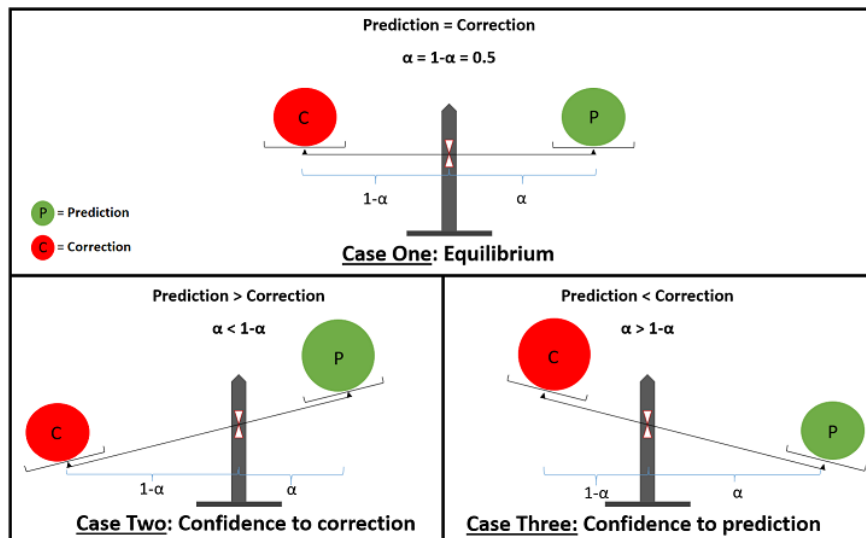


FIGURE 4.4 – illustration of the adjusting effect played by alpha in the residual rebalancing the probability distributions

In case if the covariance matrix pdfs of prediction and correction are equal and $\alpha = 1 - \alpha = 0.5$, so the equilibrium is achieved, and the confidence is equally distributed between the covariance matrices representing the prediction and correction (case one). But if this α becomes greater than $1 - \alpha$ so the confidence tends to the prediction, and it is converted to the correction if α is less than $1 - \alpha$.

Another case is also treated by α , where even if the prediction is greater than the correction, the confidence will not remain by the side of prediction, but it is shifted to the correction side if the α is less than the $1 - \alpha$ (case two). The same scenario can be applied in case the prediction is less than the correction. Where the confidence is not on the side of the correction but it is transmitted to the prediction side if the α is higher than the $1 - \alpha$ (case three).

The suitable α and its effect on the α -RD make the weighting much easier, by changing the value of α . This property in α -RD opens the capability to create residuals more robust and reliable to the modeling error *vs.* sensors faults, where the value of α adjusts the residual according to the type of application.

4.4.3 Establish A Residuals Parameterization Policy Based On Operational Requirements And Changes In Navigation Context

Taking into account the different purposes for the use of an adaptive diagnosis explained in section 3.3.1, the adaptive diagnosis is proposed in this section based on multiple reasons. First, we are dealing with two models, the evolution model and the observation model. The limitations that restrain the odometer sensor, as well as the limitations of GNSS, due to many different causes listed in section 2.2.2 and 2.2.1 respectively, lead us to rely on neither of the two models. On the other hand, we cannot avoid the fact that observations in good environment (open sky and/or LOS for example) can be very useful for an accurate estimation. In order to avoid such suspicion in the decision of the reference model, the adaptive diagnosis is proposed as a solution to the problem encountered.

For the choice of the α value at each instant k , and knowing that there is no reliable reference between the two models, we propose a solution to weight the two models equally through α balance. The following equation take into consideration the covariance matrix $\Sigma_{k/k-1}$ of the prediction step representing the evolution model, and the covariance matrix $\Sigma_{k/k}$ of the correction step representing the observation model, then weight equally the matrices.

$$\alpha |\Sigma_{k/k-1}| = (1 - \alpha) |\Sigma_{k/k}| \quad (4.27)$$

this equation leads to the weighted value of α :

$$\alpha = \frac{|\Sigma_{k/k}|}{|\Sigma_{k/k-1}| + |\Sigma_{k/k}|} \quad (4.28)$$

which is written in informational form as :

$$\alpha = \frac{|Y_{k/k-1}|}{|Y_{k/k}| + |Y_{k/k-1}|} \quad (4.29)$$

One can notice that regardless of their original weights, using the equality in equation 4.29, the weight is equally distributed between the prediction and correction *pdfs*. The adaptive α avoids the problem of model's reference faced along the trajectory by proposing a new residual at each instant k .

Based on the interpretation in figure 4.4, our proposed equation 4.29 for calculating α can be interpreted in the same balance. Where, in figure 4.5, we can see that whatever the case is, equilibrium will surely occur. This equilibrium is achieved by α which redistributes the difference between the two edges of the balance to equalize the two sides.

Through this proposed solution, the problem at the level of model reference is solved, but the divergence used at each instant k will create its corresponding residuals related to the value of α . In such way, the generation of the two *pdfs* representing the faulty-free and the faulty cases will be another problem to be solved.

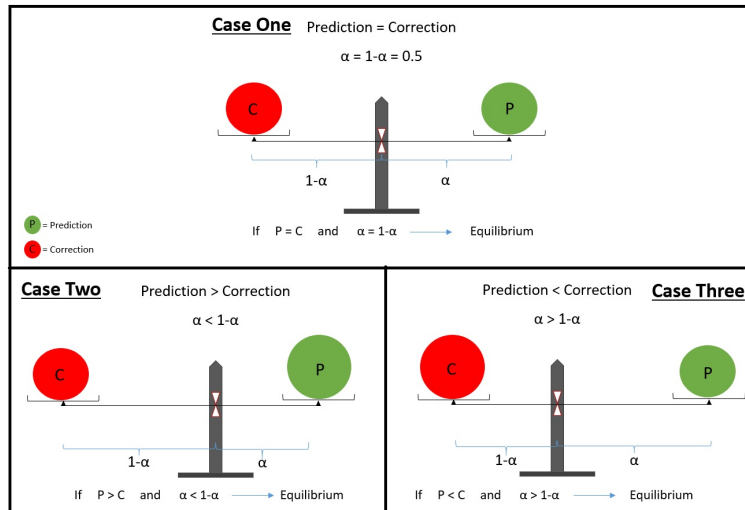


FIGURE 4.5 – Physical interpretation for α balanced

4.4.4 An Infinity Of Residuals Implies An Infinity Of Statistical Characterization ... How To Solve ?

The policy chosen in treating the adaptive diagnosis leads to an infinity of residuals, which implies an infinity of statistical characterization. In fact, creating the two *pdfs* for an infinite values of α will be hard and will take a lot of time. So, to avoid such problems, we propose a simple solution by creating mathematical models able to estimate the two *pdfs*. The diagram in figure 4.6 shows the procedure used to create these models.

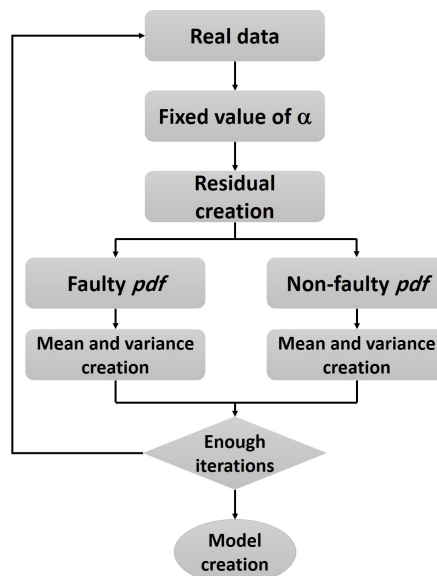


FIGURE 4.6 – Diagram to create two probability distributions

Using real sensors data, for many values of α , residuals are calculated and the two *pdfs* for faulty and non-faulty cases are created through a non-

supervised learning method for each value of α . Then, the means and the variances are extracted and plotted with respect to α . Hence, a function that approximates these values is created. This function represents the mathematical model to estimate a new value of α (figure 4.7).

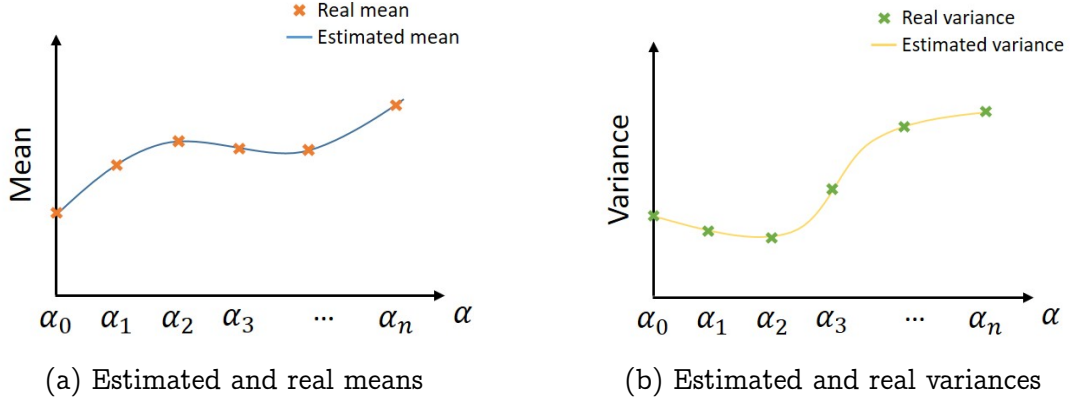


FIGURE 4.7 – Extracting estimated means and variances from real values

Mean and variance Models created take the following mathematical form :

1. For non-faulty cases :

$$\begin{aligned} M_{nf} &= \sum_{i=1,n} a_i \alpha^i \\ V_{nf} &= \sum_{j=1,n} b_j \alpha^j \end{aligned} \quad (4.30)$$

2. For faulty cases :

$$\begin{aligned} M_f &= \sum_{k=1,n} c_k \alpha^k \\ V_f &= \sum_{m=1,n} d_m \alpha^m \end{aligned} \quad (4.31)$$

Where a , b , c , and d are considered as constant values. Using the above models, one is able to approximate the mean and variance for the new value of α in order to create the two *pdfs*.

4.4.5 α -Rényi Criterion Generalizing Threshold Optimization

a. α -Rc design

Based on the equation (4.19), the informational gain associated to the decision u_j , represents the α -Rényi divergence between the *a priori* and a *posteriori* distributions. This gain can be written as :

$$RD_\alpha(p(H/u_j)||p(H)) = \frac{1}{\alpha - 1} \log \sum_{i \in \{0,1\}} (p(H_i/u_j))^\alpha (p(H_i))^{1-\alpha} \quad (4.32)$$

Therefore, the α -Rényi criterion represented by the summation of the informational gain corresponding to decisions u_0 and u_1 , is written as :

$$Rc_\alpha = RD_\alpha(p(H/u_0)||p(H)) + RD_\alpha(p(H/u_1)||p(H)) \quad (4.33)$$

which leads to :

$$Rc_\alpha = \frac{1}{\alpha - 1} \sum_{i \in \{0,1\}} \log \sum_{j \in \{0,1\}} \left(\frac{p(u_j/H_i)}{p(u_j)} \right)^\alpha p(H_i) \quad (4.34)$$

Thus, the α -Rényi criterion is written as :

$$\begin{aligned} Rc_\alpha &= \frac{1}{\alpha-1} \log P_0(1 - P_0) \\ &+ \frac{1}{\alpha-1} \log [[P_0\gamma_1\gamma_0 + (1 - P_0)\beta_1\gamma_0]^\alpha + [P_0\gamma_1\gamma_0 + (1 - P_0)\gamma_1\beta_0]^\alpha] \\ &+ \frac{1}{\alpha-1} \log [[P_0\beta_1\gamma_0 + (1 - P_0)\beta_1\beta_0]^\alpha + [P_0\gamma_1\beta_0 + (1 - P_0)\beta_1\beta_0]^\alpha] \\ &- \frac{2\alpha}{\alpha-1} \log [P_0\gamma_0 + (1 - P_0)\beta_0] \\ &- \frac{2\alpha}{\alpha-1} \log [P_0\gamma_1 + (1 - P_0)\beta_1] \end{aligned} \quad (4.35)$$

where : $\gamma_0 = 1 - P_F$, $\beta_0 = 1 - P_D$, $\gamma_1 = P_F$, and $\beta_1 = P_D$.

b. Variation of α -Rc

The variation of α -Rc is studied through the derivative of the α -Rc with respect to a given variable v . This derivative is calculated based on equation (4.35) and written as :

$$\begin{aligned} \frac{\partial Rc_\alpha}{\partial v} &= \frac{\alpha}{\alpha - 1} \left[\frac{\sum_{i \in \{0,1\}} \gamma_i^{\alpha-1} [P_0\gamma_i + (1 - P_0)\beta_i]^{\alpha-1} \left[(P_0\gamma_0 - P_0\gamma_1 + (-1)^{i+1}(1 - P_0)\beta_i) \frac{\partial \gamma_i}{\partial v} + (-1)^{i+1}(1 - P_0)\gamma_i \frac{\partial \beta_i}{\partial v} \right]}{\sum_{i \in \{0,1\}} \gamma_i^\alpha [P_0\gamma_i + (1 - P_0)\beta_i]^\alpha} \right. \\ &+ \frac{\sum_{i \in \{0,1\}} \beta_i^{\alpha-1} [P_0\gamma_i + (1 - P_0)\beta_i]^{\alpha-1} \left[((-1)^{i+1}\gamma_i + (1 - P_0)\beta_0 - (1 - P_0)\beta_1) \frac{\partial \beta_i}{\partial v} + (-1)^{i+1}\beta_i \frac{\partial \gamma_i}{\partial v} \right]}{\sum_{i \in \{0,1\}} \beta_i^\alpha [P_0\gamma_i + (1 - P_0)\beta_i]^\alpha} \\ &\left. - 2 \sum_{i \in \{0,1\}} \frac{P_0 \frac{\partial \gamma_i}{\partial v} + (1 - P_0) \frac{\partial \beta_i}{\partial v}}{P_0\gamma_i + (1 - P_0)\beta_i} \right] \end{aligned} \quad (4.36)$$

1. for $P_F = \text{constant}$, the derivative of α -Rc with respect to P_D is written

as :

$$\begin{aligned} \frac{\partial Rc_\alpha}{\partial P_D} &= \frac{\alpha}{\alpha - 1} \left[(1 - P_0) \frac{\sum_{i \in \{0,1\}} (-1)^{i+1} \gamma_i^\alpha [P_0 \gamma_i + (1 - P_0) \beta_i]^{\alpha-1}}{\sum_{i \in \{0,1\}} \gamma_i^\alpha [P_0 \gamma_i + (1 - P_0) \beta_i]^\alpha} \right. \\ &+ \frac{\sum_{i \in \{0,1\}} \beta_i^{\alpha-1} [P_0 \gamma_i + (1 - P_0) \beta_i]^{\alpha-1} [(-1)^{i+1} P_0 \gamma_i + (1 - P_0)(1 - 2\beta_i)]}{\sum_{i \in \{0,1\}} \beta_i^\alpha [[P_0 \gamma_i + (1 - P_0) \beta_i]^\alpha]} \\ &\left. - 2 \sum_{i \in \{0,1\}} \frac{(-1)^{i+1} (1 - P_0)}{P_0 \gamma_i + (1 - P_0) \beta_i} \right] \end{aligned} \quad (4.37)$$

Based on equation (4.37) :

$$\begin{aligned} \frac{\partial Rc_\alpha}{\partial P_D} &= 0 \text{ if } P_D = P_F, \\ \frac{\partial Rc_\alpha}{\partial P_D} &> 0 \text{ if } P_D > P_F, \\ \frac{\partial Rc_\alpha}{\partial P_D} &< 0 \text{ if } P_D < P_F. \end{aligned}$$

We conclude that, α -Rc is a decreasing function on $[0, P_D[$ and an increasing function on $]P_D, 1]$ with a minimum point reached at $P_D = P_F$. So, by maximizing the α -Rc, the P_D is maximized when P_F is fixed.

2. for $P_D = \text{constant}$, the derivative of α -Rc with respect to P_F is written as :

$$\begin{aligned} \frac{\partial Rc_\alpha}{\partial P_F} &= \frac{\alpha}{\alpha - 1} \left[P_0 \frac{\sum_{i \in \{0,1\}} (-1)^{i+1} \beta_i^\alpha [P_0 \gamma_i + (1 - P_0) \beta_i]^{\alpha-1}}{\sum_{i \in \{0,1\}} (-1)^{i+1} \beta_i^\alpha [P_0 \gamma_i + (1 - P_0) \beta_i]^\alpha} \right. \\ &\frac{\sum_{i \in \{0,1\}} \gamma_i^{\alpha-1} [P_0 \gamma_i + (1 - P_0) \beta_i]^{\alpha-1} [P_0 + (-1)^{i+1} (1 - P_0) \beta_i - 2P_0 \gamma_i]}{\sum_{i \in \{0,1\}} \gamma_i^\alpha [P_0 \gamma_i + (1 - P_0) \beta_i]^\alpha} \\ &\left. - 2 \sum_{i \in \{0,1\}} \frac{(-1)^{i+1} P_0}{P_0 \gamma_i + (1 - P_0) \beta_i} \right] \end{aligned} \quad (4.38)$$

Based on equation (4.38) :

$$\begin{aligned} \frac{\partial Rc_\alpha}{\partial P_F} &= 0 \text{ if } P_F = P_D, \\ \frac{\partial Rc_\alpha}{\partial P_F} &> 0 \text{ if } P_F > P_D, \\ \frac{\partial Rc_\alpha}{\partial P_F} &< 0 \text{ if } P_F < P_D. \end{aligned}$$

We conclude that, α -Rc is a decreasing function on $[0, P_F[$ and an increasing function on $]P_F, 1]$ with an minimum point reached at $P_F = P_D$. So, by maximizing the α -Rc, the P_F is minimized when P_D is fixed.

As conclusion, in order to minimize the false alarm probability and to maximize the detection probability, it is equivalent to maximizing the α -Rc which is achieved where $P_D = P_F$.

4.4.6 Threshold Optimization Algorithm

As we are interested in minimizing the missed detection probability and maximizing the detection probability, the threshold corresponding to these conditions is found by the maximization of α -Rc.

Starting from the Bayes rule :

$$\frac{p(x/H_1)p(H_1)}{p(x)} \underset{H_0}{\overset{H_1}{\geq}} \frac{p(x/H_0)p(H_0)}{p(x)} \quad (4.39)$$

which leads to the likelihood ratio test written as :

$$\Lambda = \frac{p(x/H_1)}{p(x/H_0)} \underset{H_0}{\overset{H_1}{\geq}} \frac{p(H_0)}{p(H_1)} \quad (4.40)$$

and by setting the derivative of α -Rc in equation 4.36 to zero ($\frac{\partial Rc_\alpha}{\partial v} \Big|_{v=th} = 0$), the likelihood ratio, linked to the threshold $\frac{\partial P_D}{\partial P_F} = \Lambda$, that maximizes the α -Rc is written as :

$$\Lambda \underset{H_0}{\overset{H_1}{\geq}} \frac{a(A_{01} + A_{10}) + b(B_{01} + B_{10}) + \frac{PM}{V}}{C_{01}(A_{01} - A_{10}) - C_{10}(A_{01} + A_{10}) + d(B_{01} + B_{10}) + \frac{PN}{V}} \quad (4.41)$$

where :

$$\begin{aligned} l_{ij} &= P_0\beta_j\gamma_i + (1 - P_0)\beta_j\beta_i \\ n_{ij} &= P_0\gamma_i\gamma_j + (1 - P_0)\beta_j\gamma_i \\ A_{ij} &= l_{ij}^\alpha, \quad B_{ij} = n_{ij}^\alpha, \quad C_{ij} = n_{ij}^{\alpha-1}(1 - P_0)\gamma_0 \\ a &= [-P_0(\gamma_0 - \gamma_1) + (1 - P_0)\beta_1]n_{ij}^{\alpha-1} + [-P_0(\gamma_0 - \gamma_1) - (1 - P_0)\beta_0]n_{ji}^{\alpha-1} \\ b &= l_{ij}^{\alpha-1}P_0\beta_1 - l_{ji}^{\alpha-1}P_0\beta_0 \\ d &= P_0\gamma_0 - (1 - P_0)(\beta_0 + \beta_1)l_{ij}^{\alpha-1} - P_0\gamma_1 + (1 - P_0)(\beta_0 - \beta_1)l_{ji}^{\alpha-1} \\ P &= (n_{ij}^\alpha + n_{ji}^\alpha)(l_{ij}^\alpha + l_{ji}^\alpha) \\ M &= 2P_0^2(\gamma_0 - \gamma_1) + 2P_0(1 - P_0)(\beta_0 - \beta_1) \\ N &= 2(1 - P_0)(\gamma_1 - \gamma_0) + 2(1 - P_0)^2(\beta_1 - \beta_0) \\ V &= P_0^2\gamma_0\gamma_1 + (1 - P_0)P_0\gamma_0\beta_1 + (1 - P_0)P_0\beta_0\gamma_1 + (1 - P_0)^2\beta_0\beta_1 \end{aligned} \quad (4.42)$$

with :

$$i = \bar{j} \in \{0, 1\}$$

The threshold optimization algorithm is given as follows :

4.5 A Fault Tolerant Architecture based on UIO

In the field of diagnostic and monitoring, the FDI methods are considered as the robust solution for uncertainties and unknown disturbances in a complex

Algorithm 1: Threshold optimization based on α -Rc

```

Estimate  $P_0$ ;
 $\alpha$ - $Rc_{max} = 0$ ;
for  $\lambda = \lambda_{min}$  to  $\lambda_{max}$  do
    calculate the corresponding  $P_D^\lambda$  and  $P_F^\lambda$ 
    calculate  $\alpha$ - $RD_\lambda$ 
    if  $\alpha$ - $RD_\lambda > \alpha$ - $Rc_{max}$  then
         $\alpha$ - $Rc_{max} = \alpha$ - $RD_\lambda$ ;
         $P_D^{opt} = P_D^\lambda$ ;
         $P_F^{opt} = P_F^\lambda$ ;
         $\lambda_{opt} = \lambda_\lambda$ ;
    end
end
end

```

dynamic systems. As mentioned in the previous sections, there are a great variety of model based FDI methods in the literature. Therefore, model-based FDI is in fact designed on a number of idealised hypotheses. First, concerning the mathematical model used as an accurate replica of the dynamic system. And second the inability to anticipate problems arising from practical systems as inescapable perturbations and model uncertainties, which lead to bias in the residual, hence, a wrong response to unexciting fault in the sensor. Based on this point, the robustness in FDI is directly related to the impact of system uncertainties on the FDI method performance. Thus, a robust FDI method must generate residuals sensitive to faults and not to uncertainties and/or unknown perturbations. One of the most used implementations is the concept of the disturbance decoupling principle. Where the Unknown Input Observers has been widely studied and has been successfully applied in several fields of application.

UIO is defined in (J. CHEN et al., 2012) as : "*An observer is defined as an unknown input observer for the system, if its state estimation error vector approaches zero asymptotically, regardless of the presence of the unknown input (disturbance) in the system*".

The general concept of the UIO design is to decouple the perturbations from the state estimation error. In other words, the idea is to extract an observable subsystem from the original system, and in this sub-system the fault(s) of interest are revealed, while the rest of the fault(s) are not. Then an observer gain is obtained through Kalman filter family (figure 4.8). Therefore, the choice of the information filter makes a lot of sense and is more suitable for this type of architectures. Where in the informational form, it will suffice to remove the contribution of each observation in order to isolate the fault.

Before any UIO based FDI design, three questions should studied :

1. what are the suitable conditions to achieve multi-fault isolation ?
2. what is the limit of faults removed simultaneously ?
3. What is the best design for multi-fault isolation method ?

In the literature, two different type of UIO design approaches are exist. The first study supposes some *a priori* information about the immeasurable inputs, where, the second suggests to reconstruct the state of the linear system through an observer able to deal with the presence of unknown inputs. Noting that, UIO methods are designed for a linearized system around an operating point. Hence, for a good performance results the linearization should not lead a large difference between the linear created model and the non-linear behavior. Thus, in order to design a non-linear UIO method, three main points should be taken into consideration :

1. Techniques based on non-linear state transformation,
2. Techniques based on linearization,
3. observers for particular classes of nonlinear systems.

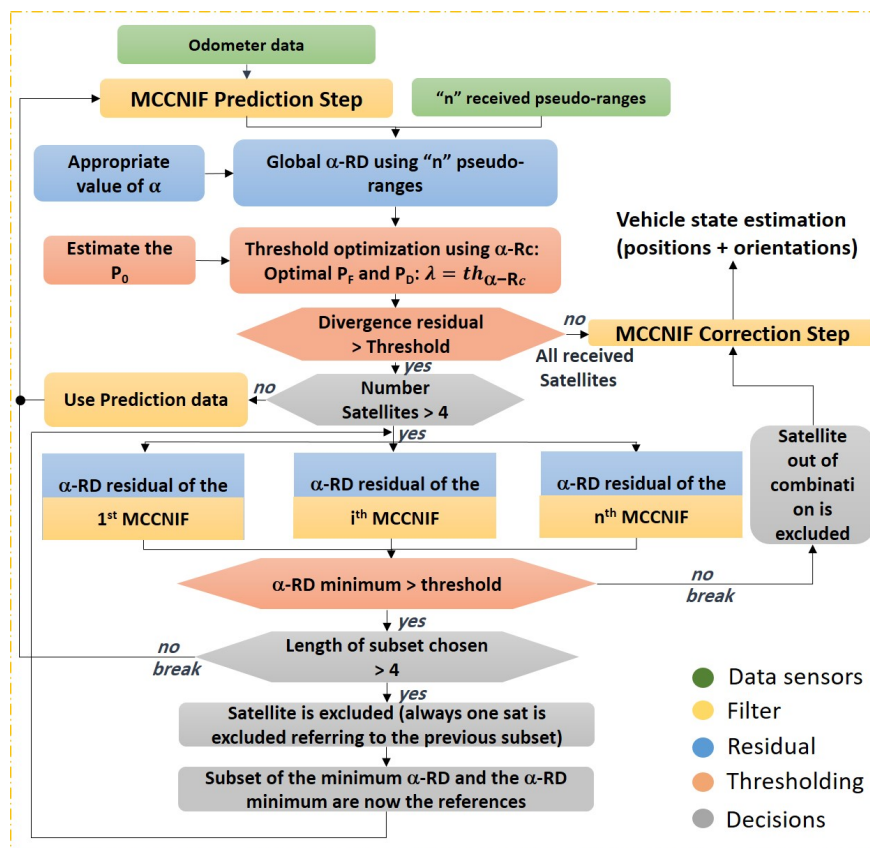


FIGURE 4.8 – UIO architecture design

A brief example in figure (figure 4.8) of the UIO architecture is presented. Where, the MCCNIF is chosen as the main estimator, then, subsets of MCCNIF are used for each possible combination of satellites. Thus, a residual is calculated for each subset and compared with the optimized threshold. The details of the process are presented in chapter 4, and 5.

4.6 Chapter Conclusion

In this chapter, we presented the proposed approach. Where, the role of each part in the approach is discussed in different sections, in order to highlight each proposed contribution. First, an introduction to the proposed framework is presented, and a table summarizing the problems that may be encountered in an experiment is shown, along with proposed solutions. Next, the approach is described through a block diagram showing the details of each part of the algorithm. The first one is focusing on the fusion sensors part, and the relevance of choosing robust criterion for a robust estimator. Based on the given explanation, a filter called MCCNIF is proposed and developed. Going to the diagnosis section, we proposed a parametric residuals design based on α -RD, followed by an interpretation for the impact of the parameter α on the residuals. The originality that α -RD offers is that the residuals can be related to the environment through the α parameter. One of the solutions to select the value of α is proposed by the concept of α balance, that assure the equilibrium between the evolution and observation models. By proposing an infinity of residuals, an infinity of faulty and non-faulty distributions must be created. Hence, a mathematical models were proposed to solve such problem. Going to the decision part, α -Rc for adaptive thresholding is proposed and developed. In addition, the design of the α -Rényi criterion for an optimized decision making is shown. Finally, and after the decision is made, a fault tolerant architecture based on separation algorithm is proposed. The UIO design was proposed and the reason of the choice was explained.

Chapter 5

Application : Robust and Fail-Safe Outdoor Localisation of an Autonomous Vehicle

5.1 Chapter Introduction

The previous chapters were dedicated to the explanation of the concept of proposed AFTF approach as well as relevant terms were defined. This algorithm is applied in this chapter on a real application and the results are presented in a way to highlight the effect of each main part of the algorithm. The whole framework is tested in real conditions using an autonomous vehicle multi-sensor localization task in different stringent environments. Where, a combination of the GNSS with the odo data by a tight coupling, through a robust optimality criterion, the maximum correntropy criterion, and a fault detection and isolation strategy, for a robust and fault tolerant multi-sensor fusion approach is presented, taking advantage of the information theory. The new estimator filter will be presented and discussed combining the advantages of the NIF under the MCC. Where, the NIF deals fairly with nonlinearity problems, and the MCC shows good performance with non-Gaussian noises, especially with shot noises and Gaussian mixture noises. To detect and isolate the erroneous measurements, an adaptive diagnosis approach through an FDI layer, based on α -RD between the a priori and a posteriori probability distributions, is proposed. Then, an adaptive threshold is calculated as a decision-making part of the proposed framework based on the α -Rc.

5.2 Technical Aspects

In this section and before introducing the experimental results and how the proposed algorithm is applied using GNSS/odo fusion, a brief introduction, for the type of data and the main tools used for the experiments, is presented.

5.2.1 Data Acquisition Equipment Details

The equipment needed and used for data acquisition in the experimental results are detailed as following :

1. odometer data

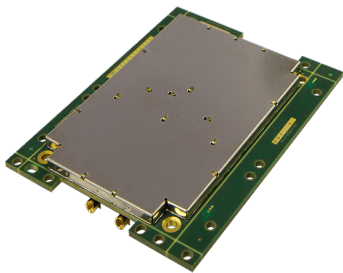
Data are mainly calculated from the encoder, related to the vehicle wheels, that acquires the data from the Can-Bus of the car, with a frequency of 50Hz, in the form of (Δ, ω) , representing the elementary displacement and elementary rotation respectively.

2. References data (ground-truth)

In order to create trajectory references, an accurate GNSS receiver must be used. In our experiments, we were based on the Septentrio receivers in certain trajectories, and on the PwrPak7 of Novatel in the others. They both use RAIM solution, and are multi-constellation, where, tracks all known and future GNSS signals from GPS, GLONASS, Galileo, BeiDou, IRNSS, QZSS, and SBAS.

— Septentrio receivers

The AsteRx4 (figure 5.1a) and the PolaRx5 (figure 5.1b) are two types of Septentrio receivers used for ground-truth creation. Both are multi-frequency engine receiver, that provide high accuracy and functionality, with up to 20 Hz data output rate. In addition, the AsteRx4 is a triple-frequency engine with dual antenna receiver, and can deliver high accuracy scalable to cm (centimeter) level using RTK (Real-time kinematic) solution, and dm (decimeter) level through PPP (Precise Point Positioning).



(a) AsteRx4 receiver



(b) PolaRx5 receiver

FIGURE 5.1 – Septentrio receivers

— PwrPak7 receiver

PwrPak7 is also a high accuracy receiver offered by NovAtel. It delivers scalable GNSS with internal storage (16 GB) and INS options

with up to 100 Hz maximum data rate, and can reach an RTK accuracy level of $1\text{cm} + 1\text{ppm}$ (*parts - per - million*).



FIGURE 5.2 – PwrPak7 - NovAtel receiver

3. U-blox receiver

EVK-M8P receiver is one of the lowest cost and most available option offered by u-blox, that provides access to the raw GNSS position signals (pseudo-range and carrier phase). It is used to apply our proposed approach, in order to see how we are able to deliver, and reach the accuracy, and the precision provided by the Septentrio and NoVatel.

5.2.2 Trajectories details

The equipment mentioned above are used in different trajectories for data collection and experiment tests. We present the real 2D view, using Google Earth software, in figure 5.3 illustrating the trajectories. Where for collecting the statistical data needed to create the distributions (faulty and non-faulty), we used the same installation with the same receivers and equipment using all the six trajectories (C1, C2, C3, C4, C5, and C6). Then, some of these trajectories (C1, C3, C4) interesting in term of faults are chosen in order to implement, and present the results. It is possible to provide the results for each of these trajectories, but this will be redundant because the same behavior in the results is repeated in each of them. Then, we detailed the acquisition information for each trajectory in the table 5.1.



FIGURE 5.3 – Trajectories references

TABLE 5.1 – Data acquisition information for trajectories

Trajectory name	Acquisition location	Number of epochs	Trajectory length
C1	Villeneuve-d'Ascq	261	1134.2 meters
C2	Villeneuve-d'Ascq	610	3444.6 meters
C3	Villeneuve-d'Ascq	1477	9844.71 meters
C4	Villeneuve-d'Ascq	370	348.85 meters
C5	Villeneuve-d'Ascq	-	467.45 meters
C6	Villeneuve-d'Ascq	-	2473.02 meters

5.2.3 Development And Processing Tools

Within the framework of our developments, we have adopted the use of a software whose purpose is to perform GNSS positioning with different types

of open GNSS receivers, called "goGPS". The goGPS is a positioning software application designed to process GNSS observations for absolute or relative positioning (HERRERA et al., 2016). It is published under a free and open-source license dedicated to the processing of GNSS raw data. The first version of goGPS was released in 2009, and was initially created for low-cost single frequency GPS receivers, but today it can fully exploit multi-constellation, multi-frequency and multi-track observations. The goGPS implements multiple algorithms to analyze the data and can currently produce epoch-by epoch solutions by Least Squares Adjustment (LSA), or multi-epoch solutions by Kalman filtering. Starting with the original version of goGPS, we integrated our algorithms as well different tested filters like the NIF, UKF, UIF, MCCEKF, MCCNIF, MCCUKF, and MCCUIF (figure 5.4). The goGPS collects input observations either by reading standard RINEX files, from low-cost or geodetic receivers, or by decoding receiver-specific binary formats. Currently, only the MATLAB version provides a graphical user interface.

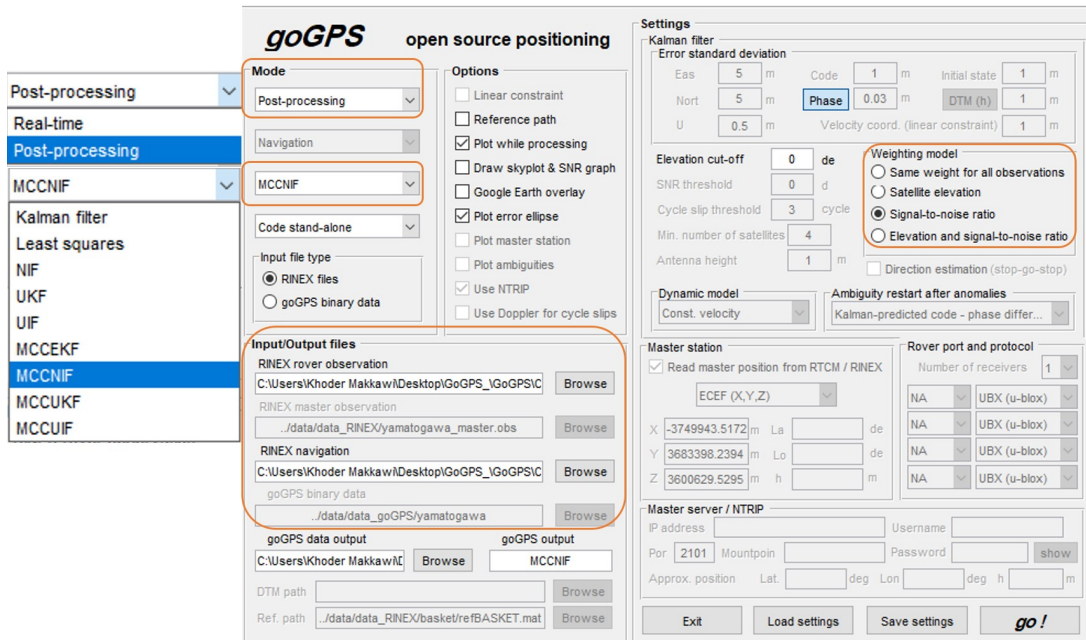


FIGURE 5.4 – goGPS interface

As we can see in figure 5.4, the MATLAB interface provided by the goGPS allow to user to choose between different weighting model : 1) weight all the observations equally, 2) as function of elevation of the satellites, 3) as function of Signal-to-Noise Ratio (SNR), and 4) as a combination of the elevation with the SNR. It also offers the possibility to run either in real-time mode, or in post-processing mode. In real-time mode the data are collected via USB port from the receiver and the master station data via internet. Otherwise, in post-processing mode the reading master and rover RINEX files are saved during the real-time acquisition data. The new incarnation of goGPS limits most of the effort required to process RINEX files.

Noting that, the philosophy of Receiver Independent Exchange Format (RI-

NEX) has been developed by the Astronomical Institute of the University of Berne for the easy exchange of the GPS data to be collected during the large European GPS campaign "EUREF 89". RINEX is the standard format that allows the treatment and elimination of measurements generated by a receiver. It allows the storage of pseudorange, carrier phase, Doppler and GNSS SNR measurements. This set of received data are defined as :

- Pseudo range measurement (or code measurement) is a measure of the propagation time required for a time mark transmitted by a satellite to reach the receiver on Earth,
- The principle of carrier phase measurement is the comparison of the phase of the wave received by the receiver with the phase of a wave generated inside the receiver, which is a replica of the satellite signal,
- Signal-to-Noise Ratio is a ratio of signal power to the noise floor of the GNSS observation, the measured SNR are directly related to carrier phase errors due to multipath (BILICH et al., 2007),
- Doppler measurement provides information on the relative speed of the receiver with respect to the satellite. It is the difference between the frequency of the received signal measured by the receiver and the frequency of the source signal emitted by the satellite.

5.3 MCCNIF Versus Classical MMSE-Based NIF Robustness Against Non-Gaussian Noises

After presenting the tools and the equipment used in our experiments, we illustrate in this section the results of the proposed algorithm by highlighting the importance of each main part in details.

The first presented results focus on the fusion part and how the filter can affect the robustness of the system. In this section, we propose a filter named "MCC-NIF". This combination allows to deal with the non-linearity problems through the NIF, and to treat the non-Gaussian noises with the MCC. To ensure an accurate and a robust estimated position, its robustness against non-Gaussian noises and in sensors fusion are tested in the following sub-sections. Where after studying the sensor fusion, an experiment of the localization system is stressed by injecting Gaussian mixture noises (MGn) in order to highlight the interest of the MCC facing non-Gaussian noises.

5.3.1 Tight GNSS/Odometer Intergration Through MCC-NIF

The fusion of GNSS pseudo-ranges and odo measurements is presented and occurred under the MCCNIF. The vehicle position and orientation are illustrated with the offset of the receiver clock and its variation in the state vector represented by :

$$X_k = [x_k \ y_k \ z_k \ \theta_k \ c\delta t_{r,k} \ c\frac{\partial\delta t_{r,k}}{\partial k}]^T \quad (5.1)$$

Where : $[x_k \ y_k \ z_k]^T$ is the position given at instant k in the Earth Centered Earth Fixed frame. c is the speed of light, θ_k the vehicle's heading, $\delta t_{r,k}$ is the clock shift of the receiver with respect to GNSS reference time and k is the sampling time.

The multi-sensor fusion is assured through two main steps that compose the MCCNIF :

1. The prediction step estimates the state vector, through the NIF, it is estimated using :
 - the information vector obtained by :

$$y_{k/k-1} = Y_{k/k-1} X_{k/k-1} \quad (5.2)$$

- the information matrix calculated using :

$$Y_{k/k-1} = [F_k P_{k-1/k-1} F_k^T + B_k (Q_u)_k B_k^T + Q_k]^{-1} \quad (5.3)$$

Considering :

Q_u is the input vector variance-covariance matrix,

F_k is the Jacobian matrix of f : $F_k = \frac{\partial f}{\partial X} |_{X=X_{k-1/k-1}}$,

It can be written as :

$$F_k = \begin{bmatrix} 1 & 0 & 0 & -\Delta_k \sin(\theta_{k-1/k-1} + \frac{T_e \omega_k}{2}) & 0 & 0 \\ 0 & 1 & 0 & \Delta_k \cos(\theta_{k-1/k-1} + \frac{T_e \omega_k}{2}) & 0 & 0 \\ 0 & 0 & 1 & 0 & 0 & 0 \\ 0 & 0 & 0 & 1 & 0 & 0 \\ 0 & 0 & 0 & 0 & 1 & T_e \\ 0 & 0 & 0 & 0 & 0 & 1 \end{bmatrix} \quad (5.4)$$

B_k is the Jacobian matrix calculated as : $B_k = \frac{\partial f}{\partial u} |_{u=u_k}$.

It can be written as :

$$B_k = \begin{bmatrix} \cos(\theta_{k-1/k-1} + \frac{T_e \omega_k}{2}) & -\frac{1}{2} \Delta_k \sin(\theta_{k-1/k-1} + \frac{T_e \omega_k}{2}) \\ \sin(\theta_{k-1/k-1} + \frac{T_e \omega_k}{2}) & \frac{1}{2} \Delta_k \cos(\theta_{k-1/k-1} + \frac{T_e \omega_k}{2}) \\ 0 & 0 \\ 0 & 1 \\ 0 & 0 \\ 0 & 0 \end{bmatrix} \quad (5.5)$$

The predicted state $X_{k/k-1}$ is computed using the state transition model :

$$X_{k/k-1} = f(X_{k-1/k-1}, u_k) + b_k \quad (5.6)$$

where :

$$f(X_{k-1/k-1}, u_k) = T X_{k-1/k-1} + A_k u_k \quad (5.7)$$

T is the model transition matrix defined by :

$$T = \begin{bmatrix} 1 & 0 & 0 & 0 & 0 & 0 \\ 0 & 1 & 0 & 0 & 0 & 0 \\ 0 & 0 & 1 & 0 & 0 & 0 \\ 0 & 0 & 0 & 1 & 0 & 0 \\ 0 & 0 & 0 & 0 & 1 & T_e \\ 0 & 0 & 0 & 0 & 0 & 1 \end{bmatrix} \quad (5.8)$$

T_e is the sampling time. A_k is the input matrix defined by :

$$A_k = \begin{bmatrix} \cos(\theta_{k-1/k-1} + \frac{T_e \omega_k}{2}) & 0 \\ \sin(\theta_{k-1/k-1} + \frac{T_e \omega_k}{2}) & 0 \\ 0 & 0 \\ 0 & 1 \\ 0 & 0 \\ 0 & 0 \end{bmatrix} \quad (5.9)$$

u_k is the input vector consisting of the elementary translation Δ and rotation ω of the vehicle : $u = [\Delta, \omega]$. And b_k is the model noise considered to be a Gaussian white noise of zero mean value and covariance matrix Q_k .

2. After pseudo-ranges reception, the equations of the correction step can be evaluated. The estimation of state vector is corrected by taking into consideration the GNSS pseudo-ranges observations. These observations measurements can be described as :

$$Z_k = H_k X_k + \epsilon_k \quad (5.10)$$

Where Z_k is the pseudo-range observations vector,
 H_k is the observation matrix which seen as :

$$H = \begin{bmatrix} \nabla H_{x_{pr}}^{x_1^s} & 0 & \nabla H_{y_{pr}}^{y_1^s} & 0 & \nabla H_{z_{pr}}^{z_1^s} & 0 & 1 & 0 \\ \vdots & \vdots \\ \nabla H_{x_{pr}}^{x_i^s} & 0 & \nabla H_{y_{pr}}^{y_i^s} & 0 & \nabla H_{z_{pr}}^{z_i^s} & 0 & 1 & 0 \\ \vdots & \vdots \\ \nabla H_{x_{pr}}^{x_n^s} & 0 & \nabla H_{y_{pr}}^{y_n^s} & 0 & \nabla H_{z_{pr}}^{z_n^s} & 0 & 1 & 0 \end{bmatrix} \quad (5.11)$$

With :

$$\begin{aligned} \nabla H_{x_{pr}}^{x_i^s} &= \frac{\partial \rho^{x_i^s}}{\partial x} = -\frac{(x_i^s - \hat{x}_{pr})}{\rho^{s_i}} \\ \nabla H_{y_{pr}}^{y_i^s} &= \frac{\partial \rho^{y_i^s}}{\partial y} = -\frac{(y_i^s - \hat{y}_{pr})}{\rho^{s_i}} \\ \nabla H_{z_{pr}}^{z_i^s} &= \frac{\partial \rho^{z_i^s}}{\partial z} = -\frac{(z_i^s - \hat{z}_{pr})}{\rho^{s_i}} \end{aligned} \quad (5.12)$$

and ϵ_k is the observation noise with a covariance matrix R_k represented as :

— For Gaussian noise :

$$R(k) = \begin{bmatrix} \sigma_{\rho_1}^2 & \cdots & 0 \\ \vdots & \sigma_{\rho_j}^2 & \vdots \\ 0 & \cdots & \sigma_{\rho_n}^2 \end{bmatrix} \quad (5.13)$$

— For mixture Gaussian noise (MGn) :

$$R(k) = \phi N(\mu_{y_1}, R_1) + (1 - \phi)N(\mu_{y_2}, R_2) \quad (5.14)$$

Where ρ is the pseudo-range that can be calculated through :

$$\rho^{s_i} = \sqrt{(x^{s_i} - \hat{x}_{pr})^2 + (y^{s_i} - \hat{y}_{pr})^2 + (z^{s_i} - \hat{z}_{pr})^2} \quad (5.15)$$

and σ^2 is the variance of noise measurements.

Hence, the corrected information vector $y_{k/k}$ and matrix $Y_{k/k}$ are respectively calculated through the Mercer kernel as it is the most used (SANTAMARIA et al., 2006) using :

$$y_{k/k} = y_{k/k-1} + \sum_{i=1}^N pI_i(k) \quad (5.16)$$

$$Y_{k/k} = Y_{k/k-1} + \sum_{i=1}^N gI_i(k) \quad (5.17)$$

Where N is the number of viewed satellites at instant k and $gI_i(k)$ and $pI_i(k)$ are seen as information contribution TMAZIRTE et al., 2014 calculated as :

$$gI_i(k) = ker_{i,k} H_{i,k}^T R_i^{-1}(k) H_{i,k} \quad (5.18)$$

$$pI_i(k) = ker_{i,k} H_{i,k}^T R_i^{-1}(k) [(Z_{i,k} - Z_{i,k/k-1}) + H_{i,k} X_{k/k-1}] \quad (5.19)$$

With

$$ker(Z_{i,k}, Z_{i,k/k-1}) = \frac{1}{\sqrt{2\pi\beta}} \exp\left(-\frac{\|Z_{i,k} - Z_{i,k/k-1}\|_{R_{i,k}^{-1}}^2}{2\beta^2}\right) \quad (5.20)$$

Where β is the kernel bandwidth. This parameter has a significant influence on the convergence of the filter as mentioned in (B. CHEN, X. LIU et al., 2017) in the theorem 4. In the literature, different method exist to calculate the kernel bandwidth. (B. CHEN, X. LIU et al., 2017) says that the kernel bandwidth can be set manually or optimized by trial and error methods. In (G. WANG et al., 2017), authors provide a new adaptive way to calculate the kernel bandwidth. In our application, and based on the statistical knowledge of the received pseudo-ranges error behavior the kernel bandwidth is estimated using the most common optimally criterion used to select this parameter, the mean integrated squared error (MISE).

5.3.2 Impact Of GNSS/Odo Fusion

This section is dedicated to show the impact of the multi-sensor fusion on the whole algorithm. Therefore, a comparison between the GNSS standalone and the GNSS/odo performances is conducted. The comparison is done without the FDI approach for both GNSS standalone and GNSS/odo. Details for the used trajectory C1 (figure 5.3a) can be found in the table 5.1. The performance of fusion can be noticed, especially with respect to the z-axis in 3D picture, by comparing the average of error on the position seen in figure 5.5 and by using table 5.2, where the mean error in the whole trajectory is much less than using GNSS/odo.

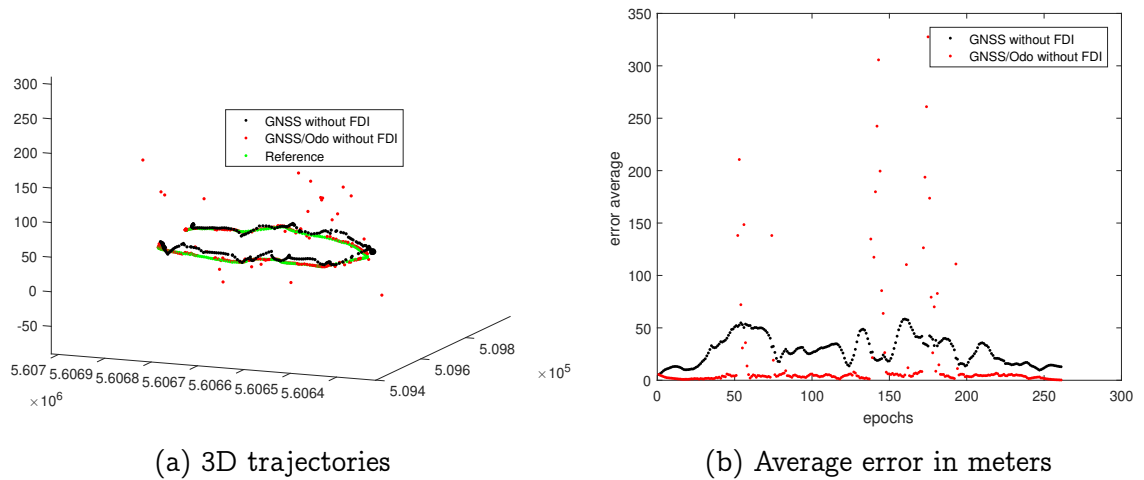


FIGURE 5.5 – GNSS vs GNSS/odo without FDI

TABLE 5.2 – Mean error for GNSS and GNSS/odo without FDI

Error type in meters	GNSS without FDI	GNSS/odo without FDI
Mean error	28.2575	17.0766

5.3.3 Impact Of MCC Compared To MMSE Criterion on non-Gaussian noises

To highlight the effect of MCCNIF when dealing with non-Gaussian noise, a heavy Mixture Gaussian noise (MGn) is injected from the epoch 204 to the epoch 254 in the trajectory "C3". Then, a comparison is made between the MCCNIF, which adopts the maximum correntropy criterion, and the UIF which adopts the minimum squared error criterion. This comparison is to show the superiority of the MCC on the MMSE when dealing with heavy MGn. Hence, the MCCNIF and the UIF are tested using GNSS/odo fusion data without the proposed FDI method.

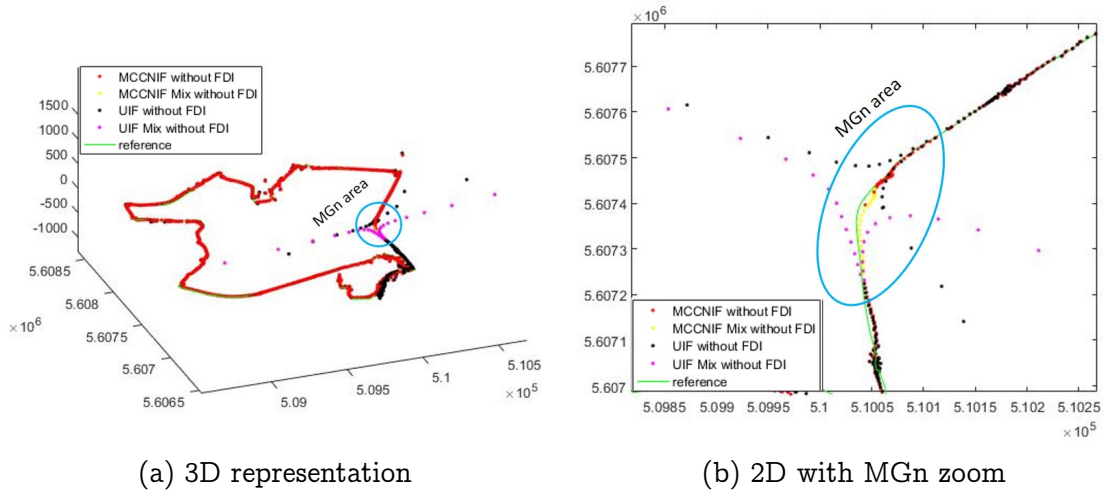


FIGURE 5.6 – MCCNIF vs UIF without FDI

The effect of the MCC on the MGn treatment can be noticed by comparing the performance of MCCNIF and UIF in the figure 5.6. Where the UIF totally diverges during the MGn injection. The MCCNIF was able to deal with this heavy MGn without any diverging and gave a better estimated position. To evaluate the performance of MCC by a different way, the average position error, represented by the median and the mean, at each epoch during the MGn injection is calculated in table 5.3.

TABLE 5.3 – Median and mean error for MCCNIF and UIF without FDI

Data type (meters)	UIF GNSS/odo	MCCNIF GNSS/odo
Median error (MGn area)	660.3594	17.8477
Mean error (MGn area)	$1.6204e^{+04}$	16.4594

This comparison ensure the ability of MCC to deal with heavy MGn and able to keep out of divergence for a robust fusion system.

5.4 Results of the Adaptive FTF proposed Framework

A robust filter for sensors fusion can ensure the availability of the system and in the most of cases the accuracy as well. But, for an autonomous vehicle navigation system, the need of the safety attribute is out of questions. Hence, in this section, we focus on the diagnosis part explained in chapter 3 and 4, to deliver the safety and avoid accuracy problems caused by feared events. Thus, two scenarios are presented based on the proposed α -RD for residuals generation. The first scenario deals with fixed α value in the whole trajectory, where the second one deals with balanced α . The results are shown and a result comparison is done in the end of the two presented scenarios.

Noting that in both scenarios, the same trajectory is compared with the same conditions and the same collected data sensors.

5.4.1 α -RD Residual Based On Unsupervised Clustering

For a fixed value of α , two *pdfs* representing the faulty and faulty free cases must be created. Hence, several kilometers of data collection are realized in different trajectories with different types of weather and through different types of environments, such as open sky, buildings, and raw of trees using the same sensors. In order to classify these residuals as faulty and non-faulty distributions, supervised learning (KOTSIANTIS et al., 2007), semi-supervised learning (X. J. ZHU, 2005) and other machine learning algorithms are proposed in the literature (SUN, 2013).

In the proposed application, there is not any information about the correct classes because of different type of errors which can occur. Our aim is to cluster input residuals that are similar together automatically without being explicitly told that these residuals belong to one class and those to a different class. The unsupervised learning, which uses the dimensionality reduction, and hence clustering of similar data points together (MARSLAND, 2014) is the appropriate choice for our application.

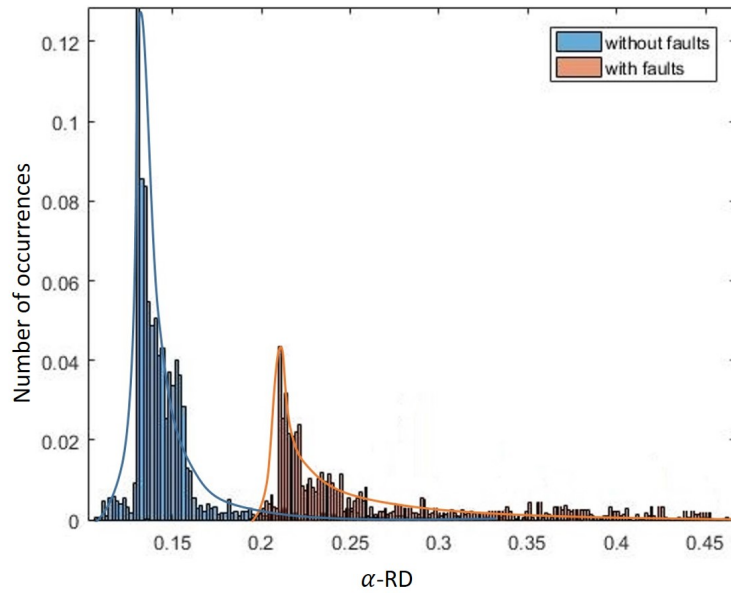


FIGURE 5.7 – Experimental data PDFs of fixed α for the cases without/with faults

In order to cluster our residuals, many methods are proposed in the literature (O. A. ABBAS, 2008),(NAGPAL et al., 2013). The α -RD residuals are clustered using the Expectation Maximization (EM) algorithm, which is a generalization of MLE to the incomplete data case (GANCHEV et al., 2008). The EM algorithm alternates between the E-step by guessing a probability distribu-

tion over completions of missing data given the current model and the M-step by re-estimating the model parameters using these completions (MOON, 1996). Figure 5.7 illustrates the two classes of non-faulty (blue) and faulty distributions (red) created using the EM clustering algorithm.

5.4.2 Impact of α -Rényi On The Detection

After the two *pdfs* are created, the threshold can be specified. In this section, and in order to illustrate the influence of the value of α on the residual, and how this value affects the detection, we used a simple fixed threshold optimized by the ROC curve. Noting that in this section, the results represent the experimental data of trajectory C4 (figure 5.3d). This curve is created by plotting the true positive rate against the false positive rate at various threshold settings (KUMAR et al., 2011), allows the comparison of diagnostic tests carried out on the same data-set. It allows to set an optimized detection threshold.

The slope at any point on the ROC curve is equal to the maximum likelihood ratio of the probability densities of the two distributions ("with" and "without" faulty data) (VEXLER et al., 2008). Then, the AUC (Area Under Curve) of the ROC curve is then calculated and the threshold is specified.

Figure 5.8 shows the α -Rényi residual before the fault detection and isolation method. Where from the epoch 197 to the epoch 204, an observation error is increasing slightly in time (The error is injected manually for the test). This kind of error usually is one of the most difficult errors to detect as it will be detected after it will has a big effect. One of the advantages of α -Rényi is a solution for a fast detection of this type of faults, where a different value of α are tested in order to illustrate their impacts on the Residual. For the value of α equals to 0.1, one can remark that is more complicated to detect this error in the first four epochs as well for the value of α equals to 0.2 for the first three epochs. But, for the values of α equal to 0.5, 0.8 and tends to 1, the slope becomes steeper each epoch, so the detection of error is much easier.

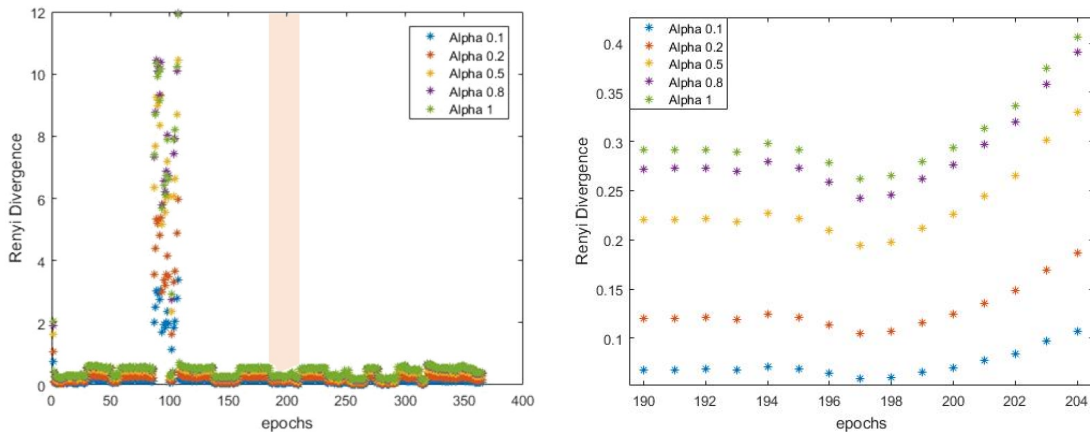


FIGURE 5.8 – Effect of α -Rényi variation on the residuals

Using the same algorithm and thresholding method for each value of α , figure 5.9 illustrates the effect of α -RD between the epochs 197 to 204, where for $\alpha = 0.1$ the error is detected in the epoch 201 and for $\alpha = 0.8$ the error is detected in the epoch 200. In plus, an error is also detected in the epoch 194 for $\alpha = 0.8$, where it is not detected using the $\alpha = 0.1$. Hence, based on the two figures 5.8 and 5.9, one can see that the sensitivity of residuals is directly linked to the fault detect-ability.

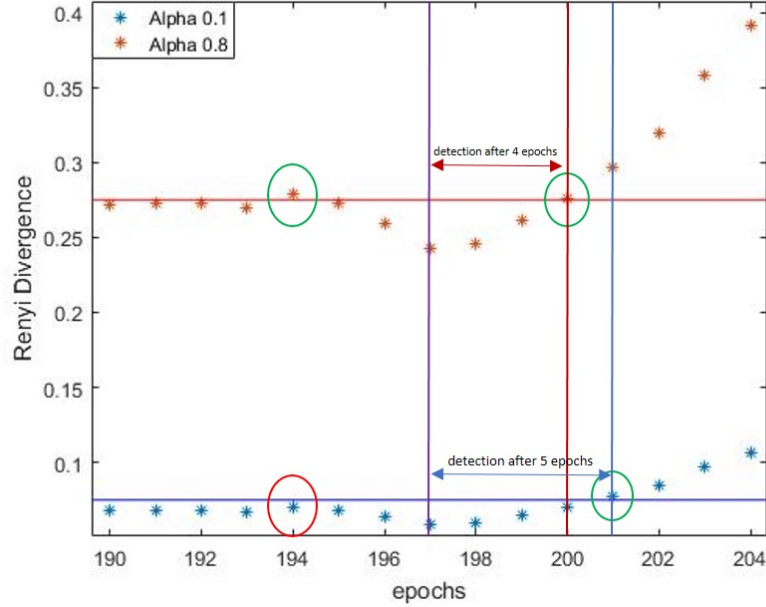


FIGURE 5.9 – Effect of α variation on the detection

5.4.3 Results using different α Strategy Scenarios

After presenting the effect of α on the residual and its impact on the detection, one can ask "how can one choose the best α value?". In chapter 3, we presented, from our point of view, the importance of the adaptive diagnosis, and why it is important to adapt the residuals taking many factors into consideration. Then, we proposed in chapter 4 the α balance as solution to adapt the value of α . In this section, we will adopt the proposed α balance, and present a comparison of the results with fixed α value ($\alpha \rightarrow 1$, so the KLD appears).

Noting that : The place of all the legends in the pictures provided don't cover any information.

Results without FDI approach

The following results in figure 5.10 illustrate the positioning estimation without any FDI algorithm on the trajectory C3 (figure 5.3c). In both views, one can see the level of error presenting especially in the z-axis.

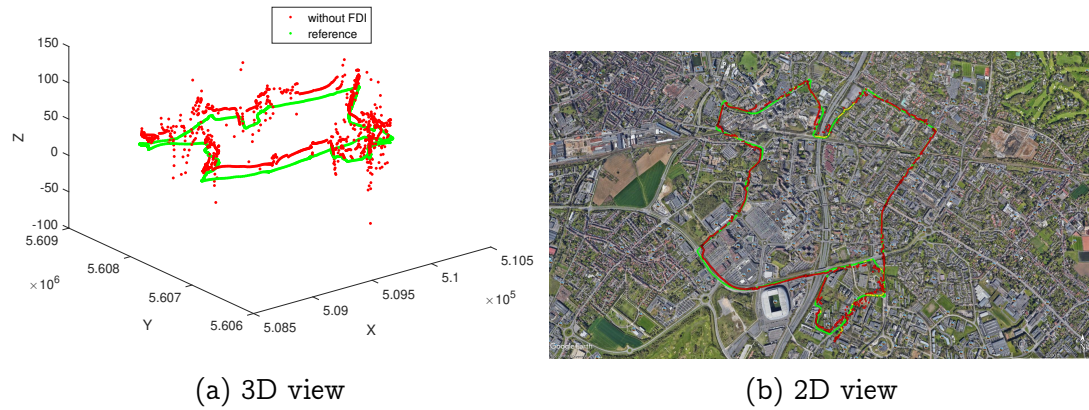


FIGURE 5.10 – Positioning estimation without FDI algorithm vs reference in 3D/2D views

These errors are due either to the multi-paths, signals reflection, NLOS, or related to the low elevation of the satellites available at the instant k . The elevation of all satellites available in this trajectory can be seen in figure 5.11.

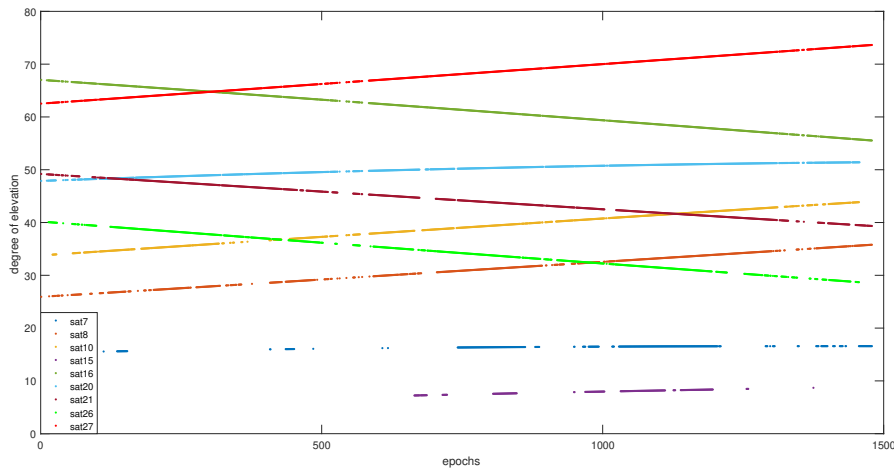


FIGURE 5.11 – Elevation of each satellites during the whole trajectory

In order to detect and isolate these errors, we will provide the results with the FDI proposed algorithm with the fixed and balanced α . But, before going to the next section, figure 5.12 illustrates the global α -Rényi residuals for the fixed and balanced α . These residuals calculated without the FDI approach show a disarrayed alignments which indicate the presence of faults.

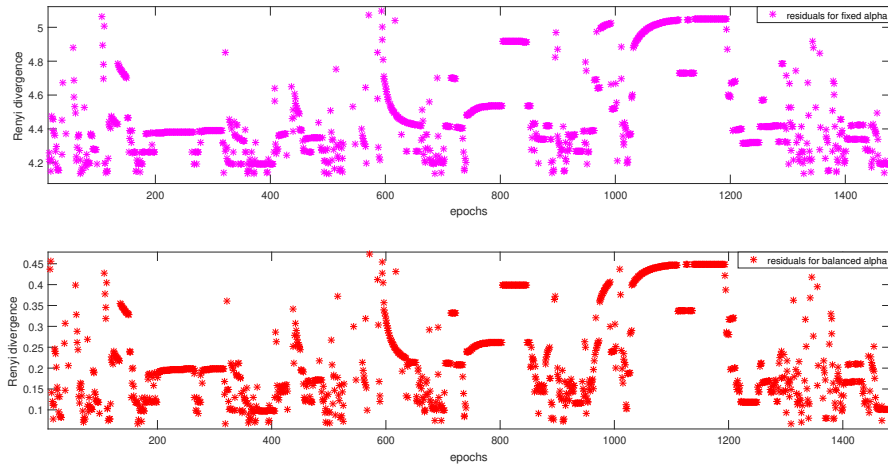


FIGURE 5.12 – α -Rényi Residuals without FDI

Results with FDI approach

As mentioned in section 3.4.3, a good residual design reduces the loss of some fault information. From this point, we will deliver two different scenarios for residual design. The first scenario residuals are generated through fixed α for $\alpha \rightarrow 1$, where the second using the balance α .

1) Residual design using fixed α

The residuals generated by the KLD for each satellites during the whole trajectory can be seen in figure 5.13.

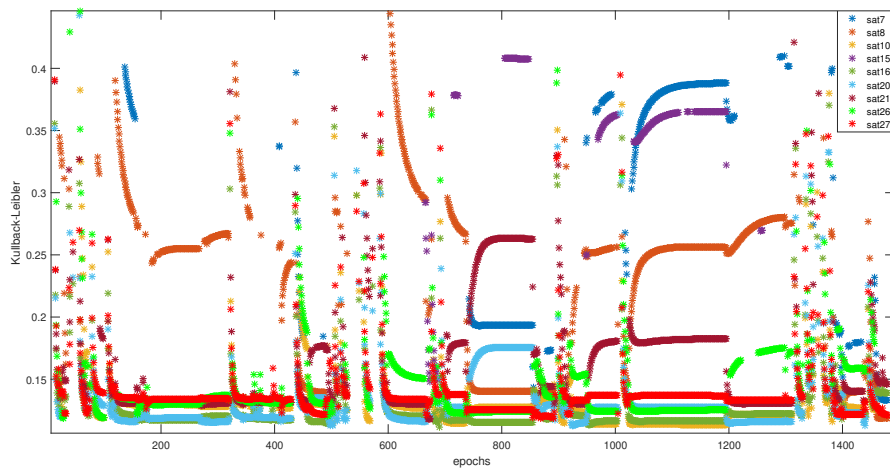


FIGURE 5.13 – Partials KLD observation for identification

The behavior of each satellite is monitored at each epoch during the whole trajectory. The detection of any erroneous behavior is carried out using the KL

criterion by optimizing the threshold value. This threshold is illustrated with the global residuals of KLD, without and with the FDI approach, in the figure 5.14.

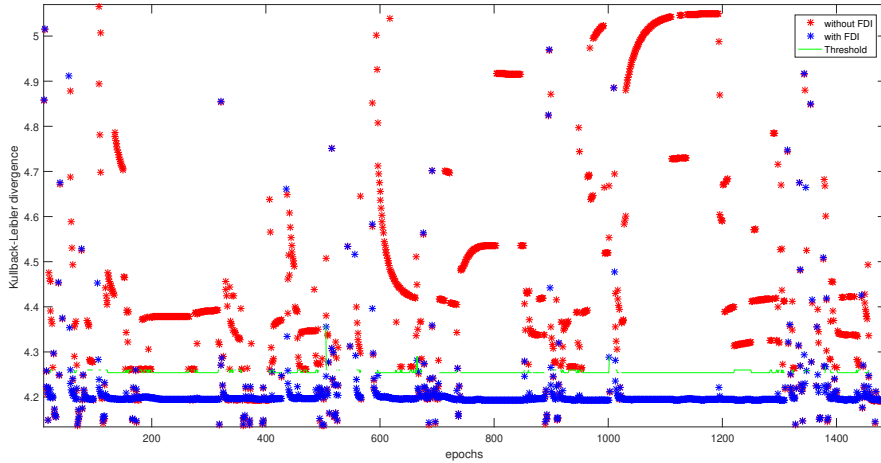


FIGURE 5.14 – KLD divergence without/with FDI with adaptive threshold

As we can see, the threshold is adaptive to the residuals, which mean that it is calculated based on a variable related to the decisions. This variable is P_0 , that takes into consideration the last 10 decisions during the past epochs, and can be calculated using equation 3.21. The P_0 representing the threshold in figure 5.14 can be seen in figure 5.15.

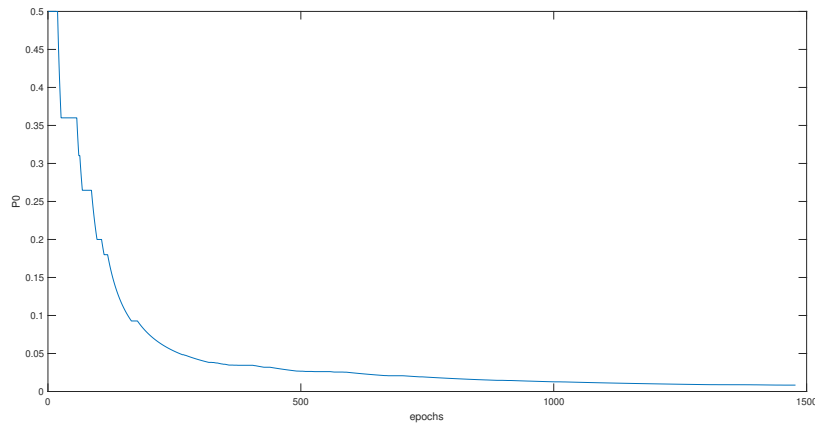


FIGURE 5.15 – P_0 during the whole trajectory

The behavior of P_0 indicated the low probability to not have a detection in the most of the epochs. Where, the value decreases as much as isolation exists in the past epochs, and vice versa.

2) Residual design using α balanced

The same structure of the fixed α will be followed in this section using the α balanced. Where, the α -Rényi residuals for each satellite are presented in the figure 5.16.

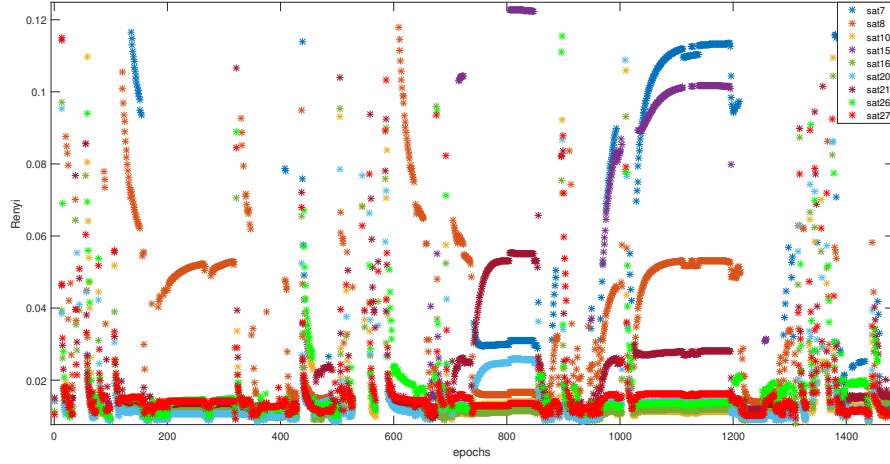


FIGURE 5.16 – Partials Rényi observation for identification

Many of the available satellites carry an erroneous information should be isolated from the final estimation, like satellites 7 (dark blue), 15 (mauve), and 8 (orange). Unlike KLD where the prediction is fully weighted by fixing α , these residuals are generated by equally weighting the prediction and correction covariance matrices. The value of α calculated to weight equally the two matrices, using equation 4.29, can be seen in figure 5.17.

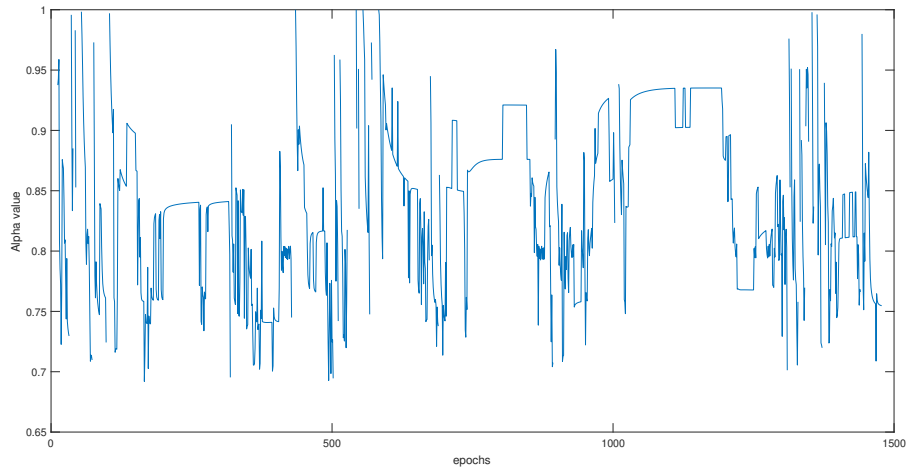
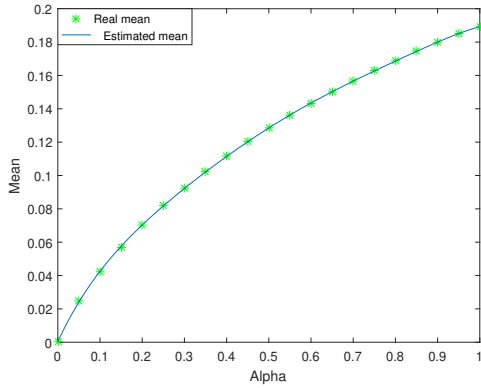


FIGURE 5.17 – Weighted Alpha balance

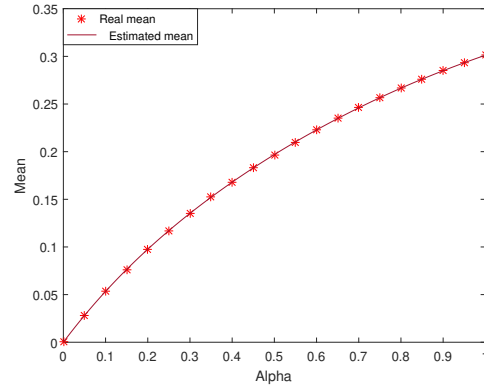
Then, the detection is occurred using an adaptive threshold optimized by the α -Rc, where each residual is judged with his corresponding criterion. Hence, referring to the problem discussed in section 4.4.4, where an infinity of residuals

implies an infinity of statistical characterization, we used the proposed models in order to estimate the mean and the variance for the corresponding value of α .

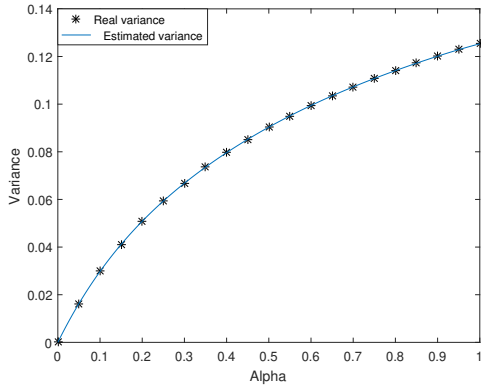
In our application, the models for estimating the means and the variances of faulty and non-faulty distributions are created by fitting the real samples (figure 5.18).



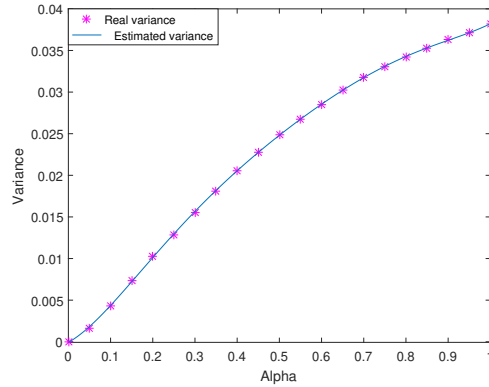
(a) Means for non-faulty distributions



(b) Means for faulty distributions



(c) Variances for non-faulty distributions



(d) Variances for faulty distributions

FIGURE 5.18 – Estimated and real means & variances for faulty and non-faulty distributions

The fitting functions for the real means and variances lead to the following mathematical models for estimating the two distributions of other value of α :

— For non-faulty cases :

$$M_{nf} = -1.2482\alpha^6 + 4.2123\alpha^5 - 5.6404\alpha^4 + 3.8677\alpha^3 - 1.5455\alpha^2 + 0.54279\alpha + 0.00039907 \quad (5.21)$$

$$V_{nf} = -0.24207\alpha^6 + 0.91051\alpha^5 - 1.4299\alpha^4 + 1.2507\alpha^3 - 0.72262\alpha^2 + 0.3587 * \alpha + 6.3904e^{-06} \quad (5.22)$$

— For faulty cases :

$$M_f = 0.11628\alpha^5 - 0.4186\alpha^4 + 0.62826\alpha^3 - 0.61309\alpha^2 + 0.58827\alpha + 9.2291e^{-05} \quad (5.23)$$

$$V_f = 0.29775\alpha^6 - 0.9601\alpha^5 + 1.2201\alpha^4 - 0.77397\alpha^3 + 0.22616\alpha^2 + 0.028363\alpha - 7.1952e^{-05} \quad (5.24)$$

These models are created by fitting the real values of means and variances, taking twenties value of α between $[0, 1]$. Where, the real means and variances are extracted using real experimental *pdfs*.

After generating the statistical characterization used for α -Rc optimization, the adaptive threshold with the global α -Rényi residuals are presented in figure 5.19.

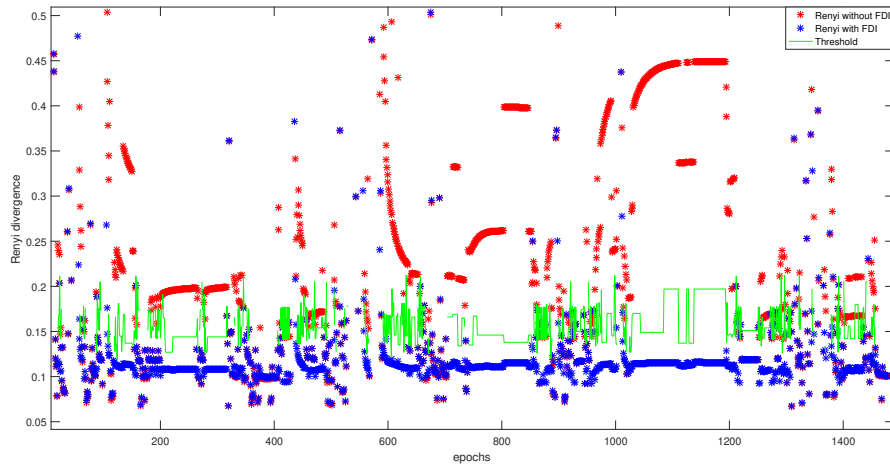


FIGURE 5.19 – Rényi divergence without/with FDI with adaptive threshold

The P_0 related to the previous threshold is seen in figure 5.20.

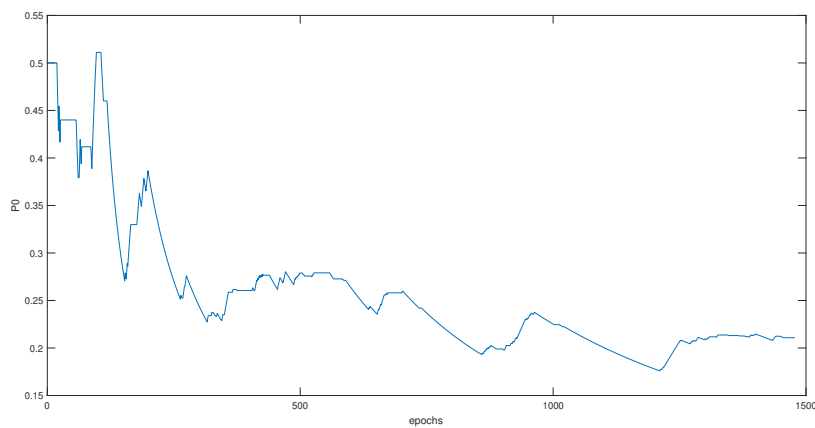


FIGURE 5.20 – P_0 during the whole trajectory

The difference in behavior between the two P_0 , and the two threshold related to the fixed and balanced α , is an indicator of a difference in the decision, which

will affect surely the final estimation.

In the next section, we will compare the final results and try to highlight the source of the differences.

3) Results comparison

In order to judge between the two scenarios, we have to see the impact of the residuals design and the resulting decisions on the estimation position. Let's first look at the effect of the two design architecture on the isolated measurements. The isolated satellites based on the fixed α are illustrated in figure 5.21.

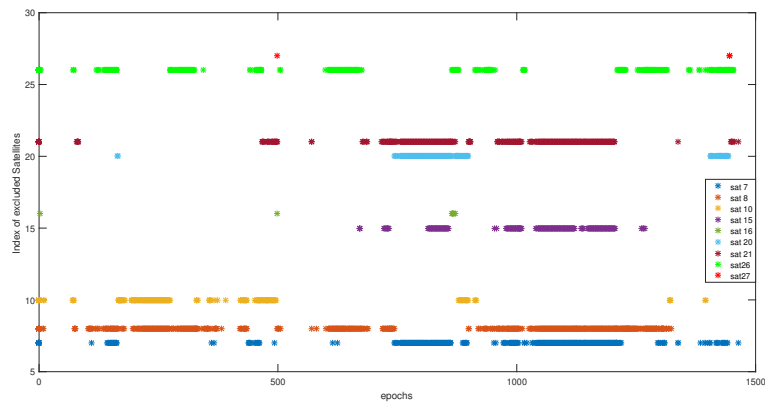


FIGURE 5.21 – index of isolated satellites using fixed α

In addition, figure 5.22 shows the isolated satellites using the α balanced scenario.

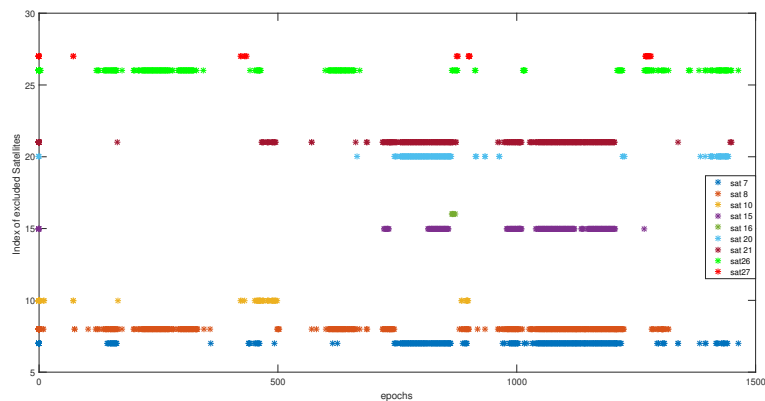


FIGURE 5.22 – index of isolated satellites using α balance

The two figures show a lot of commune isolation satellites, as well many differences present in different epochs and/or in the same epoch. Figure 5.23 shows only the differences between the isolated satellites in the two scenarios.

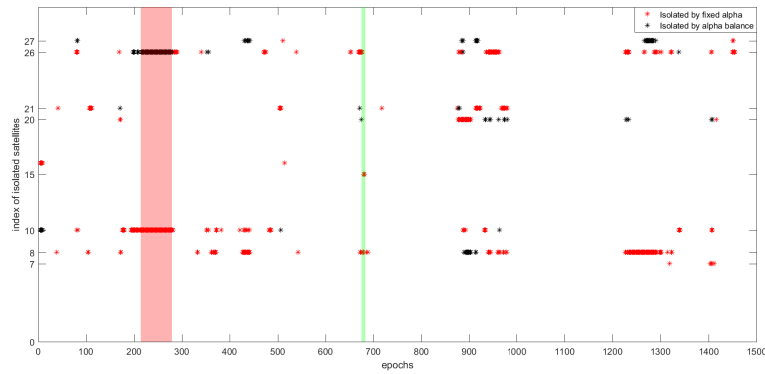
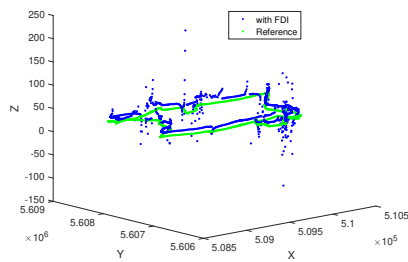


FIGURE 5.23 – The difference in decisions between fixed α and α balance

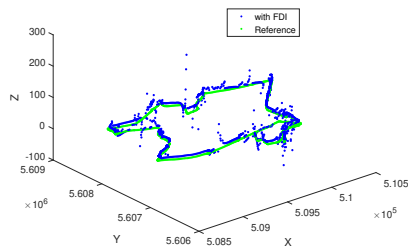
For example, in the fixed α scenario the decision was to isolate satellite 10 from epoch 215 to 278 (pink zone). Where in α balance scenario, the satellite 10 is considered non-faulty and the decision was to isolate satellite 26. The same scenario is repeated in epoch 887 with two satellites in difference, and in many different epochs. On the other hand, the fixed α in many epochs decides to isolate some satellites, where using α balance no isolation occurred. As example, from epoch 676 to epoch 681 (green zone), satellites 8 and 15 are isolated using the KLD, and used in the final estimation by the α balance. In order to judge fairly these decisions, we will presents the final positioning estimation for both scenarios in 3D and 2D views comparing each one separately to the reference using figure 5.24.



(a) 3D view using fixed α



(b) 2D view using fixed α



(c) 3D view using α balanced



(d) 2D view using α balanced

FIGURE 5.24 – Final estimation positioning with FDI approach comparison

In order to compare these results, and to deliver a clear view, we are providing in figure 5.25 the 2D view of the trajectories for the fixed and balanced α in one picture compared to the reference. In plus, we zoomed on the area corresponding to the pink zone in figure 5.23 to see the effect of each decision on the position. Noting that, the fixed α trajectory is plotted in magenta color, and the blue trajectory correspond to the α balanced.

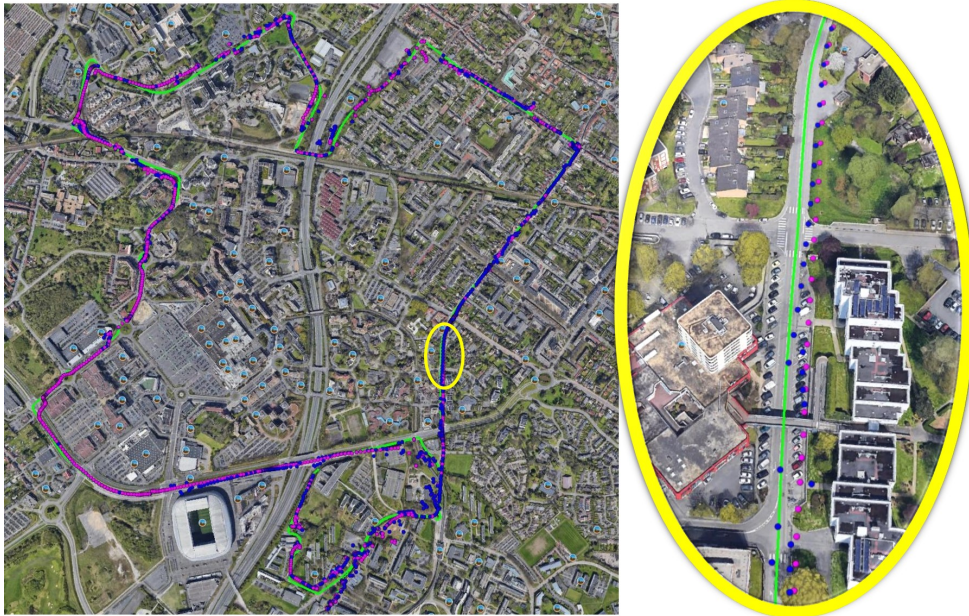


FIGURE 5.25 – The effect of the decisions between fixed α and α balance on the position

In order to evaluate the results in numerical way and show the effect of the two FDI approaches on the position estimation, table 5.4 presents the median error, the mean error, and the max error removed during the whole trajectory.

TABLE 5.4 – Type of errors removed

Error type in meters	Error removed by α balance	Error removed by fixed α	difference
Median error	5.8883	4.4228	1.4655
Mean error	5.6866	4.6615	1.0251
Max error	61.7337	55.0582	6.6755

These results underline the performance of adaptive diagnosis between the two proposed scenarios. In addition, they show that, it is not always a good policy to remove measurements from the final estimation, and to do so, adaptive diagnosis must be used taking into account different factors such as KPIs and environment. While in some cases, adaptive diagnostics can act like normal diagnostics, such as, when the vehicle is moving in the open sky over its entire trajectory. In this way, the adaptive diagnosis will provide a high degree of confidence in the observations at all times, and vice versa.

5.5 Chapter Conclusion

In this chapter, the proposed approach were tested with real experimental GNSS/odo data merging. First, the technical equipment used in the data acquisition were detailed, and the test trajectories, were presented. Then, in order to analyse and manipulate the real data, the goGPS software is used as it is a free-license software and able to deal with different type of data, especially RINEX files. Then, we presented the obtained results in order to highlight the importance and the effect of proposed algorithms in the whole approach. Starting by a discussion and illustration of the impact of the sensors fusion comparing with GNSS standalone. The comparison is made without diagnosis to focus on the impact of the sensors fusion. Later, a dedicated section that underlines the MCC impact for a robust fusion system is presented. A comparison is made in order to show how the MCC deals with heavy non-Gaussian noises in comparison with the MMSE.

For the diagnosis part, the reason of choosing α -RD for residual deign is discussed by showing the impact of the α -Rényi on the fault detection. Hence, an unsupervised clustering algorithm is used in order to create the faulty and non-faulty *pdfs*. Finally, the results were detailed through two scenarios. The first scenario uses a fixed α for residuals generation, where the second uses the α balance. The results show a difference in the decisions in order to judge which satellites should be removed. Thus, a comparison between the two scenarios is done showing the advantage of the adaptive diagnosis in the final positioning estimation.

Chapter 6

Conclusion

6.1 General Conclusion & Perspectives

6.1.1 Conclusion

In this thesis, we treated the problem of fault-tolerant localization system for autonomous vehicle. First, we introduced the concept of key performance indicators, well known in the domain of diagnostic, and also several definitions of vocabulary, acronyms and terms usually encountered in diagnostic domain. In addition, the interaction between these terms is described. Then, we highlighted the role of the multi-fusion architecture, to reach a good performance with high level of accuracy and continuity, by presenting different types of well-known sensors with their advantages and limitations. As well, we highlighted, the need of a robust estimator regarding non-linearity, and non-Gaussian *pdfs*. Hence, a presentation was done for the well-known filters in the literature, as the Kalman filter and its canonical form the non-linear information filter, the Unscented filters and the Particle filter. In chapter 3, the adaptive fault tolerant fusion was presented. After explaining the relevance of the adaptive diagnostic concept, and how the fail-safe design architecture should be related to the changing environment of a vehicle, and able to provide the KPI requirements at each moment, the target to design an adaptive diagnostic layer through residual design was shown and detailed. Different information measurements were presented for residual generation between the a priori and a posteriori distributions of the chosen estimator, and for decision-making part using threshold optimization through a suitable criterion. Before, proposing the framework, the fault tolerance concept in the multi-sensor fusion domain had to be defined. After choosing the suitable fusion architecture for the fault tolerance approach, the impact of the adaptive diagnostic was discussed. We shown that the design of a robust fault detection and isolation method can form an interesting solution. Indeed, for a changing environment of the vehicle, an adaptive residual design in a diagnostic layer has a relevant impact on the FTF architecture. The proposed approach is then detailed in chapter 4. Where, the block diagram was presented, and the problems faced with the proposed solutions were illustrated. Hence, the non-linearity and the non-Gaussian noises are faced by a proposed

filter called the nonlinear information filter under the maximum correntropy criterion. This filter adopt the MCC instead of the MMSE criterion which make it more robust against non-Gaussian noises such the mixture-Gaussian and shot noises.

Then, an adaptive FTF approach was proposed using a parametric residuals generated through the α -Rényi divergence. To adapt this parameter α , we proposed a solution called the α balance. This proposition led to a big number of statistical characterization in order to create the faulty and non-faulty distributions. A solution is proposed to this problem using a mathematical model based on non-supervised real data. For decision-making through a thresholding method for the residuals, a new criterion design based on α -RD called α -Rényi criterion was developed. This criterion holds a large choice of criterion, where we linked the criterion to the corresponding calculated divergence. For the isolation part of the diagnostic, we showed the efficiency of using the unknown input observers as separation method to isolate erroneous measurements. Finally, the whole algorithm was tested using real GNSS/odometer data using different tests trajectories. The results show good performance for the MCCNIF in the fusion part, for the adaptive diagnostic, and finally with the decision-making part.

6.1.2 Perspectives

The encouraging obtained results confirm our motivations for the choice of the methodological proposed tools, in particular the adaptive diagnostic in the informational framework. These results give suggestions for some improvements and several future research. We list below several but not exhaustive points to be treated or investigated as perspective of this work :

- Regarding the multi-sensor fusion part, like a short term perspective, we can consider the use of the INS with the GNSS/odo in tight coupling in order to reach higher level in accuracy and availability. The design of the architecture has begun in a ongoing study at the lab. We think that the use of other sensors can show more clearly the relevance of the AFTF concept. Unfortunately, in this thesis, we were not able to do it due to circumstances beyond our control linked to the access to the experimental platform in the last 8 months.
- There exist also several interesting characteristics of the Maximum Correntropy Criteria for the state estimation, specifically the managing of multi-hypothesis estimation while using non-Gaussian noise. This characteristic should be considered, and used in fault tolerant multi-sensor data fusion method when managing complex uncertainty of measurements.
- In the proposed approach, the way for selecting the parameter α for residuals generation in the adaptive diagnosis can be otherwise designed in integrating Artificial Intelligence tools like Deep Neural Network. Ac-

tually, we are working on a data driven methods to choose the suitable α corresponding to the context. The work has already launched in the frame of a PhD work in the lab.

- Regarding the decision part, we have seen that the threshold is calculated using the variable P_0 . The P_0 is calculated on the basis of the windowing method, which has some limitations regarding the rapid adaptation to each case and the heuristic way in choosing the dimension of the window. Work has started on the calculation of P_0 based on artificial intelligence tools with a joint work in the frame of a ongoing PhD in the lab, and encouraging results shall be published nearby.
- The diagnosis approach proposed is based on the fault detection and isolation. We intend to move towards the identification of sensor faults, in order to identify the amplitude of these one, and to correct them without going as far as an isolation from the fusion procedure. This aspect can be very interesting in the case where observations are limited.
- We think that the proposed framework can be applied for many different applications in different domains. In this thesis, the framework was applied on the GNSS application for single vehicle. In future work, we are planning to show the interest of the proposed framework for multi-vehicles autonomous system.
- In test and validation step of proposed approach, in some case, we were obliged to inject some additional faults and create some scenarios of faults specifically the case of multiple simultaneous faults cases. But several types of erroneous measurements and combination of simultaneous measurements errors are still not tested, because of the difficulties linked to faults labeling in real data. A new simulator that permit to reconstructs the real data with the ability of errors injection and labeling will be soon available at CRISAL lab that will permit to test and evaluate developed approach with more suitable way.

Finally, we think that one of the important contributions of this work is that it prepares the ground well for future research works with a significant impact in the short and medium term.

Bibliographie

- ABBAS, O. A. (2008). « Comparisons Between Data Clustering Algorithms. »
In : *International Arab Journal of Information Technology (IAJIT)* 5.3.
- ABBAS, T., M. ARIF et W. AHMED (2006). « Measurement and correction of systematic odometry errors caused by kinematics imperfections in mobile robots ». In : *2006 SICE-ICASE International Joint Conference*. IEEE, p. 2073-2078.
- AL HAGE, J. (oct. 2016). « Fusion de données tolérante aux défaillances : application à la surveillance de l'intégrité d'un système de localisation ». Thèse de doct.
- AL HAGE, J., M. E. EL NAJJAR et D. POMORSKI (2017). « Multi-sensor fusion approach with fault detection and exclusion based on the Kullback–Leibler Divergence : Application on collaborative multi-robot system ». In : *Information Fusion* 37, p. 61-76.
- AMINI, A., R. M. VAGHEFI, M. JESUS et R. M. BUEHRER (2014). « Improving GPS-based vehicle positioning for intelligent transportation systems ». In : *2014 IEEE Intelligent Vehicles Symposium Proceedings*. IEEE, p. 1023-1029.
- ANTOLIN, J., J. ANGULO et S. LOPEZ-ROSA (2009). « Fisher and jensen-shannon divergences : Quantitative comparisons among distributions. application to position and momentum atomic densities ». In : *The Journal of chemical physics* 130.7, p. 074110.
- AY, N. et S.-i. AMARI (2015). « A novel approach to canonical divergences within information geometry ». In : *Entropy* 17.12, p. 8111-8129.
- BADER, K., B. LUSSIER et W. SCHÖN (2017). « A fault tolerant architecture for data fusion : A real application of Kalman filters for mobile robot localization ». In : *Robotics and Autonomous Systems* 88, p. 11-23.
- BAI, L., L. ROSSI, A. TORSELLO et E. R. HANCOCK (2015). « A quantum Jensen–Shannon graph kernel for unattributed graphs ». In : *Pattern Recognition* 48.2, p. 344-355.
- BASSEVILLE, M. (2013). « Divergence measures for statistical data processing—An annotated bibliography ». In : *Signal Processing* 93.4, p. 621-633.
- BHATTACHARYA, A., D. PATI, Y. YANG et al. (2019). « Bayesian fractional posteriors ». In : *The Annals of Statistics* 47.1, p. 39-66.
- BHATTACHARYA, A., P. KAR et M. PAL (2009). « On low distortion embeddings of statistical distance measures into low dimensional spaces ». In : *Inter-*

- national Conference on Database and Expert Systems Applications*. Springer, p. 164-172.
- BILICH, A., P. AXELRAD et K. M. LARSON (2007). « Scientific utility of the signal-to-noise ratio (SNR) reported by geodetic GPS receivers ». In : *Proc. ION GNSS*, p. 26-28.
- BLANCH, J., T. WALTER, P. ENGE, Y. LEE, B. PERVAN, M. RIPPL et al. (2012). « Advanced RAIM user algorithm description : integrity support message processing, fault detection, exclusion, and protection level calculation ». In : *Proceedings of the 25th International Technical Meeting of The Satellite Division of the Institute of Navigation (ION GNSS 2012)*, p. 2828-2849.
- BOBKOV, S. G., G. CHISTYAKOV, F. GÖTZE et al. (2019). « Rényi divergence and the central limit theorem ». In : *The Annals of Probability* 47.1, p. 270-323.
- BOUSSAD, A. (déc. 2019). « Approche informationnelle pour la navigation autonome tolérante aux défauts Application aux systèmes robotiques mobiles ». Thèse de doct.
- BRAKATSOULAS, S., D. PFOSE, R. SALAS et C. WENK (2005). « On map-matching vehicle tracking data ». In : *Proceedings of the 31st international conference on Very large data bases*, p. 853-864.
- BROWN, R. G. (2003). « Receiver autonomous integrity monitoring ». In : *Global positioning system : theory and applications* 2, p. 143-165.
- BROWN, R. G., P. Y. HWANG et al. (1992). *Introduction to random signals and applied Kalman filtering*. T. 3. Wiley New York.
- CANEDO-RODRIGUEZ, A., V. ALVAREZ-SANTOS, C. V. REGUEIRO, R. IGLESIAS, S. BARRO et J. PRESEDO (2016). « Particle filter robot localisation through robust fusion of laser, WiFi, compass, and a network of external cameras ». In : *Information Fusion* 27, p. 170-188.
- CARDARELLI, D. (2002). « An integrated MEMS inertial measurement unit ». In : *2002 IEEE Position Location and Navigation Symposium (IEEE Cat. No. 02CH37284)*. IEEE, p. 314-319.
- CHEN, A., J. LI et Z. CHU (2012). « Dither signal removal of ring laser gyro POS based on combined digital filter ». In : *2012 8th IEEE International Symposium on Instrumentation and Control Technology (ISICT) Proceedings*. IEEE, p. 178-182.
- CHEN, B., X. LIU, H. ZHAO et J. C. PRINCIPE (2017). « Maximum correntropy Kalman filter ». In : *Automatica* 76, p. 70-77.
- CHEN, B. et J. C. PRINCIPE (2012). « Maximum correntropy estimation is a smoothed MAP estimation ». In : *IEEE Signal Processing Letters* 19.8, p. 491-494.
- CHEN, H.-M., P. K. VARSHNEY et M. K. ARORA (2003). « Performance of mutual information similarity measure for registration of multitemporal remote sensing images ». In : *IEEE Transactions on Geoscience and Remote Sensing* 41.11, p. 2445-2454.
- CHEN, J. et R. J. PATTON (2012). *Robust model-based fault diagnosis for dynamic systems*. T. 3. Springer Science & Business Media.

- CHEN, Z., X. LI, C. YANG, T. PENG, C. YANG, H. KARIMI et al. (2019). « A data-driven ground fault detection and isolation method for main circuit in railway electrical traction system ». In : *ISA transactions* 87, p. 264-271.
- CHIANG, K.-W. (2004). *INS/GPS integration using neural networks for land vehicular navigation applications*. NR-04589 UMI. University of Calgary Canada.
- CLAWGES, R., K. VIERLING, L. VIERLING et E. ROWELL (2008). « The use of airborne lidar to assess avian species diversity, density, and occurrence in a pine/aspen forest ». In : *Remote Sensing of Environment* 112.5, p. 2064-2073.
- COMBS, T. S., L. S. SANDT, M. P. CLAMANN et N. C. McDONALD (2019). « Automated vehicles and pedestrian safety : exploring the promise and limits of pedestrian detection ». In : *American journal of preventive medicine* 56.1, p. 1-7.
- CORNICK, M., J. KOEHLING, B. STANLEY et B. ZHANG (2016). « Localizing ground penetrating radar : A step toward robust autonomous ground vehicle localization ». In : *Journal of field robotics* 33.1, p. 82-102.
- CORRADINI, M. L. et G. ORLANDO (2007). « Linear unstable plants with saturating actuators : robust stabilization by a time varying sliding surface ». In : *Automatica* 43.1, p. 88-94.
- DAWOUD, S. (2012). « GNSS principles and comparison ». In : *Potsdam University*.
- DE DOMENICO, M., M. A. PORTER et A. ARENAS (2015). « MuxViz : a tool for multilayer analysis and visualization of networks ». In : *Journal of Complex Networks* 3.2, p. 159-176.
- DEL MORAL, P. (1997). « Nonlinear filtering : Interacting particle resolution ». In : *Comptes Rendus de l'Académie des Sciences-Series I-Mathematics* 325.6, p. 653-658.
- DENNING, P. J. (1976). « Fault tolerant operating systems ». In : *ACM Computing Surveys (CSUR)* 8.4, p. 359-389.
- EFRON, B. (1998). « RA Fisher in the 21st century ». In : *Statistical Science*, p. 95-114.
- EL FAOUZI, N.-E., H. LEUNG et A. KURIAN (2011). « Data fusion in intelligent transportation systems : Progress and challenges—A survey ». In : *Information Fusion* 12.1, p. 4-10.
- EL NAJJAR, M. E. B. et P. BONNIFAIT (2007). « Road Selection using Multi-Criteria Fusion for the Roadmap-Matching Problem ». In :
- ERVEN, T. van et P. HARREMOËS (2010). « Rényi divergence and majorization ». In : *2010 IEEE International Symposium on Information Theory*. IEEE, p. 1335-1339.
- ESCOBAR, R., C. ASTORGA-ZARAGOZA, A. TELLEZ-ANGUIANO, D. JUAREZ-ROMERO, J. HERNANDEZ et G. GUERRERO-RAMIREZ (2011). « Sensor fault detection and isolation via high-gain observers : Application to a double-pipe heat exchanger ». In : *ISA transactions* 50.3, p. 480-486.
- ESKANDARIAN, A. (2012). *Handbook of intelligent vehicles*. T. 2. Springer.

- FALCO, G., M. NICOLA et M. PINI (2018). « Positioning based on tightly coupled multiple sensors : A practical implementation and experimental assessment ». In : *IEEE Access* 6, p. 13101-13116.
- GANCHEV, K., B. TASKAR et J. GAMA (2008). « Expectation maximization and posterior constraints ». In : *Advances in neural information processing systems*, p. 569-576.
- GENG, H., Y. LIANG, F. YANG, L. XU et Q. PAN (2017). « Model-reduced fault detection for multi-rate sensor fusion with unknown inputs ». In : *Information Fusion* 33, p. 1-14.
- GERTLER, J. (1998). *Fault detection and diagnosis in engineering systems*. CRC press.
- GUAN, H., J. LI, S. CAO et Y. YU (2016). « Use of mobile LiDAR in road information inventory : A review ». In : *International Journal of Image and Data Fusion* 7.3, p. 219-242.
- HANSEN, A. (2004). « WAAS Precision Approach Metrics : Accuracy, Integrity, Continuity and Availability ». In : URL : <http://waas.stanford.edu/metrics.html> [accessed 1 November 2004].
- HARMOUCHE, J., C. DELPHA et D. DIALLO (2015). « Incipient fault detection and diagnosis based on Kullback–Leibler divergence using principal component analysis : Part II ». In : *Signal Processing* 109, p. 334-344.
- HERRERA, A. M., H. F. SUHANDRI, E. REALINI, M. REGUZZONI et M. C. de LACY (2016). « goGPS : open-source MATLAB software ». In : *GPS solutions* 20.3, p. 595-603.
- HEWITSON, S. et J. WANG (2006). « GNSS receiver autonomous integrity monitoring (RAIM) performance analysis ». In : *Gps Solutions* 10.3, p. 155-170.
- HISTACE, A. et D. ROUSSEAU (2015). « Divergence de Rényi comme mesure de contraste pour la détection d’objets dans des images bruitées ». In :
- HO, S.-W. et S. VERDÚ (2015). « Convexity/concavity of Rényi entropy and α -mutual information ». In : *2015 IEEE International Symposium on Information Theory (ISIT)*. IEEE, p. 745-749.
- HOBALLAH, I. Y. et P. K. VARSHNEY (1989). « An information theoretic approach to the distributed detection problem ». In : *IEEE Transactions on Information Theory* 35.5, p. 988-994.
- HOBZA, T., D. MORALES et L. PARDO (2009). « Rényi statistics for testing equality of autocorrelation coefficients ». In : *Statistical Methodology* 6.4, p. 424-436.
- HOWARD, A. (2006). « Multi-robot simultaneous localization and mapping using particle filters ». In : *The International Journal of Robotics Research* 25.12, p. 1243-1256.
- HU, H. et J. Q. GAN (2005). « Sensors and data fusion algorithms in mobile robotics ». In : *Technical Report : CSM-422, Department of Computer Science*.
- HUISMAN, L., P. J. TEUNISSEN et D. ODIJK (2010). « On the robustness of next generation GNSS phase-only real-time kinematic positioning ». In : *Proc. of FIG Congress, Sydney, Australia*.

- HURSKAINEN, H., J. RAASAKKA, T. AHONEN et J. NURMI (2009). « Multicore software-defined radio architecture for GNSS receiver signal processing ». In : *EURASIP Journal on Embedded Systems* 2009.1, p. 543720.
- ISERMANN, R. (2006). *Fault-diagnosis systems : an introduction from fault detection to fault tolerance*. Springer Science & Business Media.
- IZANLOO, R., S. A. FAKOORIAN, H. S. YAZDI et D. SIMON (2016). « Kalman filtering based on the maximum correntropy criterion in the presence of non-Gaussian noise ». In : *2016 Annual Conference on Information Science and Systems (CISS)*. IEEE, p. 500-505.
- JAGADEESH, G., T. SRIKANTHAN et X. ZHANG (2004). « A map matching method for GPS based real-time vehicle location ». In :
- JEN, E. (2005). « Stable or robust? What's the difference? » In : *Robust Design : a repertoire of biological, ecological, and engineering case studies, SFI Studies in the Sciences of Complexity*, p. 7-20.
- JIANG, L. (2011). « Sensor Fault Detection and Isolation Using System Dynamics Identification Techniques. » Thèse de doct.
- JOERGER, M., F.-C. CHAN et B. PERVAN (2014). « Solution separation versus residual-based RAIM ». In : *NAVIGATION : Journal of the Institute of Navigation* 61.4, p. 273-291.
- JULIER, S. J. (2006). « An empirical study into the use of Chernoff information for robust, distributed fusion of Gaussian mixture models ». In : *2006 9th International Conference on Information Fusion*. IEEE, p. 1-8.
- JULIER, S. J. et J. K. UHLMANN (1997). « New extension of the Kalman filter to nonlinear systems ». In : *Signal processing, sensor fusion, and target recognition VI*. T. 3068. International Society for Optics et Photonics, p. 182-193.
- JUNG, S., J. KIM et S. KIM (2009). « Simultaneous localization and mapping of a wheel-based autonomous vehicle with ultrasonic sensors ». In : *Artificial Life and Robotics* 14.2, p. 186.
- KADDOUR, M. (2016). « Contribution à la surveillance et au contrôle de l'intégrité d'un système de localisation GNSS ». Thèse de doct. Lille 1.
- KALMAN, R. E. (1960). « A new approach to linear filtering and prediction problems ». In :
- KALRA, N. et S. M. PADDOCK (2016). « Driving to safety : How many miles of driving would it take to demonstrate autonomous vehicle reliability? » In : *Transportation Research Part A : Policy and Practice* 94, p. 182-193.
- KAMIJO, S., Y. GU et L.-T. HSU (2015). « Autonomous Vehicle Technologies : Localization and Mapping ». In : *ESSFR* 9.2, p. 131-141.
- KHAN, M. F. et R. A. PAUL (2012). « Pragmatic Directions in Engineering Secure Dependable Systems ». In : *Advances in Computers*. T. 84. Elsevier, p. 141-167.
- KIKUTIS, R. et D. RUDINSKAS (2012). « „ARDUPILOT MEGA “AUTOPILOTO INERCINIO NAVIGACIJOS ĮRENGINIO PAKLAIDŲ ANALIZĖ ». In : *Science : Future of Lithuania* 4.4.
- KIM, H., B. LIU, C. Y. GOH, S. LEE et H. MYUNG (2017). « Robust vehicle localization using entropy-weighted particle filter-based data fusion of verti-

- cal and road intensity information for a large scale urban area ». In : *IEEE Robotics and Automation Letters* 2.3, p. 1518-1524.
- KLUGE, S., K. REIF et M. BROKATE (2010). « Stochastic stability of the extended Kalman filter with intermittent observations ». In : *IEEE Transactions on Automatic Control* 55.2, p. 514-518.
- KOTSIANTIS, S. B., I. ZAHARAKIS et P. PINTELAS (2007). « Supervised machine learning : A review of classification techniques ». In : *Emerging artificial intelligence applications in computer engineering* 160, p. 3-24.
- KULLBACK, S. (1959). *Information theory and statistics*. J. Wiley et Sons, New York.
- KULLBACK, S. et R. A. LEIBLER (1951). « On information and sufficiency ». In : *The annals of mathematical statistics* 22.1, p. 79-86.
- KUMAR, R. et A. INDRAYAN (2011). « Receiver operating characteristic (ROC) curve for medical researchers ». In : *Indian pediatrics* 48.4, p. 277-287.
- KUUTTI, S., S. FALLAH, K. KATSAROS, M. DIANATI, F. MCCULLOUGH et A. MOUZAKITIS (2018). « A survey of the state-of-the-art localization techniques and their potentials for autonomous vehicle applications ». In : *IEEE Internet of Things Journal* 5.2, p. 829-846.
- LARSEN, P. B. (2001). « Issues relating to civilian and military dual uses of GNSS ». In : *Space Policy* 17.2, p. 111-119.
- LASHLEY, M., D. M. BEVLY et J. Y. HUNG (2010). « Analysis of deeply integrated and tightly coupled architectures ». In : *IEEE/ION Position, Location and Navigation Symposium*. IEEE, p. 382-396.
- LEGENDRE, A. M. (1805). *Nouvelles méthodes pour la détermination des orbites des comètes*. F. Didot.
- LEVINSON, J., M. MONTEMERLO et S. THRUN (2007). « Map-based precision vehicle localization in urban environments. » In : *Robotics : science and systems*. T. 4. Citeseer. Citeseer, p. 1.
- LEWANDOWSKI, W. et L. TISSERAND (2010). « Relative characterization of GNSS receiver delays for GPS and GLONASS C/A codes in the L1 frequency band at the OP, SU, PTB and AOS ». In : *Bureau International des Poids et Mesures, Tech. Rep* 4.
- LI, C., B. DAI et T. WU (2013). « Vision-based precision vehicle localization in urban environments ». In : *2013 Chinese Automation Congress*. IEEE, p. 599-604.
- LIM, H. S. M. et A. TAEIHAGH (2019). « Algorithmic decision-making in AVs : Understanding ethical and technical concerns for smart cities ». In : *Sustainability* 11.20, p. 5791.
- LIU, Y., F. LIU, Y. GAO et L. ZHAO (2018). « Implementation and analysis of tightly coupled global navigation satellite system precise point positioning/inertial navigation system (GNSS PPP/INS) with insufficient satellites for land vehicle navigation ». In : *Sensors* 18.12, p. 4305.
- LOZANO, R., P. CASTILLO, P. GARCIA et A. DZUL (2004). « Robust prediction-based control for unstable delay systems : Application to the yaw control of a mini-helicopter ». In : *Automatica* 40.4, p. 603-612.

- MAKKAWI, K., N. AIT-TMAZIRTE, M. EL BADAoui EL NAJJAR et N. MOUBAYED (2019). « Fault tolerant fusion using α -Rényi divergence for autonomous vehicle localization, » in : *The 15th European Workshop on Advanced Control and Diagnosis (ACD 2019)*.
- MARSLAND, S. (2014). *Machine learning : an algorithmic perspective*. Chapman et Hall/CRC.
- MEI, W., G. SHAN et C. WANG (2011). « Practical development of the second-order extended Kalman filter for very long range radar tracking ». In : *Signal Processing* 91.5, p. 1240-1248.
- MENG, X., S. ROBERTS, Y. CUI, Y. GAO, Q. CHEN, C. XU et al. (2018). « Required navigation performance for connected and autonomous vehicles : where are we now and where are we going ? » In : *Transportation planning and technology* 41.1, p. 104-118.
- MENSING, C., S. SAND et A. DAMMANN (2010). « Hybrid data fusion and tracking for positioning with GNSS and 3GPP-LTE ». In : *International Journal of Navigation and Observation* 2010.
- MISRA, P. et P. ENGE (p. d.). « Global Positioning System : signals, measurements and performance second edition ». In : ().
- MITCHELL, H. B. (2007). *Multi-sensor data fusion : an introduction*. Springer Science & Business Media.
- MONDAL, S., G. CHAKRABORTY et K. BHATTACHARYYA (2008). « Robust unknown input observer for nonlinear systems and its application to fault detection and isolation ». In : *Journal of dynamic systems, measurement, and control* 130.4.
- MOON, T. K. (1996). « The expectation-maximization algorithm ». In : *IEEE Signal processing magazine* 13.6, p. 47-60.
- MORALES, Y., E. TAKEUCHI et T. TSUBOUCHI (2008). « Vehicle localization in outdoor woodland environments with sensor fault detection ». In : *2008 IEEE International Conference on Robotics and Automation*. IEEE, p. 449-454.
- EL-MOWAFY, A. et N. KUBO (2017). « Integrity monitoring of vehicle positioning in urban environment using RTK-GNSS, IMU and speedometer ». In : *Measurement Science and Technology* 28.5, p. 055102.
- MR, B. et P. MR (1763). « An essay toward solving a problem in the doctrine of chances. By the late Rev. Mr. Bayes, FRS communicated by Mr. Price, in a letter to John Canton, AMFRS ». In : *Philosophical Transactions*, p. 1683-1775.
- NAGPAL, A., A. JATAIN et D. GAUR (2013). « Review based on data clustering algorithms ». In : *2013 IEEE Conference on Information & Communication Technologies*. IEEE, p. 298-303.
- NIELSEN, F. (2011). « Chernoff information of exponential families ». In : *arXiv preprint arXiv :1102.2684*.
- (2013). « An information-geometric characterization of Chernoff information ». In : *IEEE Signal Processing Letters* 20.3, p. 269-272.

- NIKIFOROV, I. et B. ROTURIER (2005). « Advanced RAIM algorithms : First results ». In : *18th International Technical Meeting of the Satellite Division of The Institute of Navigation (ION GNSS 2005)*, p. 1789-1800.
- QIAN, W. et W. SHU (2015). « Mutual information criterion for feature selection from incomplete data ». In : *Neurocomputing* 168, p. 210-220.
- RADHAKRISHNAN, C., M. PARTHASARATHY, S. JAMBULINGAM et T. BYRNES (2016). « Distribution of quantum coherence in multipartite systems ». In : *Physical review letters* 116.15, p. 150504.
- RÉNYI, A. et al. (1961). « On measures of entropy and information ». In : *Proceedings of the Fourth Berkeley Symposium on Mathematical Statistics and Probability, Volume 1 : Contributions to the Theory of Statistics*. The Regents of the University of California.
- RIZOS, C. (2013). « Locata : A positioning system for indoor and outdoor applications where GNSS does not work ». In : *Proceedings of the 18th Association of Public Authority Surveyors Conference*, p. 73-83.
- ROBERT, C. et G. CASELLA (2011). « A short history of Markov chain Monte Carlo : Subjective recollections from incomplete data ». In : *Statistical Science*, p. 102-115.
- SALMANPOUR, M. S., Z. SHARIF KHODAEI et M. H. ALIABADI (2017). « Impact damage localisation with piezoelectric sensors under operational and environmental conditions ». In : *Sensors* 17.5, p. 1178.
- SANTAMARIA, I., P. P. POKHAREL et J. C. PRINCIPE (2006). « Generalized correlation function : definition, properties, and application to blind equalization ». In : *IEEE Transactions on Signal Processing* 54.6, p. 2187-2197.
- SAVAGE, P. G. (2013). « Blazing gyros : The evolution of strapdown inertial navigation technology for aircraft ». In : *Journal of Guidance, Control, and Dynamics* 36.3, p. 637-655.
- SENETA, E. (1996). « Markov and the birth of chain dependence theory ». In : *International Statistical Review/Revue Internationale de Statistique*, p. 255-263.
- SHAN, J. et C. K. TOTH (2018). *Topographic laser ranging and scanning : principles and processing*. CRC press.
- SHANNON, C. E. (1948). « A mathematical theory of communication ». In : *The Bell system technical journal* 27.3, p. 379-423.
- SINGH, S. (2015). *Critical reasons for crashes investigated in the national motor vehicle crash causation survey*. Rapp. tech.
- SUHR, J. K., J. JANG, D. MIN et H. G. JUNG (2016). « Sensor fusion-based low-cost vehicle localization system for complex urban environments ». In : *IEEE Transactions on Intelligent Transportation Systems* 18.5, p. 1078-1086.
- SUN, S. (2013). « A survey of multi-view machine learning ». In : *Neural computing and applications* 23.7-8, p. 2031-2038.
- SUNDVALL, P. et P. JENSFELT (2006). « Fault detection for mobile robots using redundant positioning systems ». In : *Proceedings 2006 IEEE International Conference on Robotics and Automation, 2006. ICRA 2006*. IEEE, p. 3781-3786.

- TANAKA, K. et M. SANO (1994). « A robust stabilization problem of fuzzy control systems and its application to backing up control of a truck-trailer ». In : *IEEE Transactions on Fuzzy systems* 2.2, p. 119-134.
- TARTAKOVSKY, A., I. NIKIFOROV et M. BASSEVILLE (2014). *Sequential analysis : Hypothesis testing and changepoint detection*. CRC Press.
- TIPALDI, G. D., D. MEYER-DELIUS et W. BURGARD (2013). « Lifelong localization in changing environments ». In : *The International Journal of Robotics Research* 32.14, p. 1662-1678.
- TMAZIRTE, N. A., M. E. EL NAJJAR, J. AL HAGE, C. SMAILI et D. POMORSKI (2014). « Fast multi fault detection & exclusion approach for GNSS integrity monitoring ». In : *17th International Conference on Information Fusion (FUSION)*. IEEE, p. 1-6.
- TONG, G., Z. FANG et X. XU (2006). « A particle swarm optimized particle filter for nonlinear system state estimation ». In : *2006 IEEE International Conference on Evolutionary Computation*. IEEE, p. 438-442.
- VAN DER MERWE, R., E. WAN et S. JULIER (2004). « Sigma-point Kalman filters for nonlinear estimation and sensor-fusion : Applications to integrated navigation ». In : *AIAA Guidance, Navigation, and Control Conference and Exhibit*, p. 5120.
- VAN ERVEN, T. et P. HARREMOS (2014). « Rényi divergence and Kullback-Leibler divergence ». In : *IEEE Transactions on Information Theory* 60.7, p. 3797-3820.
- VARSHNEY, P. K. (2012). *Distributed detection and data fusion*. Springer Science & Business Media.
- VEXLER, A., A. LIU, E. ELISEEVA et E. F. SCHISTERMAN (2008). « Maximum likelihood ratio tests for comparing the discriminatory ability of biomarkers subject to limit of detection ». In : *Biometrics* 64.3, p. 895-903.
- VIVET, D., F. GÉROSSIER, P. CHECCHIN, L. TRASSOUDAIN et R. CHAPUIS (2013). « Mobile ground-based radar sensor for localization and mapping : An evaluation of two approaches ». In : *International Journal of Advanced Robotic Systems* 10.8, p. 307.
- WANG, G., N. LI et Y. ZHANG (2017). « Maximum correntropy unscented Kalman and information filters for non-Gaussian measurement noise ». In : *Journal of the Franklin Institute* 354.18, p. 8659-8677.
- WANG, R. (2013). « 3D building modeling using images and LiDAR : A review ». In : *International Journal of Image and Data Fusion* 4.4, p. 273-292.
- WARD, E. et J. FOLKESSON (2016). « Vehicle localization with low cost radar sensors ». In : *2016 IEEE Intelligent Vehicles Symposium (IV)*. IEEE, p. 864-870.
- WIENER, N. (1949). « Extrapolation, interpolation and smoothing of stationary time series-with engineering applications' MIT Press ». In : *Google Scholar*.
- WOOD, M., P. ROBBEL, M. MAASS, R. TEBBENS, M. MEIJS, M. HARB et al. (2019). « Safety first for automated driving ». In : *Online verfügbar unter <https://www.daimler.com/documents/innovation/other/safety-first-for-automated-driving.pdf>, zuletzt geprüft am 19.11*, p. 2019.

- WU, Z., J. SHI, X. ZHANG, W. MA, B. CHEN et I. SENIOR MEMBER (2015). « Kernel recursive maximum correntropy ». In : *Signal Processing* 117, p. 11-16.
- YANG, Y. et J. XU (2016). « GNSS receiver autonomous integrity monitoring (RAIM) algorithm based on robust estimation ». In : *Geodesy and geodynamics* 7.2, p. 117-123.
- ZAARANE, A., I. SLIMANI, W. AL OKAISHI, I. ATOUF et A. HAMDOUN (2020). « Distance measurement system for autonomous vehicles using stereo camera ». In : *Array* 5, p. 100016.
- ZABALEGUI, P., G. DE MIGUEL, A. PÉREZ, J. MENDIZABAL, J. GOYA et I. ADIN (2020). « A Review of the Evolution of the Integrity Methods Applied in GNSS ». In : *IEEE Access* 8, p. 45813-45824.
- ZHANG, F., H. STÄHLE, G. CHEN, C. C. C. SIMON, C. BUCKL et A. KNOLL (2012). « A sensor fusion approach for localization with cumulative error elimination ». In : *2012 IEEE International Conference on Multisensor Fusion and Integration for Intelligent Systems (MFI)*. IEEE, p. 1-6.
- ZHENG, X. et W. WEI (2009). « Reliability study of redundant configuration of IMU fiber optic gyroscope inertial measurement unit ». In : *2009 8th International Conference on Reliability, Maintainability and Safety*. IEEE, p. 87-90.
- ZHOU, S. K. et R. CHELLAPPA (2005). « Beyond one still image : Face recognition from multiple still images or a video sequence ». In : *Face processing : advanced modeling and methods*, p. 547-567.
- ZHU, N., D. BETAILLE, J. MARAIS et M. BERBINEAU (2018). « GNSS Integrity Enhancement for Urban Transport Applications by Error Characterization and Fault Detection and Exclusion (FDE) ». In :
- ZHU, X. J. (2005). *Semi-supervised learning literature survey*. Rapp. tech. University of Wisconsin-Madison Department of Computer Sciences.